rijkswaterstaat

communications

aspects of sediment- and morphodynamics of subtidal deposits of the oosterschelde (the netherlands)

by

dr. j. h. van den berg

no. 43/1986

aspects of sediment- and morphodynamics of subtidal deposits of the oosterschelde (the netherlands)

rijkswaterstaat communications

aspects of sediment- and morphodynamics of subtidal deposits of the oosterschelde (the netherlands)

by
dr. j. h. van den berg

the hague, 1986

all correspondence and applications should be addressed to:

rijkswaterstaat
dienst getijdewateren
hooftskade 1
postbus 20907
2500 EX the hague – the netherlands

recommended catalogue entry:

Berg, J. H. van den
Aspects of sediment- and morphodynamics of subtidal deposits of the Oosterschelde (the Netherlands) / by J. H. van den Berg ; Rijkswaterstaat. – The Hague : Rijkswaterstaat, 1986. – 128 p. : ill. ; 24 cm. – (Rijkswaterstaat communications ; 43)
With refer. after each chapter.
With Dutch summary.

Contents

Summary

The present thesis consists of five articles, in all of which links are established between sedimentological aspects of sediments – mostly below the low-water line – in the Oosterschelde and either large- or small-scale morphological changes.

Large morphological changes and associated movements of sediment which occur in the tidal system of the Oosterschelde are first considered in relation to changes in the tidal discharges of this sea-arm. The link between sedimentary structures of recent deposits in the Oosterschelde, as observed in a number of excavations for construction purposes, and the morphological background to their origin is indicated. Lastly, the connection between bed-load transport and sediment transport through small-scale morphological changes in the form of the movement of sand dunes and ripple-marks, is discussed, as is the prediction of such transport with the aid of bed-load transport formulae.

Chapter 1

This introductory chapter primarily deals with the morphological development of the Oosterschelde. Long before the Christian era, the mouth of the Oosterschelde was located in the area between the islands of Schouwen and Walcheren. Until the Middle Ages the Oosterschelde was the principal outlet of the Scheldt River. However, the mouth area was much narrower than it is now. The volume of water which it carries has increased since the Middle Ages mainly as an indirect result of human intervention. Consequently the tidal flow increased, which caused considerable deepening and widening of the estuary. The completion of the Grevelingen Dam in 1964 and the Volkerak Dam in 1969 caused a further increase in the tidal discharges in the western part of the Oosterschelde and part of its northern tributary, which led to considerable scouring in this area. Part of the eroded material was carried out to sea, while a quantity of a similar order of magnitude was deposited in the southern branch of the Oosterschelde to compensate for the substantial removal of sand by human agency there during the 1960s and 1970s. An empirical link between the current-bearing cross-sectional area of tidal channels and the tidal discharge indicated that in 1983 the morphology of much of the Oosterschelde had not yet completely adjusted to the changed hydraulic conditions.

Chapter 2

The effects of the growth in the volume of water involved in tidal movements have not been confined to the Oosterschelde itself during the past century but have also been perceptible in its outer delta. Erosive processes have predominated in the part of the outer delta closest to the mouth of the sea-arm. A few large shoals which 100 years ago were dry at low tide have now virtually disappeared. The ebb channels in the mouth of the estuary have become extended a long way out to sea. As a result, a link between the two largest ebb channels, the Roompot and the Westgat, came into being in 1974, which led to a change in the flow distribution among channels in the mouth of the sea-arm. Part of the sediment eroded in the Oosterschelde and the proximal section of the outer delta was deposited in the more seaward, distal section along the edge of the ebb channels (ebb shields) and along the edge of the outer delta (terminal lobes).

Since 1960 this edge of the outer delta has become extended a considerable distance in a seaward direction, and a stratum of more than 9 metres of sand has been deposited in places. Apart from the terminal lobes and the ebb shields, the main areas of deposition have been the inside bends in the dynamic ebb channels. Sedimentation rates in excess of 8 metres within a few years have been far from exceptional here.

Chapter 3

In the 'Schaar' construction pit on the artificial island 'Neeltje Jans' in the mouth of the Oosterschelde, sediments deposited in a dynamic ebb channel of this type were excavated to a depth of 10 to 17 metres below Amsterdam Ordnance Datum. The sedimentary structure of the deposits consisted mainly of large-scale cross-bedding formed by sand dunes which moved with the dominant ebb current. It appears from old hydrographic charts that the deposits very probably date from the 18th century and came about in a small ebb channel which moved in a westerly direction along the northern flank of the Roompot. A similar sedimentary unit was found at a depth of 5 to 9 metres below AOD in the construction pit for the lock complex in the Philips Dam. However, this was not an inside bend deposit from an active ebb channel but the filling of a passive flood channel which formed on the southern flank of the Krammer during the construction of the Grevelingen Dam (1962–1964). On account of the hydraulic changes caused by this dam, the Krammer underwent a spectacular process of curving out and deepening. In association with this, the aforementioned flood channel soon became silted up and the sedimentary sequence found in the construction pit came about.

From the preserved sedimentary structure it can be deduced that the large-scale cross-bedding at both sites were formed by dunes with a sinusoidal crest and a maximum height of about 2 metres. It was possible to calculate the propagation rate of the bedforms on the basis of thin mud drapes deposited during the turning of the tide and perceptible in the sloping strata. The mean propagation rate calculated for the deposits in the 'Schaar' construction pit was 278 m per annum and that for the excavation in the work island for the Philips Dam was 158 m per annum. There are strong indications that all the ripples which passed the site of the Philips Dam excavations during the period of rapid sedimentation contributed towards the sedimentary sequence which has been preserved.

The considerable similarity between the sedimentary structure of both deposits gives reason to suppose that the same applies to the deposits in the 'Schaar' construction pit. This would suggest an accumulation rate of 0.8 to 0.9 m per month. Soundings show that such extreme values are indeed possible in the smaller ebb channels in this area.

Chapter 4

Above the large-scale cross-bedding unit in the 'Schaar' construction pit, a deposit was opened up which came into being during the silting up of a channel up to 11 m deep which formed here in the 19th century. The sediment in the channel consists of a deposit 5 m thick comprising a rhythmic alternation of sediments originally deposited as flasers and as laminated alternations of sand and silt. Individual strata could be followed for hundreds of metres and were not interrupted by erosion. The alternation is found to be associated with the change of the seasons: the flaser and laminated strata correspond to the cold half of the year (winter) and to the warm half of the year (summer) respectively. This relationship can be demonstrated with reference to the growth and mortality of autochthonous populations of a few common molluscs and the extent of bioturbation, which is relatively great in the laminated strata.

The thickness of the pairs of strata deposited in summer and winter ranges from 20 to 60 cm. The accumulation rate which can thus be calculated corresponds with data from hydrographic charts and also with the growth of a population of sea-urchins which lived in the channel, as deduced from the upward increase in the diameter of tunneling traces in the sediment.

The difference in the physical sedimentary structure between the summer and winter strata arises from a difference in the critical bed shear stress at which sediment begins to move, which reached a higher value in the summer. As a result there was no bed-load transport in the summer, the bed was flat and the

suspended sediment was deposited in parallel laminations and preserved in that form. In the winter the critical bed shear stress could be exceeded and small ripples were created in the bed, as a result of which strata were deposited in a flaser structure. The increased binding between sand particles caused by the increase in the critical bed shear stress value in the summer is probably attributable to the greater organic matter content of the silt which is deposited at that time of year.

Chapter 5

In this chapter the relationship between the bed-load transport, the sediment transport associated with the movement of ripples and dunes, and current velocity is discussed. There are hardly any reliable direct measurements of the bed-load transport in the field. This is primarily because of the problems of accurate and representative sampling. The verification of bed-load transport formulae is therefore based mainly on the results of flume experiments, which have the disadvantage that they relate to very shallow water, not exceeding a few decimetres, and cannot be expected to be representative of most natural situations involving depths of metres to which the formulae are applied. As an alternative to direct sampling, for example with sand traps, the bed-load transport can be measured indirectly by studying the movement of bedforms in the channel bed. Results of flume experiments show that in general the bed-load transport can be measured fairly accurately in this way.

It was possible to obtain a varied series of data which were usable for verification purposes from 9 locations in large and small rivers and from 3 locations in tidal areas using this bed-load transport calculation method.

These data were used to test Van Rijn's bed-load transport formula and a modified version of the Kalinske-Frijlink formula, which seemed the most appropriate formulae for application to the range from fine sand to gravel. The latter of these formulae produced the best results: the transport figure calculated using it differed by a factor of less than 2 from the value derived from the movement of ripples in 37 out of a total of 43 sets of river data (86%).

Samenvatting

In dit proefschrift zijn 5 artikelen bijeengebracht, die met elkaar gemeen hebben, dat sedimentologische aspekten van voornamelijk beneden de laagwaterlijn gelegen sedimenten van de Oosterschelde en klein- of grootschalige morfologische veranderingen met elkaar in verband worden gebracht.
Allereerst wordt aandacht besteed aan grote morfologische veranderingen in de zin van wijzigingen in de ligging van platen en geulen en daarmee gemoeide sedimentverplaatsingen die optreden in het getijsysteem van de Oosterschelde in relatie tot veranderingen in de getijdebieten van deze zeearm. Daarnaast wordt de samenhang aangegeven tussen sedimentaire strukturen van recente afzettingen van de Oosterschelde, die in enkele bouwputten waren ontsloten, met de morfologische achtergrond van hun ontstaan. Tenslotte wordt ingegaan op de samenhang van het bodemtransport en het sedimenttransport dat kan worden afgeleid uit kleine morfologische veranderingen, in de vorm van de verplaatsing van bodemribbels, en op de voorspelling van dit transport met behulp van bodemtransportformules.

Hoofdstuk 1
In dit inleidend hoofdstuk wordt voornamelijk ingegaan op de morfologische ontwikkeling van de Oosterschelde. Reeds lang voor het begin van de jaartelling was de monding van de Oosterschelde gesitueerd in het gebied tussen de eilanden Schouwen en Walcheren. Tot in de Middeleeuwen vormde de Oosterschelde de voornaamste benedenloop van de Schelde. De breedte van het toenmalige mondingsgebied was echter veel minder groot dan die van de tegenwoordige zeearm. Voornamelijk als indirekt gevolg van menselijk handelen is de komberging van de Oosterschelde vanaf de Middeleeuwen sterk vergroot. De toename van de getijstroom die dit tot gevolg had leidde tot een sterke verdieping en verbreding van het estuarium. Door de sluiting van de Grevelingendam (1964) en de Volkerakdam (1969) nam het getijvolume in het trajekt Krammer-mondingsgebied verder toe, waardoor hier sterke verdiepingen optraden. Een gedeelte van het geërodeerde materiaal werd naar zee afgevoerd. Een hoeveelheid van dezelfde orde van grootte kwam terecht in de zuidelijke tak van de Oosterschelde ter kompensatie van de omvangrijke zandwinningen die hier in de zestiger en zeventiger jaren plaatsvonden. Uit een empirisch verband tussen het stroomvoerend oppervlak van de dwarsdoorsnede van getijgeulen en het getijdebiet blijkt dat in een groot deel van de Oosterschel-

de de morfologie in 1983 zich nog niet geheel aan de veranderde hydraulische omstandigheden had aangepast.

Hoofdstuk 2
De effekten van de toename van de getijdebieten bleven de afgelopen 100 jaar niet beperkt tot de Oosterschelde zelf, maar waren ook merkbaar in de buitendelta van deze zeearm. In het nabij de monding gelegen deel van de buitendelta overheersten erosieve processen. Enkele grote, bij laagwater droogvallende platen, die hier een eeuw geleden nog werden aangetroffen zijn nu vrijwel volledig verdwenen. Verder breidden de ebscharen in het mondingsgebied zich sterk in zeewaartse richting uit. Hierdoor ontstond in 1974 een verbinding tussen de twee grootste ebscharen, de Roompot en het Westgat, hetgeen leidde tot een wijziging van de debietverdeling van de geulen in het mondingsgebied. Een deel van het in de Oosterschelde zeearm en het kustnabije deel van de buitendelta geërodeerde sediment kwam in het verder zeewaarts gelegen, distale gedeelte tot afzetting langs de rand van de ebscharen (ebschilden) en op de rand van de buitendelta.
Sedert 1960 breidde deze rand van de buitendelta zich sterk in zeewaartse richting uit waarbij plaatselijk een laag van meer dan 9 m zand werd afgezet. Naast het deltafront en de ebschilden vormden de binnenbochten van de dynamische ebgeulen de meest belangrijke afzettingsmilieus. Sedimentatie snelheden van meer dan 8 m in enkele jaren waren hier geen uitzondering.

Hoofdstuk 3
In de bouwput 'Schaar', gesitueerd op het kunstmatige eiland 'Neeltje Jans' in het mondingsgebied van de Oosterschelde was op een diepte van 10 tot 17 m beneden NAP een afzetting ontsloten die ontstaan is in zo'n dynamische ebgeul. De sedimentaire struktuur van deze afzetting bestaat voornamelijk uit grote scheefgelaagde eenheden, gevormd door bodemribbels die met de dominante ebstroom meebewogen. Uit oude hydrografische kaarten kan worden opgemaakt dat de afzettingen hoogstwaarschijnlijk dateren uit de 18e eeuw en ontstaan zijn in een kleine ebschaar die zich langs de noordelijke flank van de Roompot naar het westen verplaatste.
Een soortgelijke sedimentaire eenheid werd op een diepte van 9 tot 5 m beneden NAP aangetroffen in de bouwput voor het sluizencomplex in de Philipsdam. Het betreft hier echter geen binnenbocht afzetting van een aktieve ebschaar, maar de vulling van een passieve vloedschaar, die zich ten tijde van de aanleg van de Grevelingendam (1962–1964) aan de zuidelijke flank van het Krammer vormde.

Door de hydraulische veranderingen die deze dam teweeg bracht, onderging het Krammer een spektakulair proces van uitbochting en verdieping. In samen-

hang daarmee verzandde genoemde vloedschaar in korte tijd en ontstond de sedimentaire sequentie die in de bouwput ontsloten was.
Uit de sedimentaire strukturen kan worden opgemaakt dat de grote scheefgelaagde eenheden in beide ontsluitingen gevormd zijn door ribbels met een sinusoïdale kamlijn en een maximale hoogte van ca. 2 m. Aan de hand van dunne sliblaagjes die tijdens de stroomkentering over de ribbel werden afgezet en die in de scheefgelaagde eenheden kunnen worden herkend, kon de voortplantingssnelheid van de ribbels worden vastgesteld. Deze bedroeg voor de afzettingen in de bouwput Schaar en de ontgraving in het werkeiland van de Philipsdam respektievelijk gemiddeld 278 en 158 m per jaar. Er zijn sterke aanwijzingen dat alle ribbels die tijdens de periode van snelle sedimentatie ter plaatse van de Philipsdam ontsluiting voorbijtrokken bijgedragen hebben aan de bewaard gebleven sedimentaire sequentie.
De grote overeenkomst tussen de sedimentaire struktuur van beide afzettingen doet vermoeden dat dit ook bij de afzettingen in de bouwput "Schaar" het geval was. Dit zou neerkomen op een akkumulatie snelheid van 0.8 tot 0.9 m per maand. Uit peilingen blijkt dat dergelijke extreme waarden in dit gebied in kleinere ebscharen inderdaad mogelijk zijn.

Hoofdstuk 4
In de bouwput 'Schaar' was boven het scheefgelaagd pakket een afzetting ontsloten die ontstond bij de verzanding van een tot 11 m diepe geul die zich hier in de vorige eeuw vormde. De geulvulling bevat een 5 m dikke laag die bestaat uit een ritmische afwisseling van in oorsprong als flasers en als gelamineerde slib-zand alternaties afgeze sediment. Afzonderlijke lagen kunnen over honderden meters worden vervolgd en worden niet door erosie afgesneden. De afwisseling blijkt samen te hangen met de wisseling der seizoenen: de flaser en gelamineerde lagen korresponderen respektievelijk met het koude (winter) en warme (zomer) halfjaar. Deze relatie kan worden aangetoond aan de hand van de groei en mortaliteit van autochtone populaties van enkele veel voorkomende schelpdieren en de mate van bioturbatie, die in de gelamineerde lagen relatief groot is.
De dikte van de zomer-winter coupletten varieert van 20 tot 60 cm. De akkumulatie snelheid die hiermee kan worden berekend komt overeen met gegevens van hydrografische kaarten en korrespondeert ook met de groei van een populatie zeeklitten die in de geul leefde, zoals die kan worden afgeleid uit de opwaartse toename van de diameter van graafsporen in het sediment.

Het verschil in de fysische sedimentaire struktuur tussen de zomer- en winterlagen is het gevolg van een verschil in de kritieke bodemschuifspanning van het begin van sedimentbeweging, welke 's zomers een hogere waarde aannam. Daardoor trad 's zomers geen bodemtransport op en was er sprake van een

vlakke bodem waarop het gesuspendeerde sediment in parallelle laminaties tot afzetting kwam en gepreserveerd bleef. 's Winters kon de kritieke schuifspanning wel overschreden worden en ontstonden kleine bodemribbels waarmee een flaser gelaagdheid werd opgebouwd.
De grotere binding tussen de zandpartikels die de toename van de kritieke waarde van de schuifspanning 's zomers veroorzaakte hangt waarschijnlijk samen met het hogere organisch stofgehalte van het slib dat gedurende de zomer bezinkt.

Hoofdstuk 5
In dit hoofdstuk wordt aandacht besteed aan de relatie tussen het bodemtransport, het sedementtransport dat gemoeid is met de verplaatsing van bodemribbels en de stroomsnelheid.
Betrouwbare direkte metingen van het bodemtransport in het veld zijn nauwelijks voorhanden. Dit wordt vooral veroorzaakt door problemen die een nauwkeurige en representatieve bemonstering met zich meebrengt. De verifikatie van bodemtransportformules is daarom voornamelijk op resultaten van experimenten in stroomgoten gebaseerd. Dergelijke proeven hebben als nadeel dat ze betrekking hebben op zeer ondiep water – hooguit enkele decimeters – waarvan niet mag worden verwacht dat ze representatief zijn voor de meeste natuurlijke situaties met waterdiepten in de orde van meters, waarop de formules worden toegepast.
Als alternatief voor de direkte bemonstering, met bijvoorbeeld zandvangers, kan het bodemtransport indirekt worden gemeten aan de hand van de ribbelverplaatsing. Uit resultaten van gootproeven blijkt, dat op deze wijze het bodemtransport in het algemeen vrij nauwkeurig kan worden bepaald.
Met op dergelijke wijze berekende bodemtransporten kon van 9 lokaties in kleine en grote rivieren en van 3 situaties in getijdegebieden een gevarieerde reeks van voor verifikatie bruikbare gegevens worden verkregen.
Hiermee zijn de bodemtransportformule van Van Rijn en een aangepaste versie van de formule van Kalinske-Frijlink, die het meest voor toepassing in het bereik van fijn zand tot grind in aanmerking leken te komen, beproefd. Laatstgenoemde formule gaf de beste resultaten: bij 37 van in totaal 43 sets van riviergegevens (86%) week het met de formule berekende transport minder dan een faktor 2 af van de uit de ribbelverplaatsing afgeleide waarde.

1. Introduction

In this thesis a number of papers on sedimentological and morphological topics are brought together in which, as a common theme, morphological changes in recent, mainly subtidal, environments are discussed. Attention is paid to small-scale periodic bed-level changes that are related both to the migration of bedforms and to large-scale changes in channel and shoal systems.

In chapter 2 the morphological impact of a small increase in tidal discharges through the mouth of the Oosterschelde to the ebb-tidal delta of this inlet is discussed. In chapter 3 and 4 the preservation of sedimentary structures of recent subtidal deposits studied in some of the construction docks of the Delta Project in the Oosterschelde is related to hydrographic changes.

The author not only studied sediment dynamics in terms of morphological change and sedimentary products: more fundamental sedimentological research was done on the physical processes that create morphological change and sedimentation. This research is reported in the final chapter, which deals with predicting the bed-load transport and the sediment transport involved in the migration of bedforms in fluvial and tidal environments.

In chapter 2, 3 and 4, aspects of morphological change in the Oosterschelde are described and related to the subjects discussed. Below, by way of introduction, the role of these morphological changes in the evolution of the Oosterschelde tidal system will be outlined.

Evolution of the Oosterschelde tidal system

The southwest part of the Netherlands is almost completely blanketed by Holocene sediment, which is 20 to 40 meters thick in places. It developed under the influence of the rising sea level, on a slightly westward dipping surface of Pleistocene fluvial deposits and aeolian coversands (HAGEMAN, 1969). Most of the deposit was laid down behind a transgressive coastal barrier (PONS ET AL., 1963). The sequence is divided into two clastic units (Calais and Dunkirk) composed of fine siliciclastic sands and finer sediments that were deposited during periods of marine incursions through the barrier, separated by a peat layer (Holland Peat). Peat formation in this area started about 4500 BP (VAN RUMMELEN, 1978). Under the influence of the Dunkirk marine incursions

most peat accumulation stopped in Roman times. However, peat formation continued locally until early mediaeval times. During the main period of peat accumulation the area was made up of an extensive marsh, protected from the sea by an almost closed barrier and crossed by the estuary of the Scheldt river. For most of the period the main outlet of the Scheldt river seems to have been at the present location of the Oosterschelde mouth. (VAN RUMMELEN, 1978; ZAGWIJN, 1986).

Until the Middle Ages the Oosterschelde course remained the main distributary of the Scheldt river. At the same time it was part of a system of tidal inlets and channels formed by the latest Dunkirk incursions, which to some degree were connected with each other and with the Rhine-Meuse-Scheldt fluvial systems. Presumably, the early Oosterschelde consisted of only one major channel, which was relatively narrow as compared with its present dimensions (WILDEROM, 1964). Fig. 1.1A shows a palaeogeographic reconstruction of the situation around 800 AD. Between 1100 and 1300 AD most of the salt marshes bordering the estuary were embanked (WILDEROM, 1964; 1968; DEKKER, 1971. See also Fig. 1.1B). Within the embanked areas natural accretion of silt and clay ceased and the surface of these polder areas fell significantly, because the peat and clay settled as a result of the artificially improved drainage. Large areas were lowered even more by the extensive stripping of surficial peat layers, mainly for mining the salt, that was deposited during the Dunkirk inundations. Finally, a lowering of the land relative to the sea level resulted from tectonic drop and a continuing rise in sea level. The rate of this relative sea-level rise will not have been much different from the present rate in this area, which according to measurements at tidal gauges is in the order of 0.2 m per century (DE RONDE, 1983).

Because of the lowering of the land it became exceedingly difficult to restore storm induced dike-bursts. Mainly for this reason but also because of political reasons and a decline in the economic prosperity of the region which resulted in a serious lack of financial means to improve or even maintain the embankments, by the end of the Middle Ages considerable areas remained inundated after storm floodings and changed into a tidal landscape of shoals and channels. As a result the tidal prism of the estuary increased. At the entrance of the estuary the effects of this increase started to become apparent after 1400 AD when the main channel of the Oosterschelde developed a large meander. This caused considerable coastal retreat in the island of Schouwen-Duiveland to the north (Fig. 1.3). During one of the most dramatic storm surge disasters in 1530, very large polderland areas neighbouring the Oosterschelde, especially in the easternmost part of the present basin, were drowned and became part of the tidal system. As a result of the basin enlargement the tidal prism of the estuary must have increased by at least 50%.

This caused a further widening of the mouth of the Oosterschelde accompanied

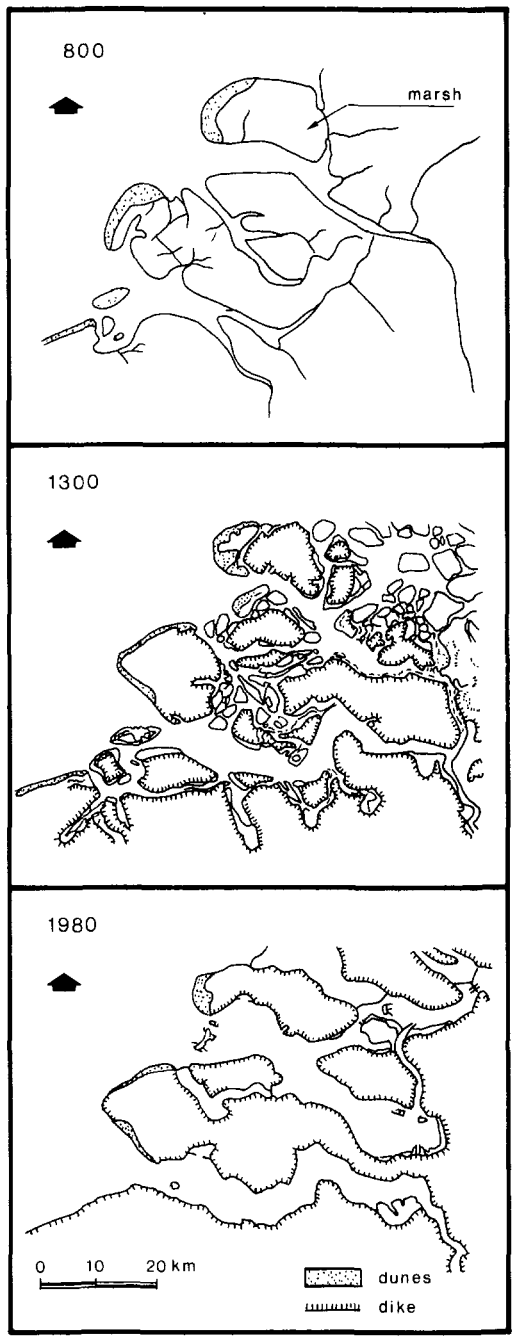

Fig. 1.1 Embanked areas and marshes (some tidal) in the southwestern part of the Netherlands in 800 AD: after THURKOW ET AL. (1984); 1300 AD: after BEEKMAN (1952), and at present

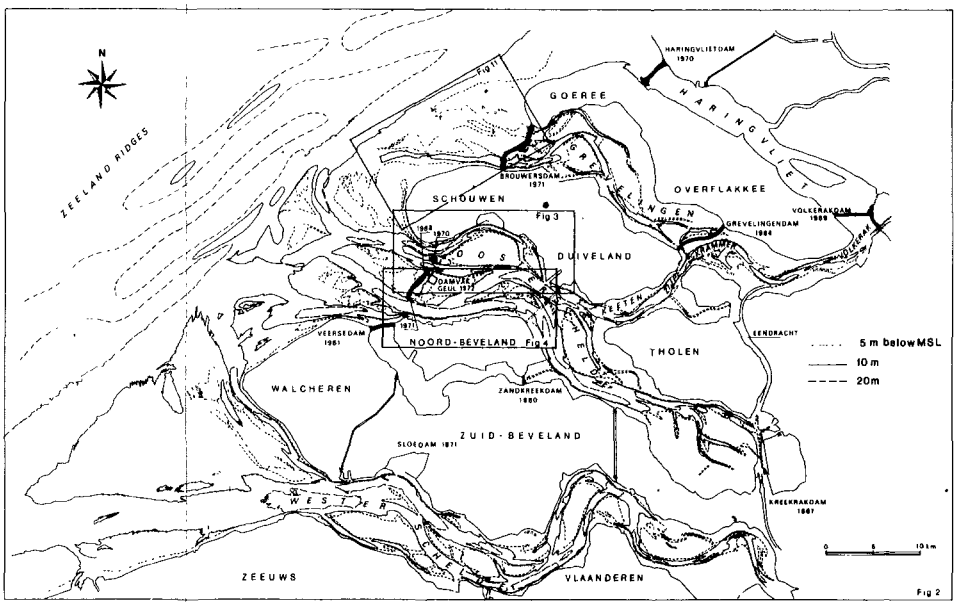

Fig. 1.2 Bathymetry of the southwestern Netherlands with dates of the main channel closures (situation in 1980)

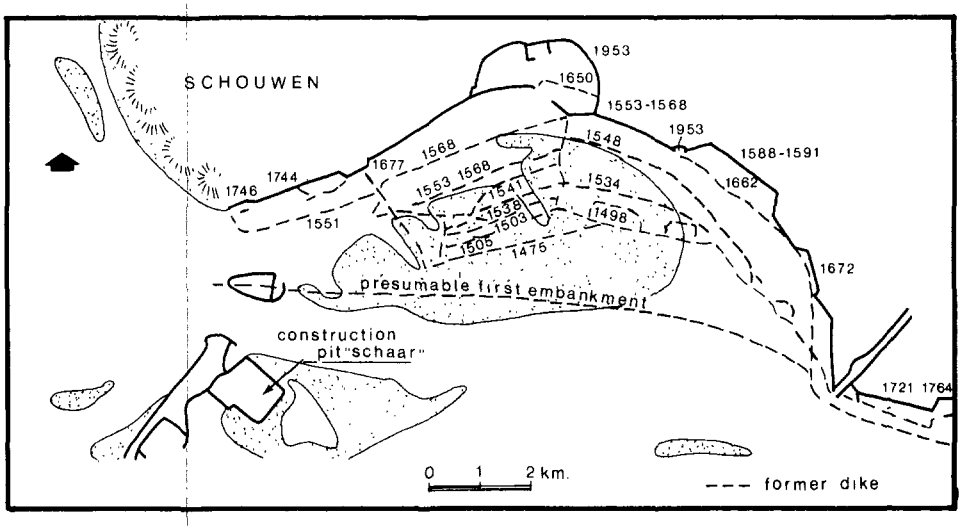

Fig. 1.3 The retreat of the southern coastline of Schouwen (modified after WILDEROM, 1964; for location see Fig. 1.2)

by the gradual development of a second major channel (the Roompot) in the southern part of the inlet (Fig. 1.4). Not only did this second channel accommodate the extra tidal discharges caused by the widening of the inshore tidal basin; it must also have taken over some of the Hammen discharge, since the Schouwen coastal retreat ceased after 1600 AD. A chart published in 1637 ('Comitatus Zeelandiae Novissima Descriptio Auct.Petrum Verbist') indicates a maximum depth in the Roompot of 10 m. On a map of 1670 ('De Cost van Zeelandt begrijpende in sich de gaten als van de Wielingen, ter Veere Zierikzee, Brouwershaven, Goeree en de Maes') the maximum depth indicated has increased to 17 m. On both maps the maximum depth of the Hammen is 17 m.

In the 18th century, apart from the widening of the mouth of the estuary a further deepening of the channels occurred. On the first detailed hydrographic map covering the Oosterschelde, which shows the situation at the beginning of the 19th century ('Carte réduite des côtes des Pays-Bas', by Beautemps-Beaupré, published in 1817), the Roompot channel is shown to reach a depth of 30 m, which is 13 m deeper than indicated on the map of 1670. The depth of the Hammen channel increased by 10 m to 27 m.
In the 1970's in the construction dock of the sills of the Storm Surge Barrier in the mouth of the Oosterschelde at a depth of 10 to 17 m below Mean Sea Level deposits that were probably formed in the 18th century in a secondary ebb channel branching off the Roompot. The morphodynamic background of their origination are described in chapter 3.

In the Middle Ages the present tidal connection through the Zijpe channel consisted of a broad shoal area with some shallow channels of minor importance (Fig. 1.1B); the northern branch of the present day Oosterschelde (the Krammer-Volkerak area, see Fig. 1.2 for location) was part of the Grevelingen tidal system.

In 1575, during the 80-year war Spanish-Dutch war, Spanish troops succeeded in wading through the Zijpe area (DE BRUIN, 1953). This situation of apparent tidal watershed between the Oosterschelde and Grevelingen tidal basins lasted until the beginning of the 18th century. Then, quite suddenly, erosion started and before the century was out a depth of 24 m had been sounded. This scouring of the Zijpe channel points to a drastic increase in the influence of the Oosterschelde tidal system in this area. The expansion can be explained by considering the implication of further deepening of the estuary upon the propagation of the tide: since the velocity of propagation of a tidal wave travelling through an inlet is proportional to the square root of the water depth, in the Zijpe area the dramatic deepening of the estuary must have caused an important advancement of the tide coming from the Oosterschelde. Thus it is hypothesed that south of

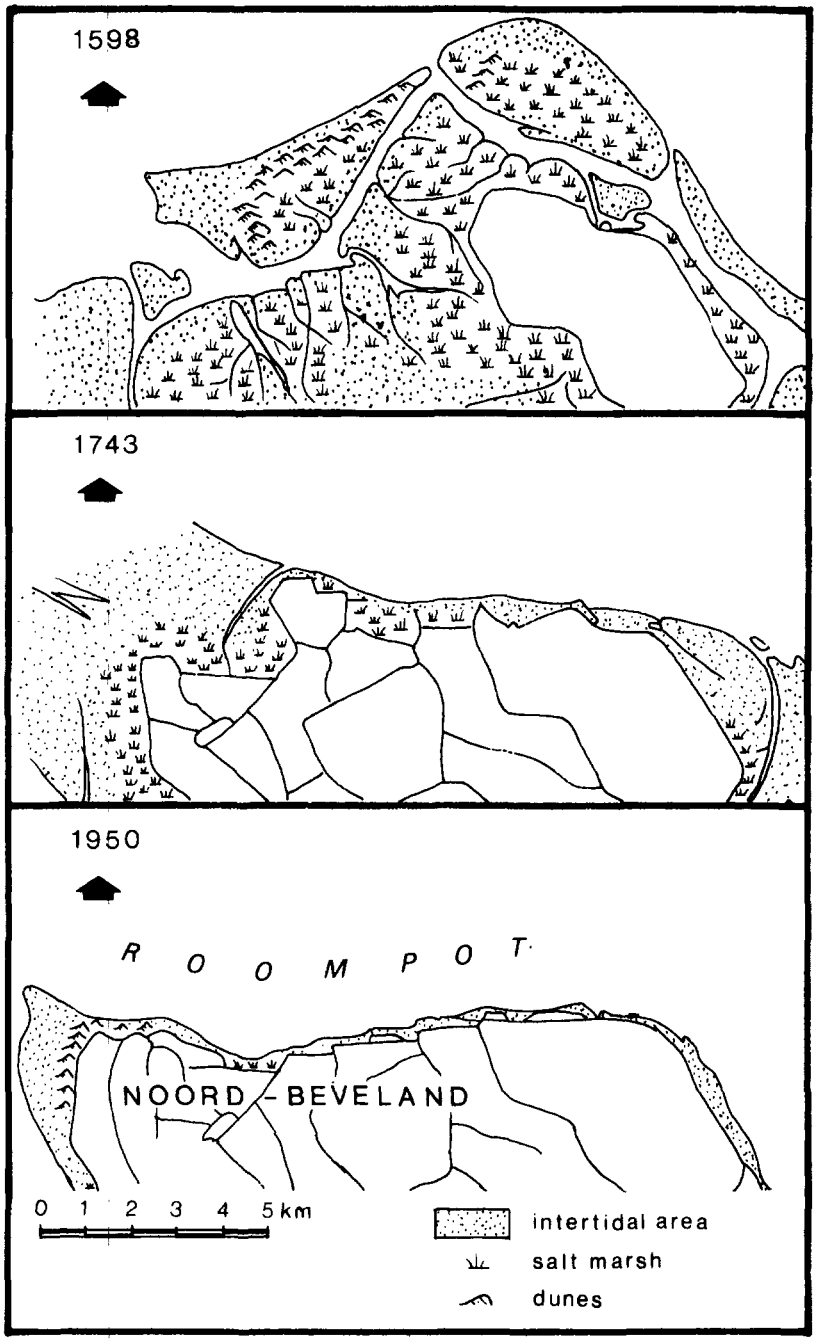

Fig. 1.4 Gain and loss of land in the northern part of the isle of Noord-Beveland (modified after DE BRUIN & WILDEROM, 1961; for location see Fig. 1.2)

the original 'watershed' in the Zijpe the water level did rise and fall sooner than further north, resulting in a tidal water movement through the Zijpe area dominated by the tide in the Oosterschelde. By capturing part of the tidal discharges through the Krammer-Volkerak area the tidal prism of the Oosterschelde increased again, causing further scouring and deepening of the major channels. This in turn can explain the further expansion of tidal influence of the Oosterschelde tidal system into the Krammer-Volkerak area, causing the rapid scouring of the Zijpe channel.

The expansion of the tidal system of the Oosterschelde continued in the 19th and 20th century. Because a further widening was hindened by improved coastal defense works erosional processes mainly resulted in a further deepening of the western part of the sea-arm and the northern tributary. By 1960 the Roompot and Hammen channels had reached depths of 51 m and 35 m, respectively. In the Zijpe channel the maximum depth increased to 38 m. Large amounts of sediment were transported seawards and contributed to an expanding ebb-tidal delta. This process is described in detail in chapter 2.
In the construction dock of the Oosterschelde Storm Surge Barrier on top of the sediments which presumably originated during the 18th century a channel-fill deposit was exposed which, according to hydrographic maps, was laid down in the period 1880-1940. This deposit (which mainly consists of a sequence of seasonal rhythmites) and its hydrographic background, are described in chapter 4. The growing influence of the Oosterschelde tidal system in the Krammer-Volkerak area reduced the tidal prism of the Grevelingen inlet. By way of counteraction in the Grevelingen basin processes of sedimentation dominated: according to calculations based on hydrographic charts made in the period 1872–1962 a net deposition of 0.3 10^8 m^3 occurred (HARING, 1964). After 1933 the reduction of tidal prism becomes also noticeable in a gradual degradation of the outer delta of the Grevelingen sea-arm: along the delta front erosive processes dominated, whereas some siltation occurred in the channels of the proximal part of the tidal delta.

Until mediaeval times the Oosterschelde remained the major course of the Scheldt river. However, during the 14th century the shipping route to Antwerp started to divert to the Westerschelde (DENUCÉ, 1933), indicating the growing importance of the Westerschelde as a distributary of the Scheldt river.
In the 16th century the channel connecting the Oosterschelde with the Scheldt river through the Kreekrak (see Fig. 1.2 for location) silted up, becoming shallow enough to be waded through at low tide. The abandonment of the Oosterschelde as a river distributary was finally completed artifically in 1867 and 1871, when dams were built to shut off the last connections with the Westerschelde.

Hydraulic implications of the channel closures of the Delta Project before 1983

After 1959 the tide characteristics of the Oosterschelde tidal system changed, as a result of the Delta Project works. This project envisions the closure or partial closure of the inlets of the Veerse Gat, Oosterschelde, Grevelingen and Haringvliet and the construction of a number of secondary dams within the tidal basins. A review of closure dates is presented in Fig. 1.2.
The hydraulic situation just before the start of the first closure is well documented by series of discharge measurements at several transects of the tidal system. The same holds for the hydraulic change caused by the closure of the Grevelingen dam and of the Volkerak dam. In Fig. 1.5 the tide-integrated results of some discharge measurements (ebb and flood volumes) have been compiled. The data presented refer to conditions of mean tidal range and average discharge of the rivers Rhine and Meuse.
The initial situation (1959) was characterized by an important surplus of flood discharge in the Zijpe area, which was compensated for by an ebb surplus in the Grevelingen and Haringvliet. As a result, only small amounts of fresh water from river discharge penetrated into the original Oosterschelde basin. A measurable dilution only occurred at periods of high river discharge (PEELEN, 1967).
As a result of the construction of the Grevelingen dam (1962–1964) part of the tidal prism of the Grevelingen sea-arm was added to the Oosterschelde tidal system. At the entrance of the Grevelingen inlet some of the loss in tidal discharge was compensated for by an 8% increase of the tidal range in the Grevelingen basin, caused by an improved resonance of the tidal wave in the remaining basin. For the same season, the closure of the Volkerak in 1969 caused an important increase in the tidal range of the northern tributary of the Oosterschelde, amounting to more than 50% in the northernmost part of the channel near the closure dam.
This resulted in an increase in the tidal prism of the Oosterschelde. At the mouth of the Oosterschelde the ebb volume increased by about 8%. The increase in the flood volume was about 6%. Also indicated in Fig. 1.5 are the yearly averages of the tidal range in 1959, 1968 and 1972. It appears that changes in the tidal range are not restricted to the Oosterschelde and Grevelingen, but have also occurred at stations like Flushing and Westkapelle,which are situated practically beyond the influence of the various closures of the Delta project.
These changes are mainly related to the 18.61 year cyclic rotation of the plane of the lunar orbit with respect to the ecliptica, which along the Dutch coast causes a tidal variation with an amplitude of about 3% of the tidal range (DE RONDE, 1983).
Minima of this variation were reached in 1932, 1950 and 1969. Thus, in the period 1969 to 1978, after the closure of the Volkerak, the tidal range at the

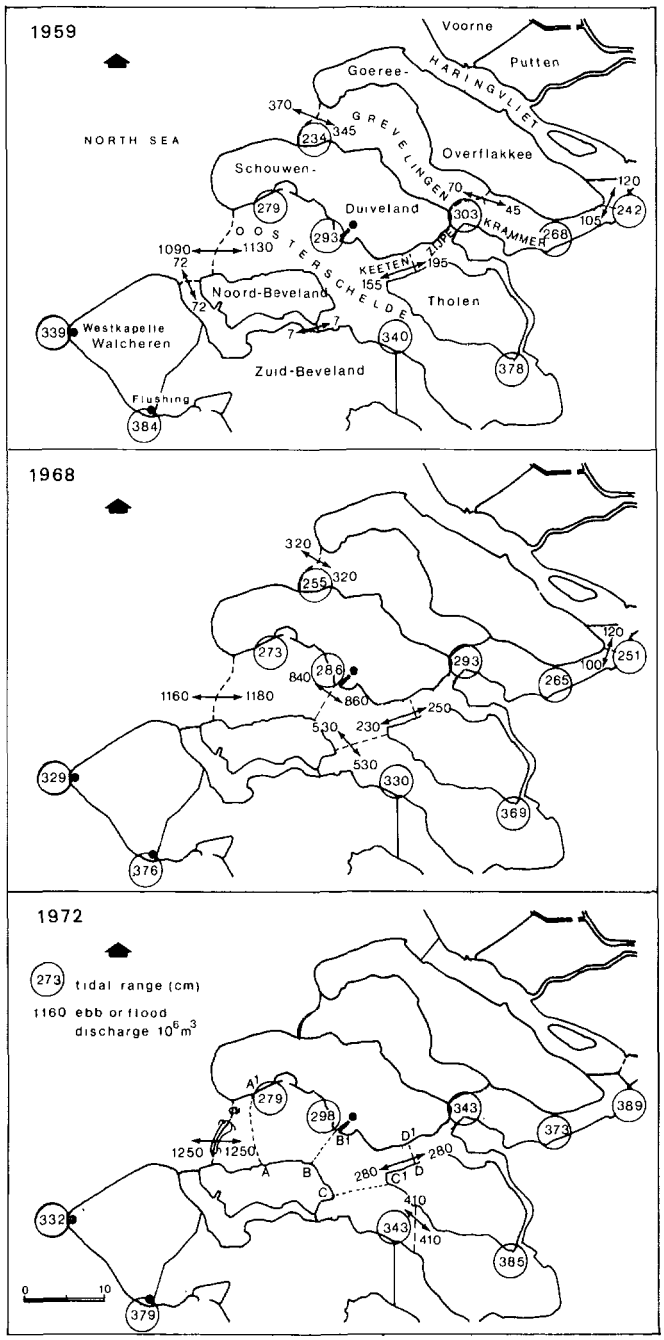

Fig. 1.5 Changes of ebb and flood discharges and of tidal range in the Grevelingen and Oosterschelde tidal systems after 1959

entrance of the Oosterschelde increased by about 3% (see Fig. 1.6).
Since the magnitude of the tidal prism of the Oosterschelde is proportional to the tidal range it is suggested in chapter 2 that this increase of 3% would result in a similar increase in the value of the mean tidal prism in this period.
However, results of accurate measurement of basin geometry executed in 1968 and 1983 indicate, that the effect of the increase in tidal range was counteracted by a reduction of the same magnitude in the storage capacity of the basin.
This reduction mainly resulted from the construction of a number of artificial islands and from topographical changes related to the canalization of the Eendracht channel.

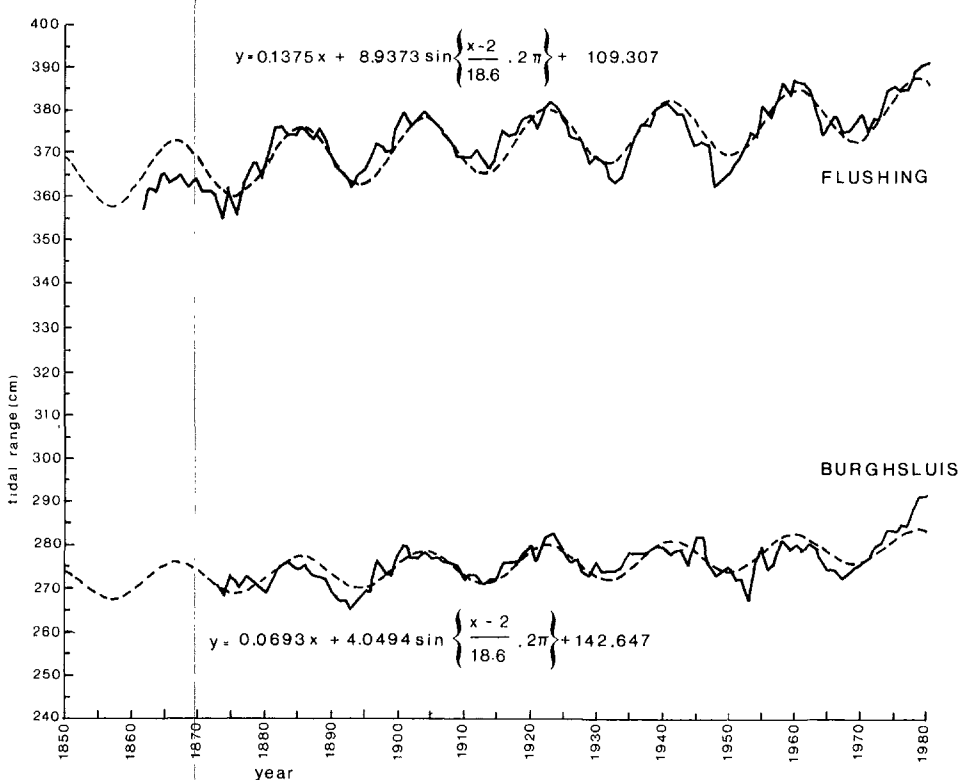

Fig. 1.6 The tidal range at Flushing and Burghsluis during the past century. Data kindly provided by Mr. J. G. de RONDE, Rijkswaterstaat, The Hague

The reaction of the sediment balance to hydraulic change

Using data from large number of tidal inlets along the Atlantic coast of North America O'BRIEN (1969) found a constant ratio between tidal prism (P) and

the cross-sectional area of the inlet entrance below Mean Sea Level (A_c). This relation can be written as

$P = 13158\ A_c$ $(m^3\ tide^{-1})$

In the same way a proportionality factor 12195 was found by VAN DER KREEKE & HARING (1979) for some tidal inlets in the southwestern part of the Netherlands. Using this relation and data of hydrographic charts, plus the results of the discharge measurements mentioned above, the tidal prism of the Oosterschelde system have been estimated to have increased by 25% since 1872 (for further details, see chapter 2).
Data from the Westerschelde indicate that approximately the same relation is valid for cross-sections within that estuary (DE JONG & GERRITSEN, 1984):

$EV = 12800\ A_c + 12.6\ 10^6$ $r = 0.991$

in which EV = ebb volume $(m^3\ tide^{-1})$ r = regression coefficient

For conditions of fine sand, such as found in the Dutch tidal waters, similar relations also hold for individual channels in a wide range of tidal situations for individual channels in the Westerschelde and the Dutch Wadden Sea, and DE JONG & GERRITSEN (1984) found:

Westerschelde:
ebb-dominated channels : $EV = 13000A_c + 21.1\ 10^6$ $r = 0.949$
flood-dominated channels: $FV = 13000A_c + 23.2\ 10^6$ $r = 0.989$

Waddenzee:
ebb-dominated channels : $EV = 13500A_c + 1.4\ 10^6$ $r = 0.987$
flood-dominated channels: $FV = 14400A_c - 5.2\ 10^6$ $r = 0.992$

in which FV = flood volume $(m^3\ tide^{-1})$

For the present analysis, data from discharge measurement carried out in a number of transects across the mouth of the Grevelingen and the Oosterschelde in 1959 and within the Oosterschelde sea-arm in 1982–1983 were used.
The results are presented in Fig. 1.7. Note that the relation found does not differ significantly from the ratio of inlet cross-section and tidal prism found by VAN DER KREEKE & HARING (1979). Therefore, it is concluded that the latter ratio also holds for inshore cross-sections of the Oosterschelde tidal system.
The morphological response to the hydraulic change initiated by the Delta project works was studied using detailed sounding maps of the area, which were

made almost annually from 1959 onwards. In this present analysis the maps of the Grevelingen and Oosterschelde areas made in 1960, 1965, 1970, 1975, 1980 and 1983 were used. In those years the intertidal areas were also surveyed. My calculations used interpolated depth values in a regular 200 × 200 m grid.

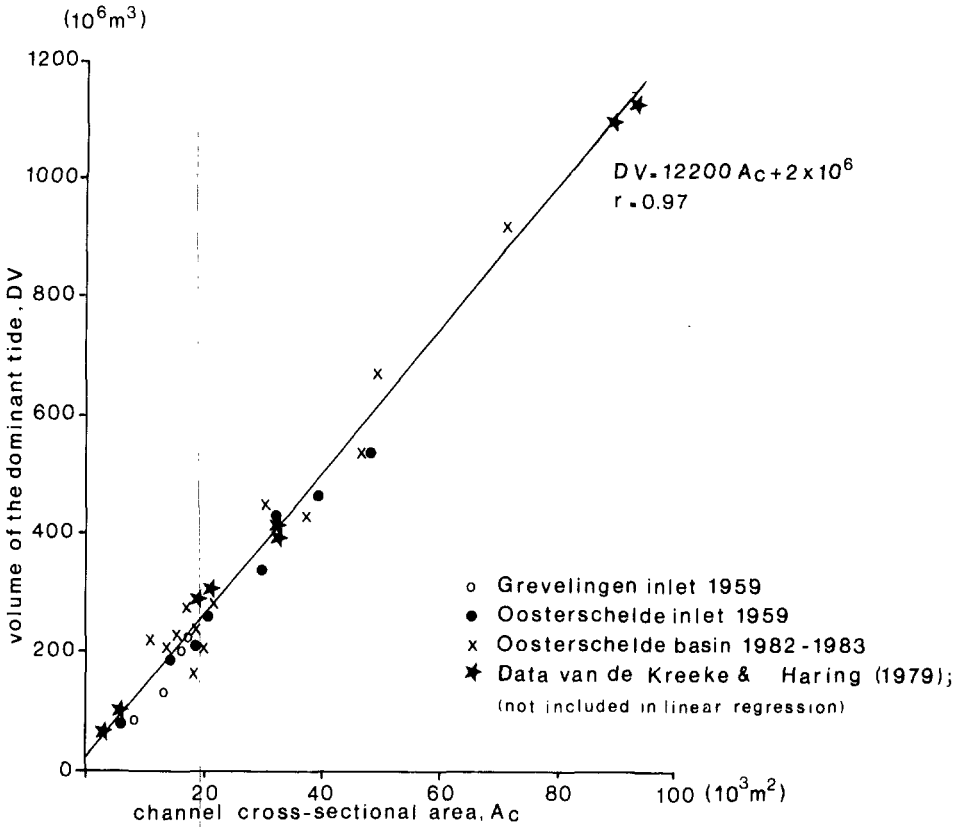

Fig. 1.7 Volume of the Dominant Tide (DV) as a function of Channel Cross-sectional Area below Mean Sea Level (A_c)

In the distal part of the outer deltas a grid of 400 × 400 m was used. Some general information on the soundings may be found in chapter 2; part of the grid schematization is shown in Fig. 1.4 of that chapter.
As is shown in Fig. 1.9 the area considered comprises the tidal system of the Oosterschelde and Grevelingen, because it includes both the inshore basins as well as the offshore tidal deltas. Using the interpolated depth values per grid square, the net erosion and sedimentation of the whole area were calculated for each of the periods between the survey years successively. To the resulting balance was added the amount of sediment that was removed from the area by

dredging activities. In this way a 'natural' budget of overall gain or loss of sediment was obtained. The results are presented in Fig. 1.8. It appears that the system as a whole is reasonably well-balanced in the sense that net natural sediment gain from or loss to the surrounding environments is small. The final results over the 1960–1983 period of a gain of 34 10^6 m^3 or a raise of 0.036 m is not significant when spread over the whole area of 955.4 10^6 m^2 because it could reflect the inaccuracy of the data used.

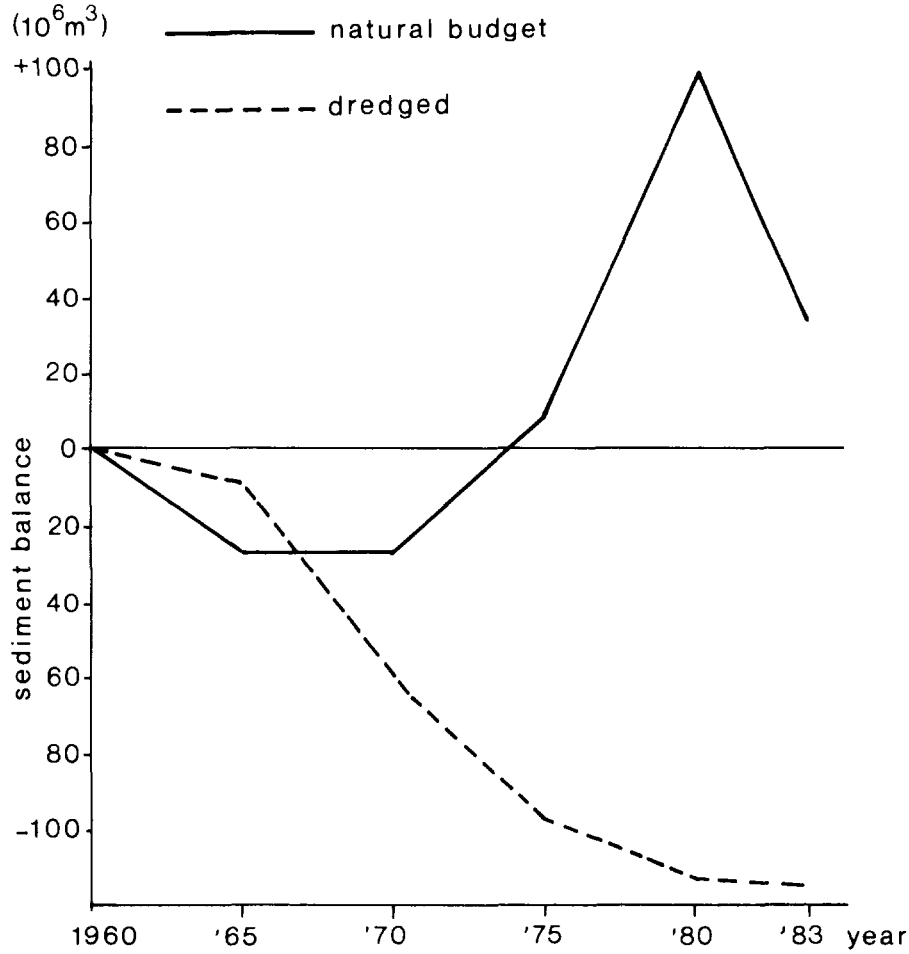

Fig. 1.8 Sediment budget of the Oosterschelde and Grevelingen tidal systems 1960–1983

The picture in 1980, however, was anomalous. This remarkable deviation from the general trend apparently resulted from some relatively large systematic errors incurred when the map makers reduced the sounded depths to the Ordnance Datum. I found these errors in the soundings of the Outer Delta areas

and in the levellings of some inshore shoals and therefore decided to exclude1980 from further calculations.
Note that the unreliability of the 1980 data came to light only after indications of serious errors arose during my analysis of the sediment budget. The data on the sediment budget of the outer delta of the Oosterschelde were published (chapter 2) before I had discovered the discrepancy. From the present data record of 1975 and 1983 it is now obvious that the use of 1980 data in that earlier paper resulted in an overestimation of the rate of deposition in the ebb-tidal delta of the Oosterschelde in the period 1975–1980.

To investigate the impact of hydraulic change on the internal sediment balance of the Oosterschelde and Grevelingen tidal systems, the area was divided into a number of segments that represent the inshore branches of the systems and the proximal and more distal parts of the ebb-tidal deltas. The results of the calculations are presented in Fig. 1.9. Within the western part of the Oosterschelde and its northern branch it, the reaction to the increase in tidal discharges is obvious: the closure of the Grevelingen dam in 1964 and resulting increase in tidal discharges in the Krammer-Zijpe area caused a considerable erosion and widening of these channels (Fig. 1.9B).
This process is described in detail for the Krammer area in chapter 3. The material eroded was partly deposited on both sides of the reach that had the largest relative increase of tidal discharges: the Keeten and the Volkerak areas. The closure of the Volkerak dam in 1969 caused erosive processes to continue and to extended to the Keeten area (Fig. 1.9 C–D).
To illustrate the process of channel widening and deepening in the various parts of the Oosterschelde, the change in profile of some characteristic cross-sections is shown in Fig. 1.10.
After 1959 the ebb and flood volumes in the western part of the Oosterschelde increased by about 10% (see Fig. 1.5). Calculations using with the grid data on depth values indicate that the water content below Mean Sea Level of the latter area increased by 5%.

Given that cross-sectional area below Mean Sea Level (i.e. volume below Mean Sea Level) is proportional to tidal discharge, in 1983 this area had not yet adjusted morphologically to the hydraulic change caused by the closure of the Grevelingen and Volkerak dams. In the Zijpe-Krammer area the relative increase in the content below Mean Sea Level was of about the same magnitude as that in tidal volume, and this indicates that a state of dynamic equilibrium has been achieved there. In the Keeten area, however, only 10% of the morphological adjustment has been reached. This is probably because the subsoil of the Keeten channel, which consists of clayey material of Tiglian age (lower Pleistocene), is not easily erodible.

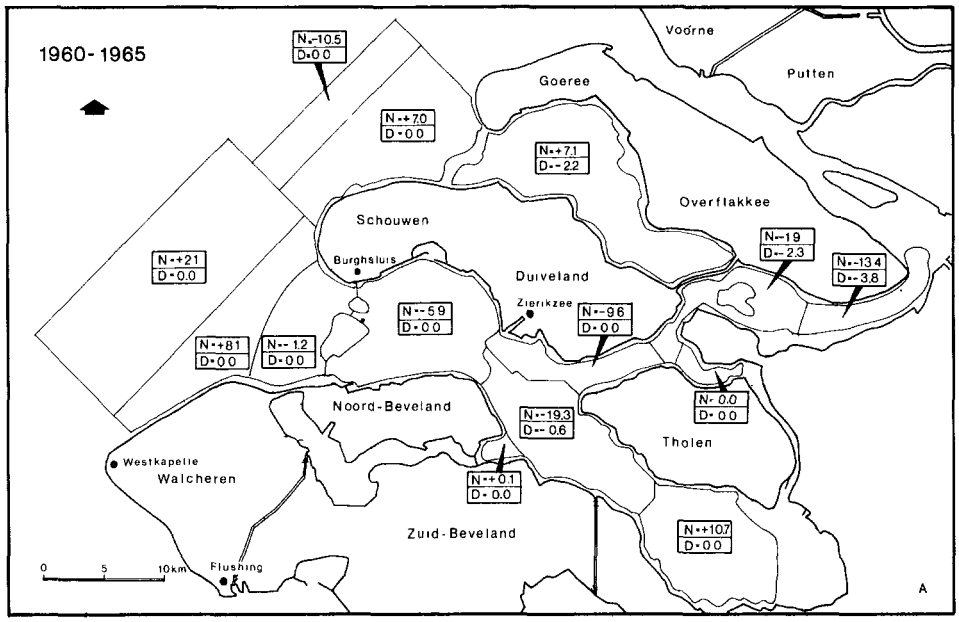

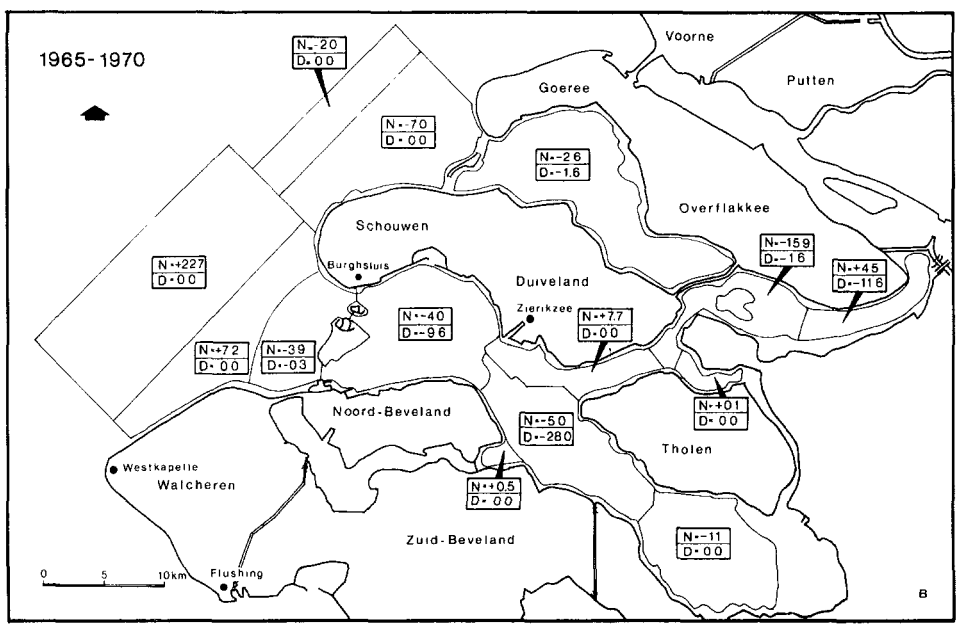

Fig. 1.9 Sediment budgets of the various parts of the Oosterschelde and Grevelingen tidal systems since 1960; Sediment gain in 10^6 m^3: N = by natural processes; D = by dredging

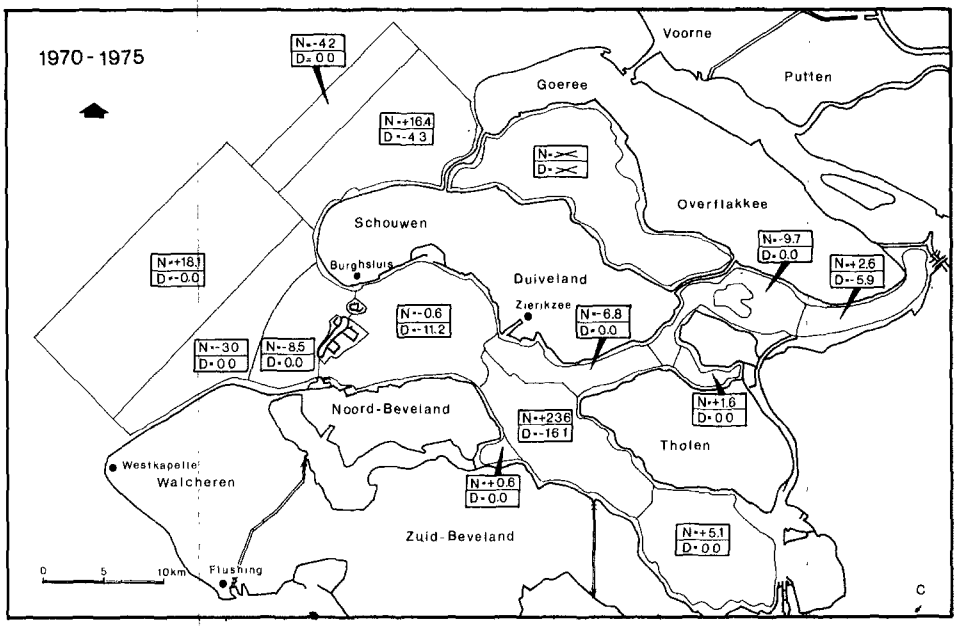
1970 - 1975
N=-42
D=0.0
N=+16.4
D=-4.3
N=><
D=><
N=+18.1
D=-0.0
N=-3.0
D=0.0
N=-8.5
D=0.0
N=-0.6
D=-11.2
N=-6.8
D=0.0
N=-9.7
D=0.0
N=+2.6
D=-5.9
N=+1.6
D=0.0
N=+23.6
D=-16.1
N=+0.6
D=0.0
N=+5.1
D=0.0
Voorne
Putten
Goeree
Overflakkee
Schouwen
Burghsluis
Duiveland
Zierikzee
Noord-Beveland
Tholen
Westkapelle
Walcheren
Zuid-Beveland
Flushing
0
5
10km
C

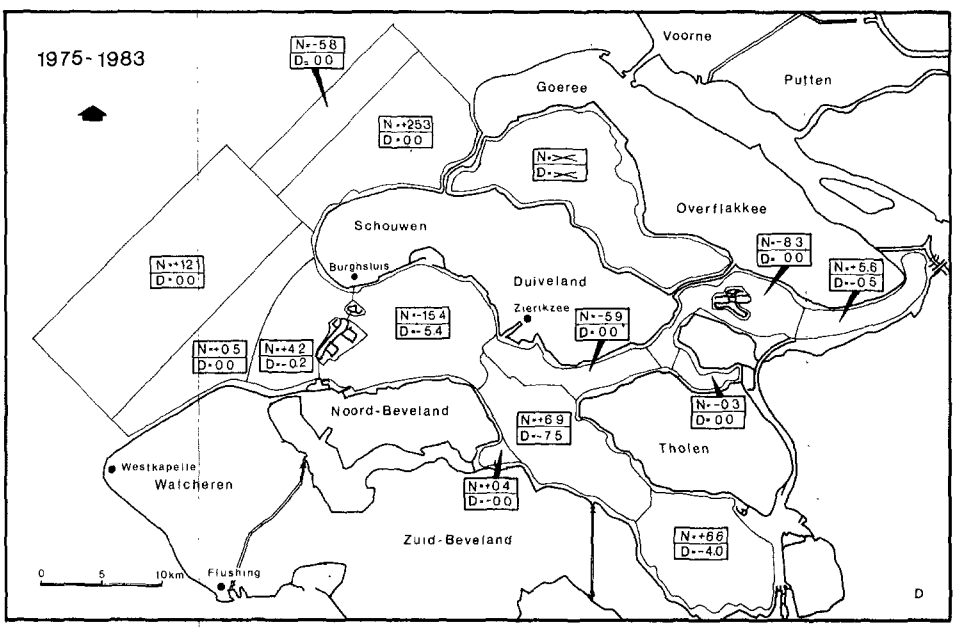
1975 - 1983
N=-5.8
D=0.0
N=+25.3
D=0.0
N=><
D=><
N=+12.1
D=0.0
N=+0.5
D=0.0
N=+4.2
D=-0.2
N=-15.4
D=-5.4
N=-5.9
D=0.0
N=-8.3
D=0.0
N=+5.6
D=-0.5
N=-0.3
D=0.0
N=+6.9
D=-7.5
N=+0.4
D=-0.0
N=+6.6
D=-4.0
Voorne
Putten
Goeree
Overflakkee
Schouwen
Burghsluis
Duiveland
Zierikzee
Noord-Beveland
Tholen
Westkapelle
Walcheren
Zuid-Beveland
Flushing
0
5
10km
D

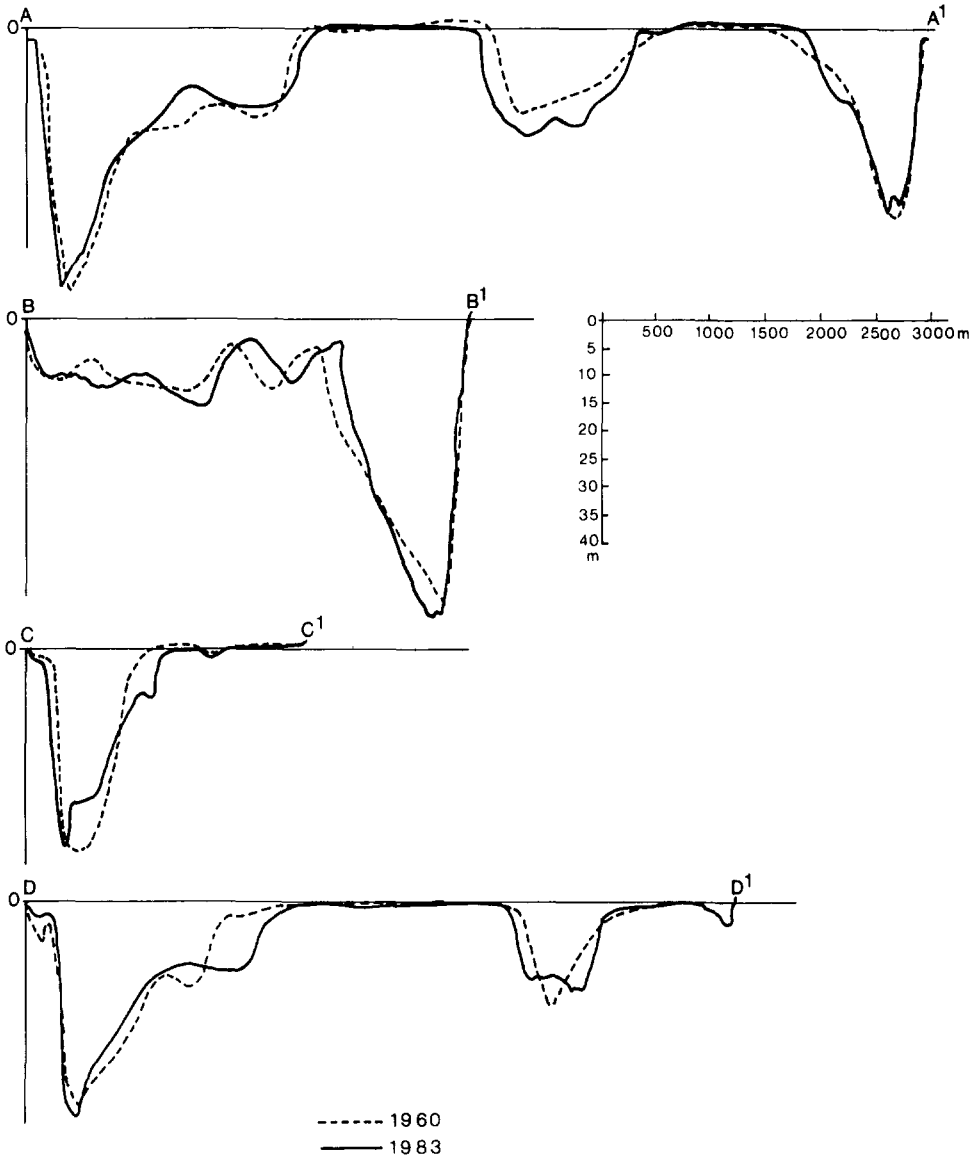

Fig. 1.10 Changes in some cross-sections of the Oosterschelde in the period 1959–1983. For location, see Fig. 5

Part of the sediment eroded within the basin has been transported seaward and has contributed to a continuing expansion of the ebb-tidal delta of the Oosterschelde (see also chapter 2). In contrast to this the closure of the Brouwersdam resulted in an acceleration of the process of degradation of the outer delta of the Grevelingen inlet. The original tidal channels formed by the in- and offshore

movement of the tide through this inlet now become filled in. Close to the barrier the channel fill deposits mainly consist of mud and in some places a layer of 7 m of this material has already formed. The delta front is subject to erosion, especially in the zone between the isobath of 10 and 4 m below mean Sea Level. The eroded sand is transported in an onshore direction, where part of it is temporarily stored in an elongated transgressive bar, which lies parallel to the strike of the delta front and is locally exposed at low tide (see Fig. 1.11). This onshore transport of sediment could be explained by the asymmetric orbital motion of shoaling waves, because the stronger onshore motion is more effective in transporting the bed material (SILVESTER, 1974; KOMAR, 1976).
The sediment transport mainly consists of well-sorted fine sands with a median diameter of about 200 microns. Therefore, by far most of the sediment is transported as suspended load. As will be shown in chapter 5 the sediment transport involved in the migration of ripples or dunes equalizes about the bed-load transport. From measurements of the dune migration and the suspended load transport in a channel of the Oosterschelde it was deduced that the bed-load transport accounted for only about 5% of the total sediment transport by the tidal currents (VAN DEN BERG, 1985). Huge amounts of sediment are transported back and forth with the tide; the sediment transport involved in the morphodynamic change of channels and shoals certainly is one order of magnitude smaller. Note, that the resultant sediment transport from one compartment of the tidal system to another, discussed in this paper, will even be smaller. Nevertheless, this resultant transport on a yearly base still refers to millions of cubic metres.

Discussion and conclusions

Since Roman times the tidal prism of the Oosterschelde has increased dramatically. As a result erosional processes dominated, causing a deepening and widening of the estuary. Human interferences gradually became important; since the early Middle Ages the cause of the large hydraulic and morphological changes could even mainly be traced back to man's activity. A climax of interference was reached with the channel closures of the Delta Project. It has been found that in the last 20 years relatively small hydraulic changes caused by these works have had important repercussions in terms of morphological change and the sediment balance within the tidal systems. Compared with the net internal shift of sediment within the inshore tidal basins and connected outer deltas, the resultant sediment exchange with the North Sea shelf has been small.
In the period 1960–1983 erosion in the basins was mainly concentrated within the western part of the Oosterschelde and up into the Krammer area of the

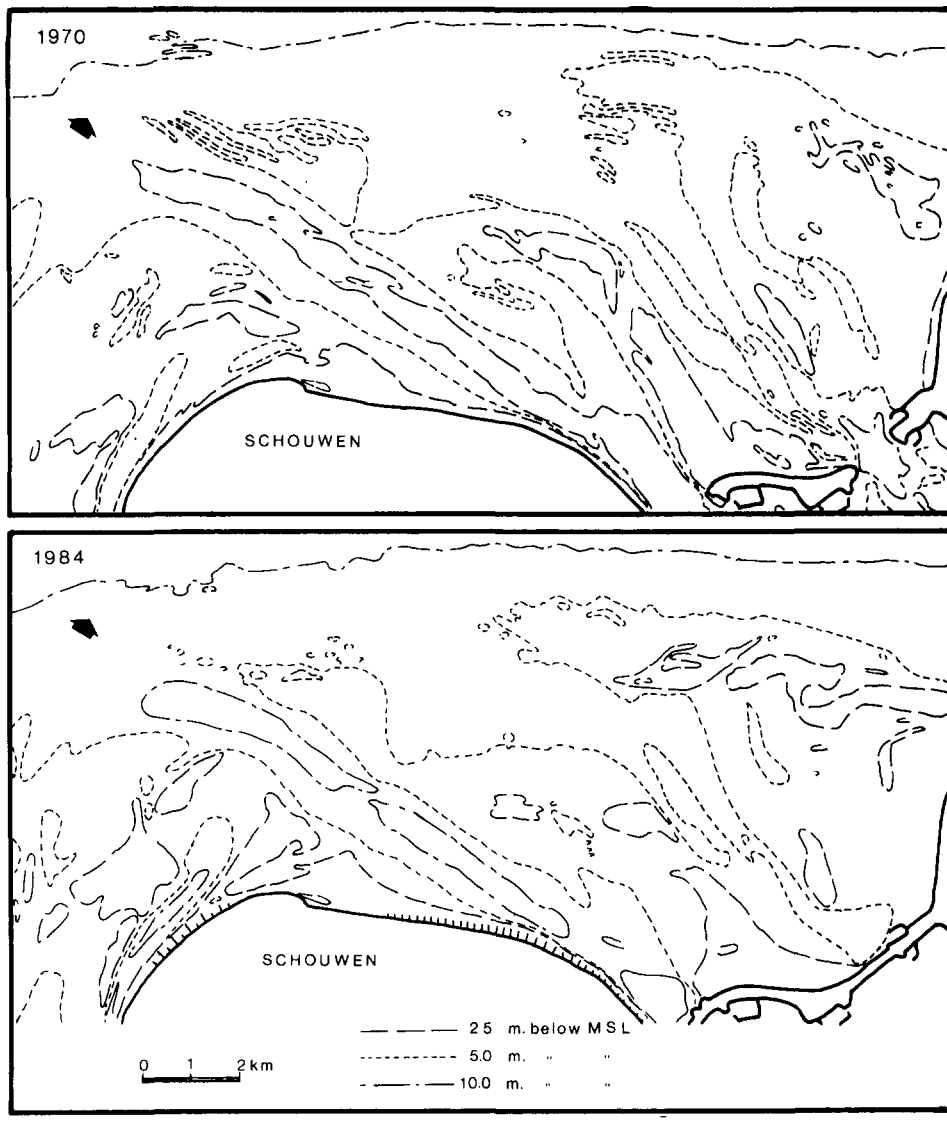

Fig. 1.11 Hydrographic change in the Grevelingen outer delta after the closure of the Brouwersdam. For location, see Fig. 1.2

northern tributary of this sea-arm. Calculations using data from a grid schematization of the area (Fig. 1.8) indicate that some of the material eroded was transported seawards: some 0.7 10^8 m^3 were added to the expanding ebb-tidal delta of the Oosterschelde. Another flux of sediment was directed to the blind arms of the Oosterschelde, near to the channel closures of the Kreekrak, the Zandkreek and the Volkerak. A relatively large share of the resulting deposits is composed of fine material with a diameter less than 50 μm (mud), which settled

in the channels close to the closure dams, as a result of the reduced current velocities. It has been estimated that in the Volkerak channel the mud forms roughly 40% of the sediment (TERWINDT, 1977).
Furthermore, since 1970 an important sediment flux has been directed to the southern branch of the Oosterschelde. This flux is favoured by the siltation of channels that have been widened by extensive dredging activities in this area.
According to my calculations using the grid data, after the closure of the Volkerak dam the inshore basin of the Oosterschelde and the proximal part of the adjacent ebb-tidal delta were deprived of some 0.5 10^8 m^3 of sediment, which is about the amount removed by dredging. This suggests that in this period no sediment loss occurred by natural processes. On the other hand, the sediment gain of 0.3 10^8 m^3 that was calculated for the distal part of the ebb-tidal delta indicates an export of sediment from the basin. Part of this discrepancy can be the unreliability of the sediment budget calculations; another part can be attributed to the fact that part of the erosion along the margins of the sea-arms was not considered because these areas were not included in the grid schematization. Bearing the latter in mind it is concluded that after 1969 the Oosterschelde still experiences a loss of sediment by natural processes.
As is shown in Fig. 1.9, after 1970 in the proximal part of the outer delta of the former Grevelingen inlet 0.3 10^8 m^3 more sediment was deposited than could have been supplied by erosion of the distal part of the tidal delta. Directional properties of the magnitude of the wave energy flux along the outer delta margin together with a gradual fining of bottom sands from the mouth of the Oosterschelde towards the outer delta of the former Haringvliet estuary and the behaviour of spoil dumped north of the latter ebb-tidal delta all point to a longshore sand transport along the outer deltas to the northeast (TERWINDT, 1973). Therefore, certainly part of the sediment trapped in the proximal part of the Grevelingen outer delta has come from the Oosterschelde. In addition, the evolution of the sediment balance of the Oosterschelde and Grevelingen tidal systems (Fig. 1.8) suggest a resultant supply of sediment from the adjacent shelf. However the accuracy of the budget calculations does not allow this to be stated with certainty.

References

BEEKMAN, A. A. 1952. Geschiedkundige Atlas van Nederland III: Zeeland.
DE BRUIN, M. P. 1953. Tussen Krammer en Keeten, Mosselkreek en het Slaak (Sint-Philipsland en omgeving). Tijdschrift K.N.A.G. Tweede Reeks, LXX: 20–34.
DE BRUIN, M. P. & M. H. WILDEROM 1961. Tussen afsluitdijken en deltadijken – Noord-Beveland, geschiedenis van strijd, nederlaag en overwinning op het water – Littooy & Olthoff (Middelburg) : 304 pp.
DE JONG, H. & F. GERRITSEN 1984. Stability parameters of Western Scheldt

estuary. Proc. 19th Coastal Eng. Conf., Houston. ASCE: 3078–3093.
DE RONDE, J. G. 1983. Changes of relative mean sea level and of mean tidal amplitude along the Dutch coast. In: Ritsema, A. R. & A. Gürpinar (eds): Seismicity and seismic risk in the offshore North-Sea area : 131-4.142.
DEKKER, C. 1971. Zuid-Beveland. De historische geografie en de instellingen van een Zeeuws eiland in de Middeleeuwen. Thesis, Amsterdam, Assen, 684 pp.
DENUCÉ, J. 1933. De loop van de Schelde van de zee tot Rupelmonde in de XVe eeuw. Veritas; Antwerpen: 24 pp.
GERRITSEN, F. & H. DE JONG 1984. Stabiliteit van doorstroomprofielen in het Waddengebied. Rijkswaterstaat, Vlissingen. Nota WWKZ-84.V016. 51 pp.
HAGEMAN, B. P. 1969. Development of the Western part of the Netherlands during the Holocene. Geol. & Mijnb., 48:373–388.
HARING, J. 1964. Een onderzoek naar de bodem- en geulveranderingen in het Deltagebied. Rijkswaterstaat, Den Haag, nota K243. 7 pp.
KOMAR, P. D. 1976. The transport of cohesionless sediments on continental shelves. In: Stanley, D. J. & D. J. P. Swift (eds): Marine sediment transport and environmental management: 107–125.
O'BRIEN, M. P. 1969. Equilibrium flow areas of inlets on sandy coasts. ASCE, J. Waterw. Harbors Div., 95 (WW1): 43–51.
PEELEN, R. 1967. Isohalines in the Delta areas of the rivers Rhine, Meuse and Scheldt. Neth. J. Sea Res., 3: 575–597.
PONS, L. J., S. JELGERSMA, A. J. WIGGERS, J. D. de JONG 1963. Evolution of the Netherlands coastal area during the Holocene. Verh. KNGMG, Geol. Serie, XXI–2: 197–208.
SILVESTER, R. 1974. Coastal Engineering, II Sedimentation, estuaries, tides, effluents, and modelling. Dev. in Geotechn. Eng. 4B: 67 pp.
TERWINDT, J. H. J. 1973. Sand movement in the in- and offshore area of the SW part of the Netherlands (Geol. & Mijnbouw 52: 69–77.
TERWINDT, J. H. J. 1977. Mud in the Dutch delta area. Geol. & Mijnbouw 56: 203–210.
THURKOW, A. J., J. D. H. HARTEN, H. KNIPPENBERG, L. PRINS, J. RENES, J. SCHRIJF, J. A. J. VERVLOET, J. C. VISSER, P. A. M. VAN WIJK 1984. Atlas van Nederland deel III: Bewoningsgeschiedenis: 23 pp.
VAN DE KREEKE, J. & J. HARING 1979. Equilibrium flow areas in the Rhine-Meuse Delta. Coast. Eng. 3: 97-111.
VAN RUMMELEN, F. F. F. E. 1978. Toelichting bij de Geologische kaart van Nederland 1 : 50.000, Noord-Beveland, Rijks Geol. Dienst, Haarlem: 138 pp.
WILDEROM, M. H. 1964. Tussen afsluitdijken en deltadijken II: Noord-Zeeland; Littooy & Olthoff, Middelburg: 415 pp.
ZAGWIJN, W. H. 1986. Geologie van Nederland I: Nederland in het Holoceen. Staatsuitgeverij, Den Haag.

2. Morphological changes of the ebb-tidal delta of the Oosterschelde during recent decades

Reproduced from Geologie & Mijnbouw vol. 63 (4), 1984, pages 363–375 by permission of the editors.

Abstract

The ebb-tidal delta of the Oosterschelde consists of a complicated system of shifting channels and shoals. From 1959 onwards detailed soundings of the area have been carried out almost yearly and thus the most important morphological changes in the last 25 years have been established. An attempt has been made to trace the impact of 'Delta-Project' constructions which have already been completed upon the trend of the morphological evolution. Attention is paid to implications of this investigation for the study of fossil examples of ebb-tidal deltas. A main conclusion is that a rather small increase in tidal discharge at the entrance of the Oosterschelde basin resulted in a remarkable and rapid expansion of the ebb-tidal delta.

Introduction

The ebb-tidal delta of the Oosterschelde is part of a series of coalescing tidal deltas adjacent to the North Sea shelf. They are formed in front of the coast by tidal currents passing through a number of tidal inlets and estuaries connected with the Rhine-Meuse-Scheldt fluvial system. The sediment of the inlets and tidal deltas largely consists of fine to medium sand (TERWINDT, 1973).

The vertical tide in the tidal delta is essentially semidiurnal. The mean tidal range in the Oosterschelde outer delta varies between 3.4 m at the coalescense of the Oosterschelde and Westerschelde tidal deltas and 2.8 m at the inlet entrance. The median grain size varies between 150 and 350 μm. The coarsest sediments are generally found in the deepest parts of the channels. For the current and sand transport patterns in the coastal area of the SW Netherlands

prior to the closure of the Haringvliet estuary (1970) and the Grevelingen (1971) see TERWINDT (1973).
The sand is transported by both waves and currents, resulting in a complicated circulation of sediments governed by the presence of ebb and flood channels. A general picture of the present current velocity pattern is given by VOOGT & ROOS (1980) and SIEGENTHALER (1982).
The 'Delta Project' is bringing about major changes in the tidal current pattern and sediment transport in the area. As shown in Figure 1 several major dams have already been built.

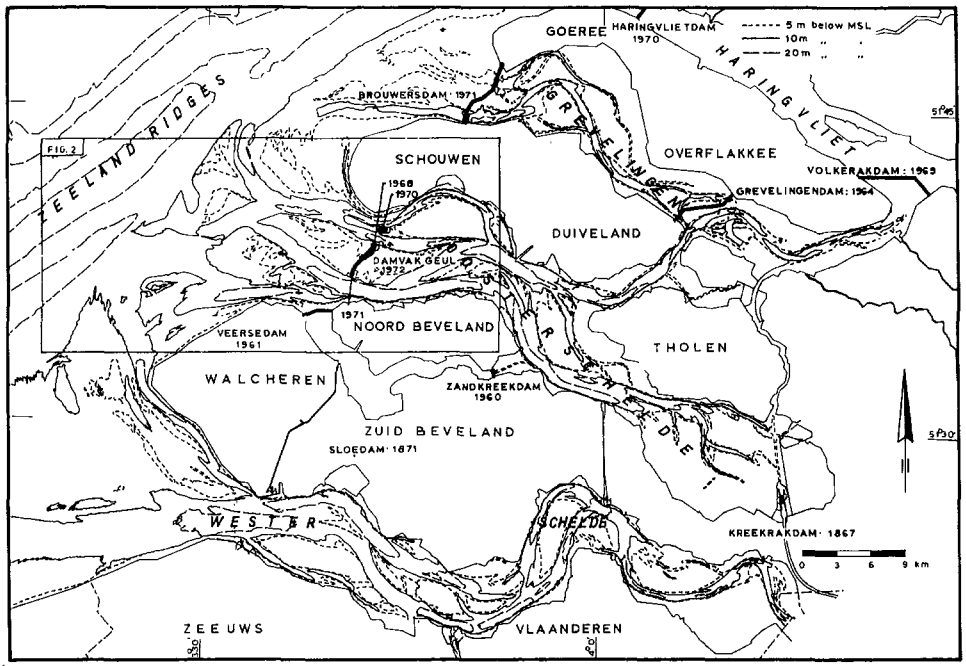

Fig. 2.1 Bathymetry of the southwestern Netherlands with dates of the main channel closures

With the construction of a storm surge barrier in the mouth of the Oosterschelde and two secondary dams within the sea-arm, the project is nearing completion. The storm surge barrier will be finished by the end of 1986 and will reduce the present 12 10^8 m^3 tidal prism by about 30% (ANONYMOUS, 1983).
In the proximal part of the tidal delta, tidal current velocities are expected to decrease drastically and a direct change in current pattern is expected up to a distance of 20 km off the barrier (VOOGT & ROOS, 1980). It is obvious that this will result in drastic changes in the morphodynamics of the area and may have repercussions on coastal evolution.
A study of the present hydraulic and morphodynamic system is essential to

evaluate possible changes. This paper deals with the morphological evolution of the tidal delta during the past 150 years. Attention is focused on changes in recent decades and their relationship to those parts of the 'Delta Works' already completed within the tidal basin and in the alignment of the Storm Surge Barrier.

Evolution of the tidal basin

The origin of the system of inlets and estuaries in the SW part of the Netherlands lies in the last major transgression of the Holocene – the Dunkirk incursions from 2500 B.P. onwards.
Presumably after 500 B.C. but certainly before Roman times, a large estuary – the Oosterschelde – was formed as a main distributary of the river Scheldt (VAN RUMMELEN, 1978). Only after about 700 AD the more southerly Westerschelde estuary started to form and gradually took over the fluvial discharge of the river Scheldt. This proces was finally completed artificially in 1867–1871 when two dams were built to seal the last connections between the Oosterschelde and the river Scheldt.
The early Oosterschelde had one major channel which was relatively narrow as compared to its present dimensions (WILDEROM, 1964). Storm incursions and floodings during mediaeval times widened the estuary at the expense of the neighbouring land (GOTTSCHALK, 1971). As a result the tidal prism must have increased by many hundreds of millions of cubic metres. The effect of this increase became apparent after 1400 AD when the main channel (the Hammen; Fig. 2.2) developed a large meander near the mouth of the inlet, causing a retreat of the coastline to the north to a maximum of 4 km.

After 1600 AD the increase of tidal discharge resulted in the development of a second major channel, the Roompot (see Fig. 2.2 for location), leading to a coastal retreat of Noord-Beveland and a further widening of the mouth of the estuary (VAN DEN BERG ET AL., 1980). Most of the eroded sediment must have been transported to the sea and likely has contributed to the growth of the tidal delta.

Morphological changes during the past 150 years are well-documented by a series of hydrographic charts. A selection of maps derived from these charts is presented in Figure 2.2. The figure shows that between the Roompot and Hammen channels a complex shoal area developed, cross-cut by smaller (5–15 m deep) blind-ending flood and ebb channels that were shaped by currents generated by small gradients in water-level between the two major channels at particular stages of the tidal cycle (VAN DEN BERG ET AL, 1980).

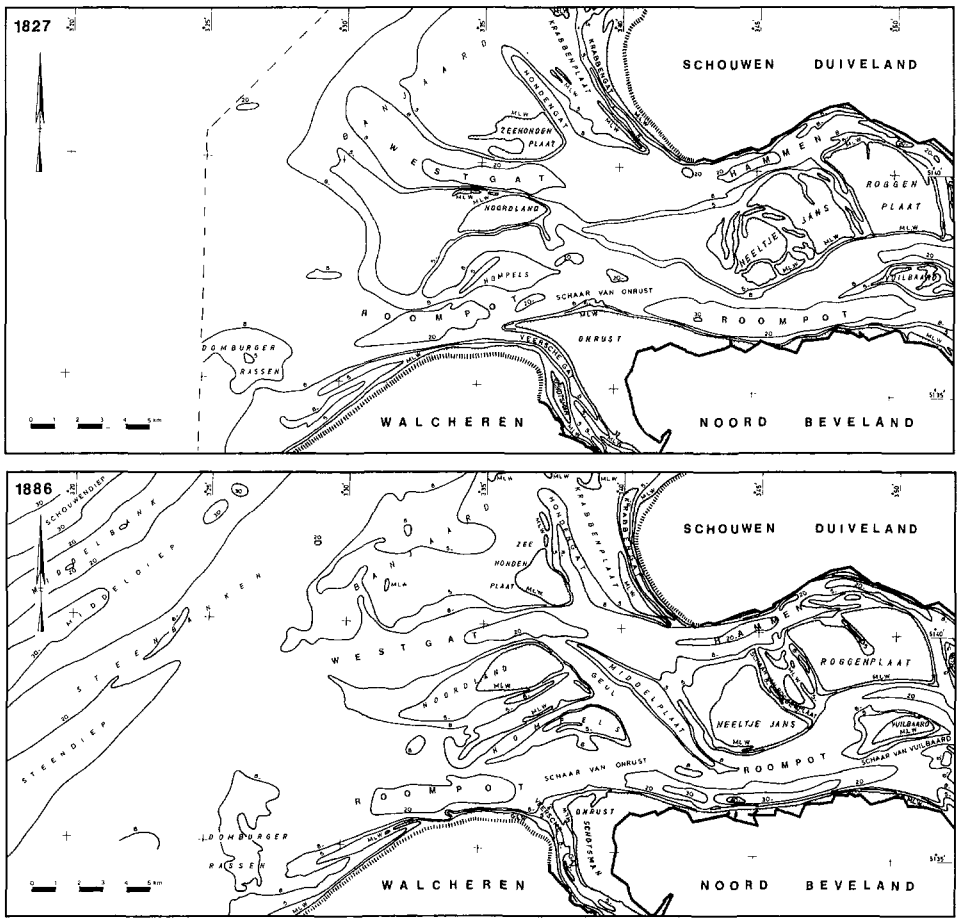

During the 20th century a third major channel has developed in the entrance area of the Oosterschelde, the 'Schaar van Roggenplaat', running NW-SE between the Hammen and the Roompot. With its development from equilibrating stream into a major channel, the 'Schaar van Roggenplaat' became more important as a transit channel like the Roompot and the Hammen, which accounts for its anticlockwise rotation. With the development of this third major channel, a permanent connection between the former two channels was established. Most of the earlier mentioned small flood and ebb channels with a similar NW-SE orientation lost their hydraulic funtion and were rapidly silted up. One of those channels, the Geul, was dammed in 1972 (Fig. 2.2).
The origin of the 'Schaar van Roggenplaat' can be considered as a response to a further increase in the tidal prism, mainly caused by human interference in the estuary; in the first half of the 20th century a considerable increase in the tidal discharge was caused by regulating works – dredging and canalization – in the northern tributary.

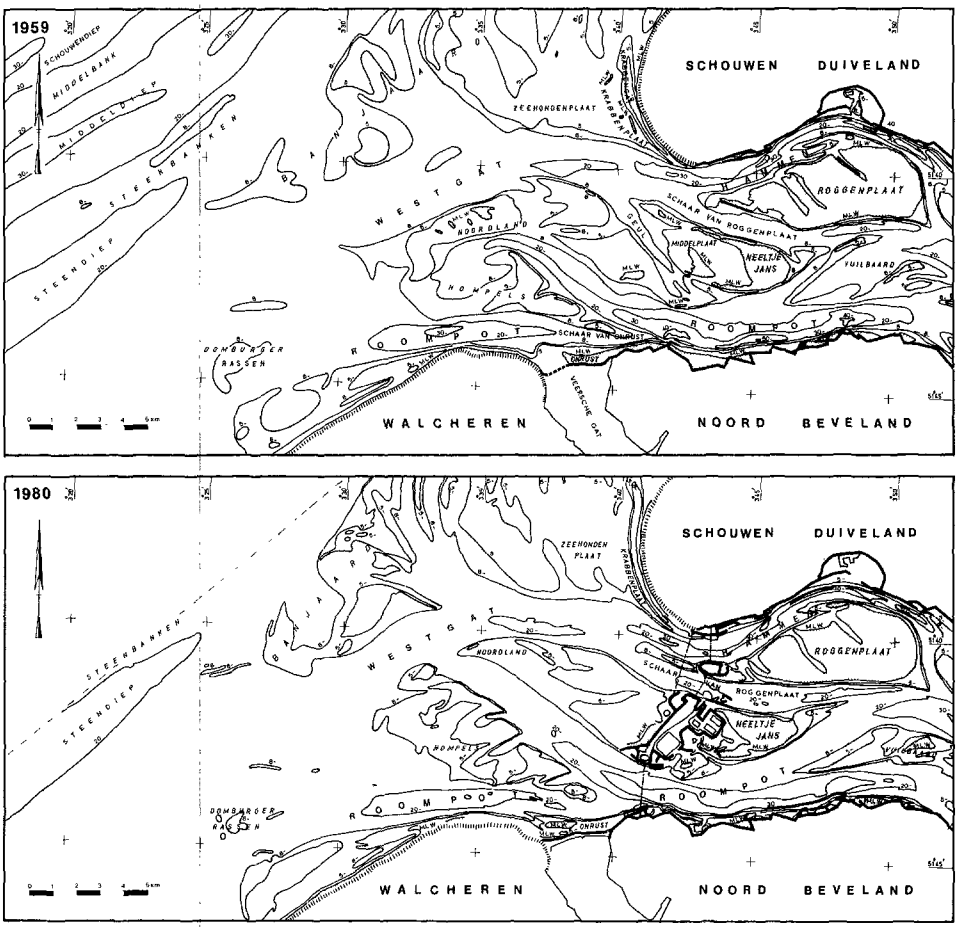

Fig. 2.2 The tidal delta of the Oosterschelde between 1827 and 1980

Since 1960 some of the closures of the Delta Project have influenced the tidal prism and other tide characteristics of the Oosterschelde. As a consequence of the closure of the Veerse Gat in 1961 the tidal prism of the sea-arm was reduced by about 5%. Before the construction of the Grevelingendam in 1962–1964 part of the ebb discharge from the Krammer-Volkerak area and, to a lesser extend, part of the flood tide, passed through the Grevelingen inlet. After this sea-arm had been dammed, these water masses were added to the tidal prism of the Oosterschelde. According to discharge measurements in the northern tributary, the tidal prism of the Oosterschelde increased by about the same quantity as it was reduced at the closure of the Veerse Gat some years earlier.
The closure of the Volkerak in 1969 caused an important change in the discharge curve and a dramatic increase in the tidal range on the northern tributary of the Oosterschelde, amounting to more than 50% in the northernmost part of

this channel near the closure dam. According to calculations using the IMPLIC numerical one-dimensional network model of the Oosterschelde (DRONKERS, 1969), the maximum ebb discharge at the mouth of the Oosterschelde increased by 12%, whereas the maximum flood movement increased by 8%.

Apart from artificially induced changes of the tidal prism one natural factor is important: tidal gauge records indicate a natural increase of 4% in the tidal amplitude along the Dutch coast over the past century (DE RONDE, 1983). According to prolonged simultaneous measurements with automatic propellor current meters (Flachsee) this increase corresponds to a similar change of the tidal volume of the Oosterschelde.
Using data from various tidal inlets in the SW part of the Netherlands, an empirical linear relationship was established between the cross-sectional area of the inlet mouth below MSL (A_c) and the maximum tidal discharge (Q) (VAN DE KREEKE & HARING, 1979):

$$A_c = 1.17\,Q \quad (m^2)$$

On the basis of this equation in conjunction with data from sounding charts and the results of the above-mentioned IMPLIC calculations, the increase in the tidal prism of the Oosterschelde since 1872 can be estimated at 25%, 9% of which has to be attributed to the damming of the Volkerak. As a consequence of this increase in tidal discharge, erosion has been dominant in most parts of the tidal basin.
Net sedimentation and erosion in the Oosterschelde and its tidal delta during the past century have been studied by HARING (1978). He analysed the change in cross-sectional area of a large number of parallel profiles through the Oosterschelde at intervals of 500 m. The changes in a profile were considered ro represent a zone of 250 m to either side of the profile and the method is therefore not very accurate. Also, the accuracy of the older sounding charts is certainly not high. This holds especially for the tidal delta area. Therefore, HARINGS's data should be considered only as indicators.
The data suggest that the Oosterschelde lost some 2.8 10^8 m^3 of sediment during the period 1872–1959, resulting in a deepening of the area below MSL of on average 0.9 m (including the northern tributary). The amount of sediment transported to the sea between 1959 and 1974 can be estimated to be about 0.6 10^8 m^3. Another 0.78 10^8 m^3 was lost as a result of dredging. In that period, 1959 to 1974, the basin was deepened by about 0.4 m.
The building of the Storm Surge Barrier in the mouth of the Oosterschelde started with the construction of three artificial islands (1968 to 1970) and a dam across the Geul channel connecting two of these islands (fig. 2.1).

As mentioned before, the Geul channel was already declining as a tidal watercourse and its damming only accelerated the process of channel abandonment. According to a series of discharge measurements carried out by the Delta Department of the Rijkswaterstaat in the mouth area in recent decades, the ebb and flood volumes of the Geul after its closure were distributed between the Schaar van Roggenplaat and Roompot channels. These measurements further indicate some loss in tidal discharge in the Hammen channel after 1972, in favour of the Roompot (Fig. 2.3), which induced morphological changes in the Oosterschelde tidal channel system, to be discussed below.

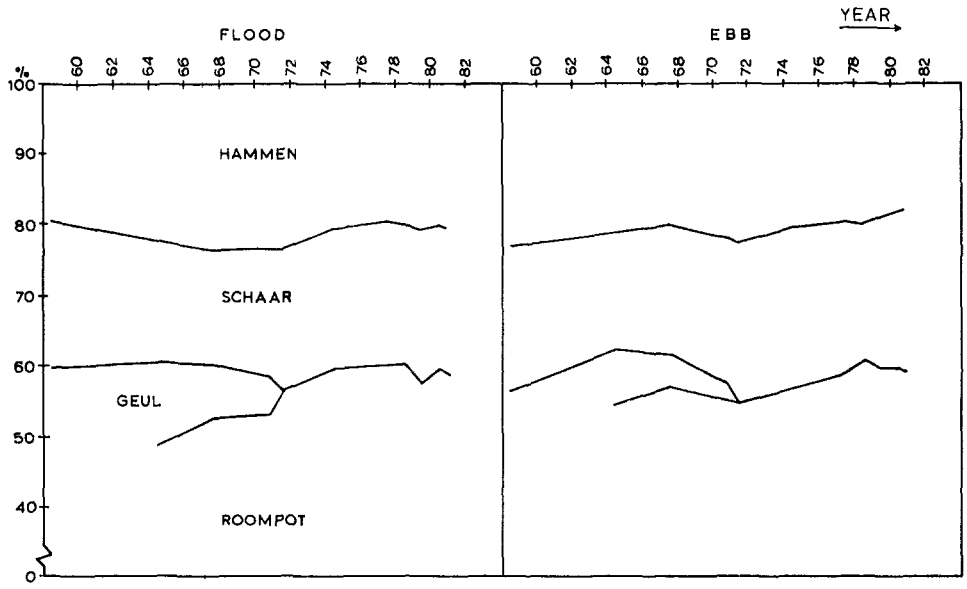

Fig. 2.3 Distribution of ebb and flood volumes among the channels in the mouth of the Oosterschelde since 1959. (Sum of ebb or flood = 100%).

Morphology and sediment budget of the outer delta in the period 1827–1962

Morphological changes in this period are shown in Fig. 2.2. The Outer Delta contained a system of rapidly shifting channels involving the transfer of huge quantities of sand. The influence of the increasing tidal discharges through the inlet is reflected in a gradual deepening of the major channels in the proximal part of the tidal delta and – less apparent – the seaward extension of the underwater delta. The coeval disappearance of the intertidal shoals suggests a similar relationship with the change in tidal prism.
With respect to the sand budget Harings's data, partly summarised in MORRA ET AL. (1961), suggest a net erosion of the proximal and southwestern

part of the outer delta between 1872 and 1962 of about 0.3 10^8 m^3 and 0.9 10^8 m^3 respectively. For the same period the amount of sediment involved in the seaward extension of the tidal delta can be estimated at 1.0 10^8 m^3. Together with the large amounts of sediment coming from the tidal basin, the total sediment export of the Oosterschelde system can be estimated at about 3.0 10^8 m^3. According to data about the sediment balance in the surrounding tidal areas, these sediments were partly transported northward along the coast and deposited in the Grevelingen and Haringvliet tidal systems, partly they were trapped on the innermost Zeeland ridges off the underwater delta front (TERWINDT, 1973). The latter is confirmed by the occurrence of a recent mollusc association including *Petricola pholadiformis* – a bivalve introduced into the North Sea around AD 1900 – in the upper layers of the sediment (LABAN & SCHUTTENHELM, 1981). In some corings this layer reaches a thickness of 2 m (C. LABAN, 1982, pers. comm.).

Morphological changes in the period 1960–1980

Data

From 1860 till 1950 sounding charts were made of the Oosterschelde system by the Hydrographic Service almost every decade. From 1959 onwards the area has been surveyed almost annually by the Delta Department of the Rijkswaterstaat (Ministry of Transport and Public Works).

The latter surveys are carried out with Decca positioning (accuracy about 15 m) according to a fixed system of 100–200 m spaced sounding tracks. The accuracy of the determination of the sounded water-depth is estimated at 0.14 m. Since inaccuracies are mainly attributable to accidental errors in the reduction to Ordnance Datum, the average error in the area surveyed in a day – about 40 km^2 – will be less than 0.1 m. Deviations become progressively less as larger areas are considered. Calculations on the sand balance were performed on the basis of interpolated depth values using 200 × 200 m and 400 × 400 m grid squares (Fig. 2.4).

The flood and ebb channels

Fig. 2.5 shows the changes in the channel pattern in the form of the migration of the 10 m below Mean Sea Level contour, which arbitrarily divides the major channels and subtidals shoals in the area. The movement of this depth contour is shown at intervals of 5 years. Obviously part of the changes has to be attributed to the inaccuracy of the survey. In flat areas such as the Domburger Rassen this may account for considerable changes in the position of the 10 m isobath, suggesting changes larger than in reality.

Nevertheless several trends are remarkable. The ebb channels of the Westgat

and the Oude Roompot have expanded rapidly towards the sea. In the period 1970–1975 this happened at an accelerated rate, leading to a coalescence of two ebb channels of the Oude Roompot and one of the Westgat ebb channels.

The tidal delta front displays a similar seaward expansion, which is spectacular in the northwest where protuding terminal lobes of ebb shields form part of it. During the period under consideration, progradation here locally amounted to 700 m, and a layer of more than 9 m of sediment was deposited (see also Fig. 2.7).

In the mouth of the Oosterschelde the aforementioned anticlockwise rotation of the Schaar van Roggenplaat channel axis and the process of Geul channel abandonment and siltation may be noted. All these trends can be explained as reactions to the 20th century increase in the tidal prism of the sea-arm. This is clearly demonstrated by the increase in rate of expansion of the major ebb channels in the period 1970–1975, just after the sudden increase in tidal discharge connected with the Volkerak closure.

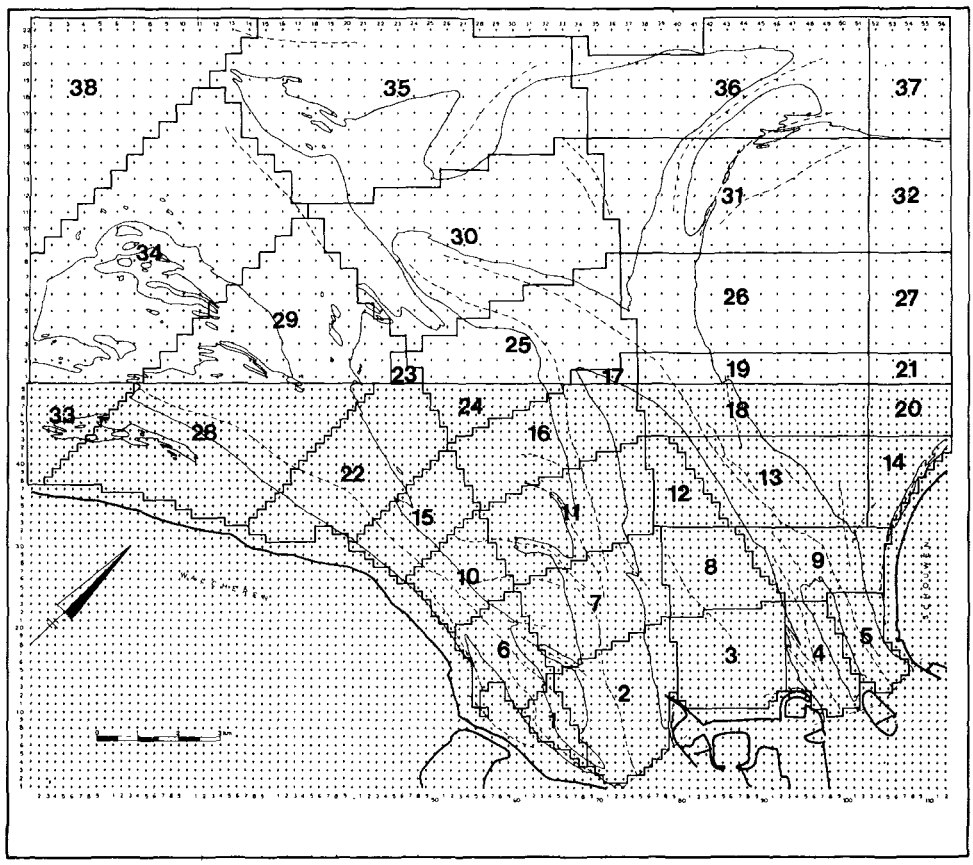

Fig. 2.4 Grid schematization and partition of the tidal delta

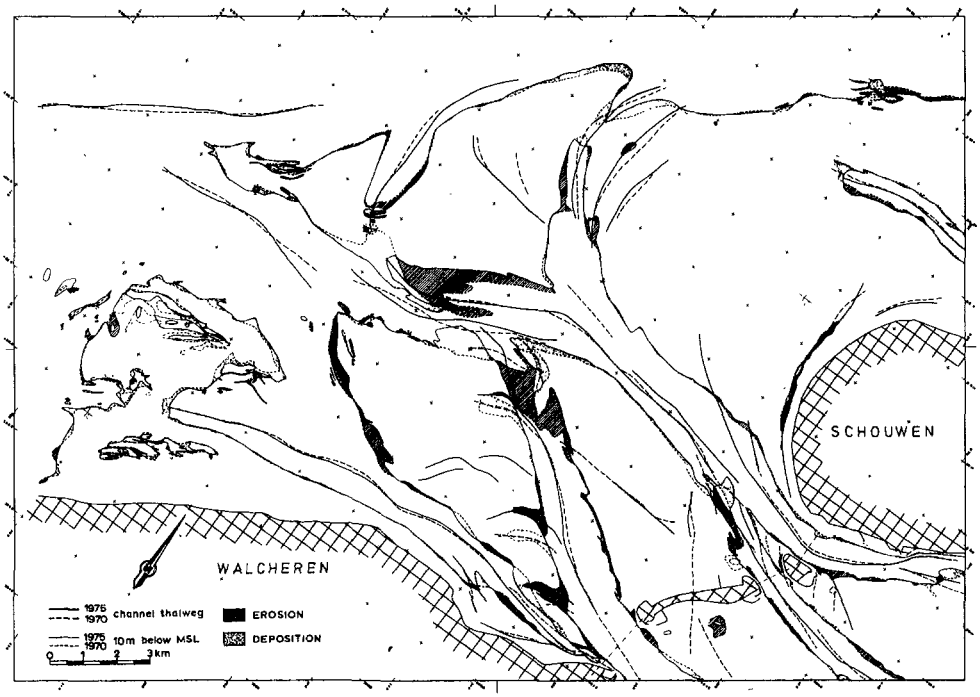
SCHOUWEN
WALCHEREN
1975
1970 channel thalweg
EROSION
1975
1970 10m below MSL
DEPOSITION
0 1 2 3km

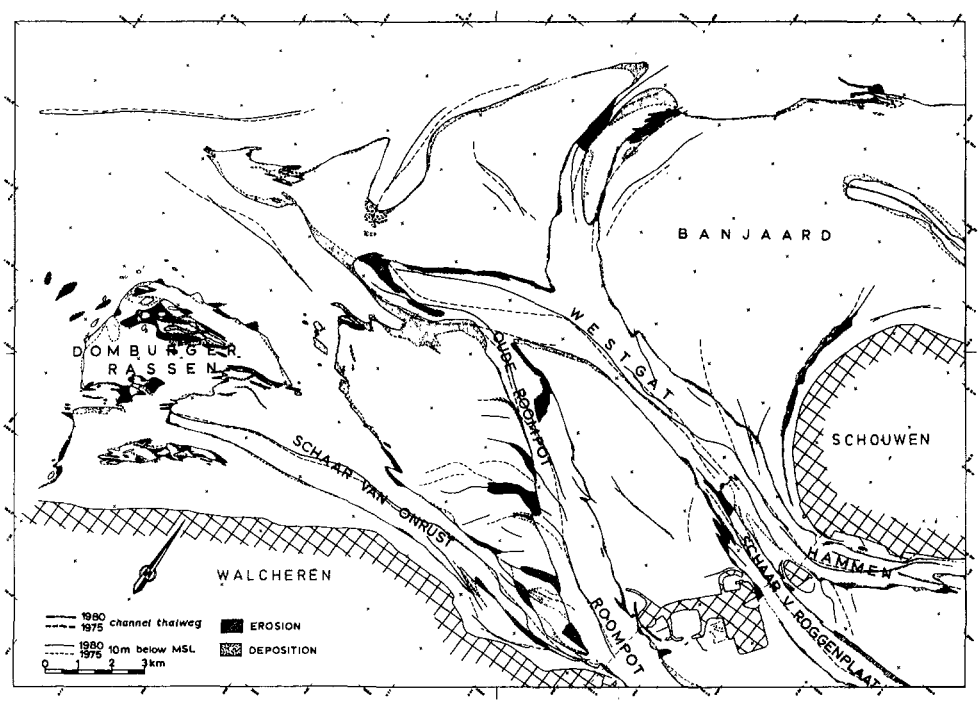
BANJAARD
DOMBURGER RASSEN
OUDE ROOMPOT
WESTGAT
SCHOUWEN
SCHAAR VAN ONRUST
HAMMEN
WALCHEREN
ROOMPOT
SCHAAR V. ROGGENPLAAT
1980
1975 channel thalweg
EROSION
1980
1975 10m below MSL
DEPOSITION
0 1 2 3km

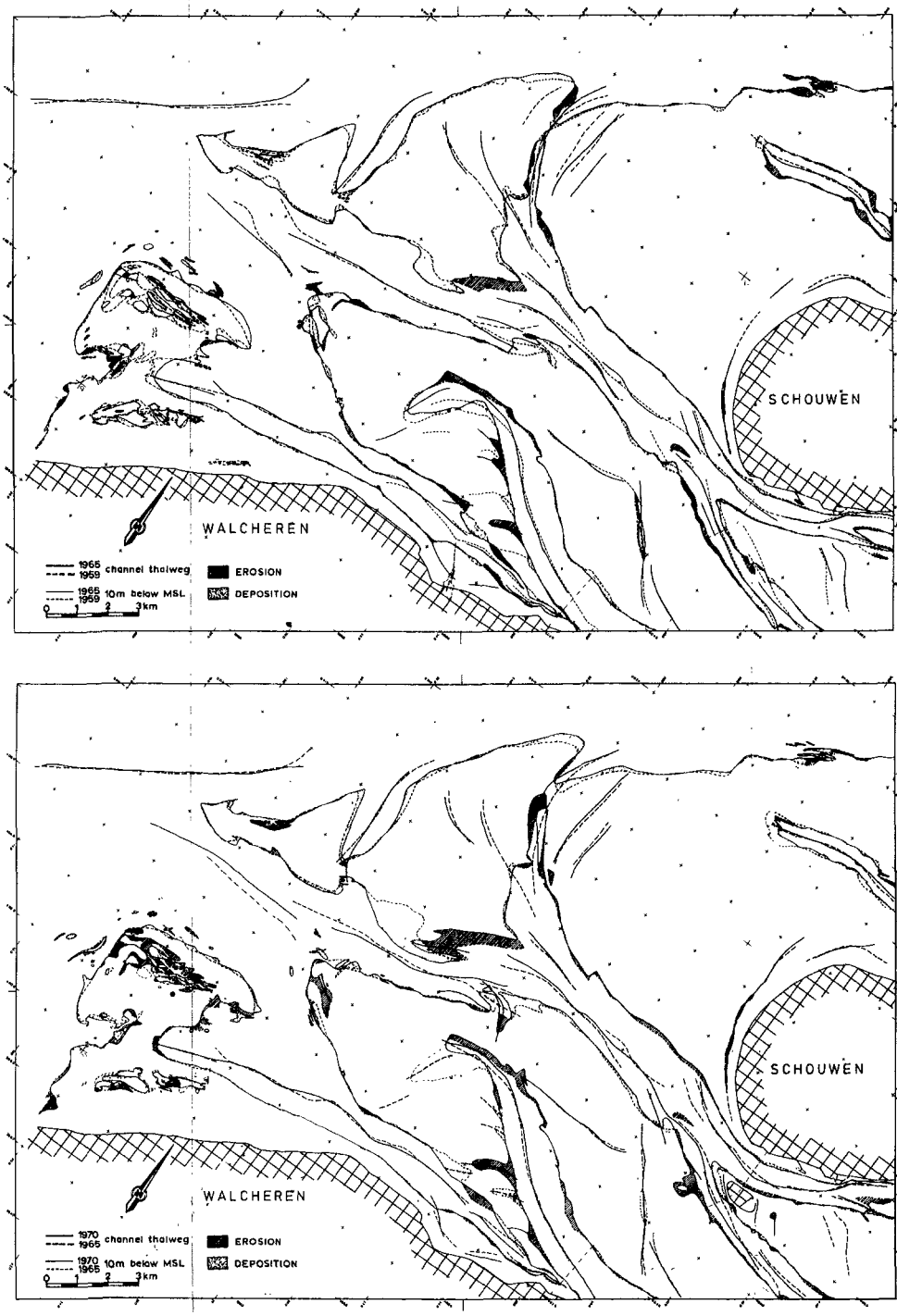

Fig. 2.5 Changes in the 10 m isobath between 1960 and 1980

At the level of the 10 m depth contour the sill between the Oude Roompot and the Westgat channel was breached in 1974. At about the same time a similar breach occurred more inshore, between the Roompot channel and an ebb channel connected to the 'Schaar van Roggenplaat' (Fig. 2.2). As a consequence of these breaches the Roompot's share of the total ebb and flood discharges in the mouth of the Oosterschelde increased from 56 to 59% (Fig. 2.3).
A further illustration of ebb channel expansion and coalescence of ebb channels is given in Figure 2.6.

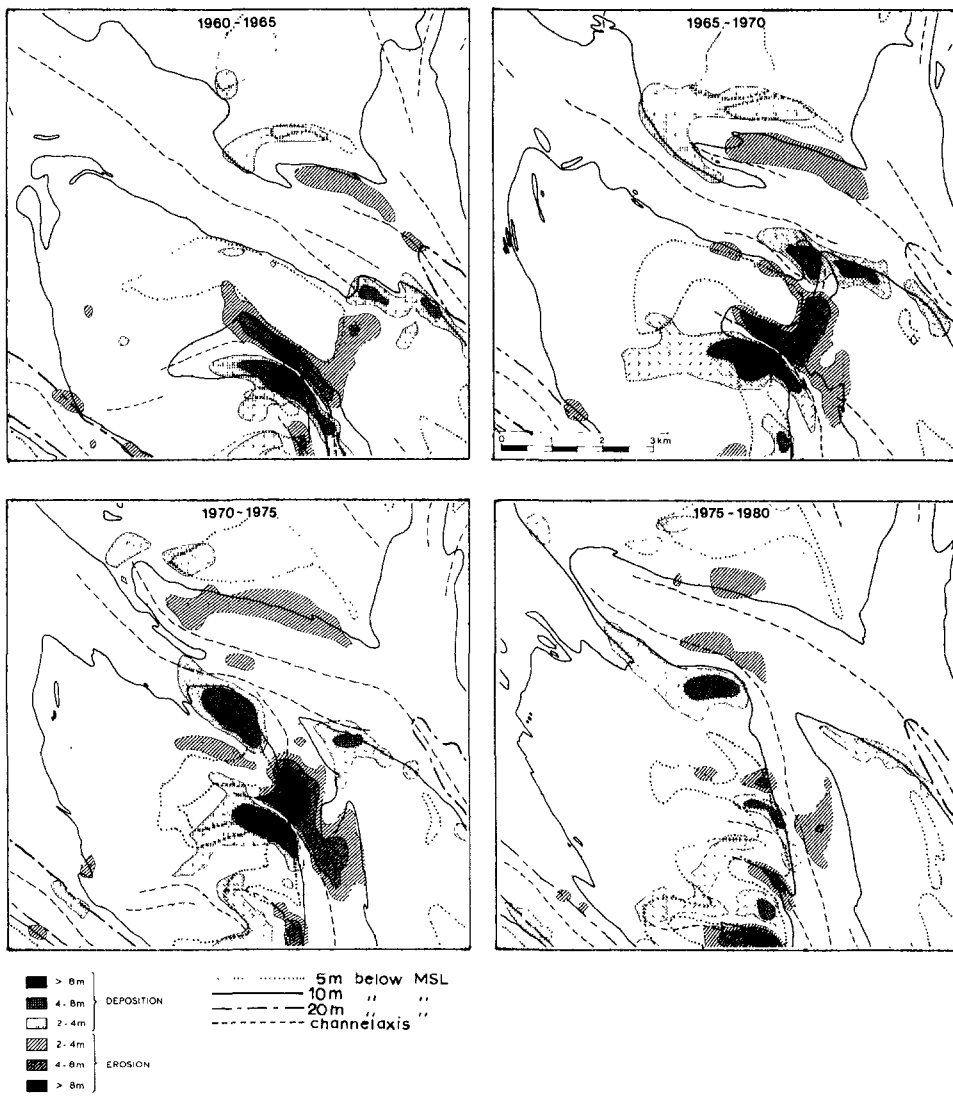

Fig. 2.6 Expanding ebb channels in the Oosterschelde tidal delta. For location see Fig. 2.7

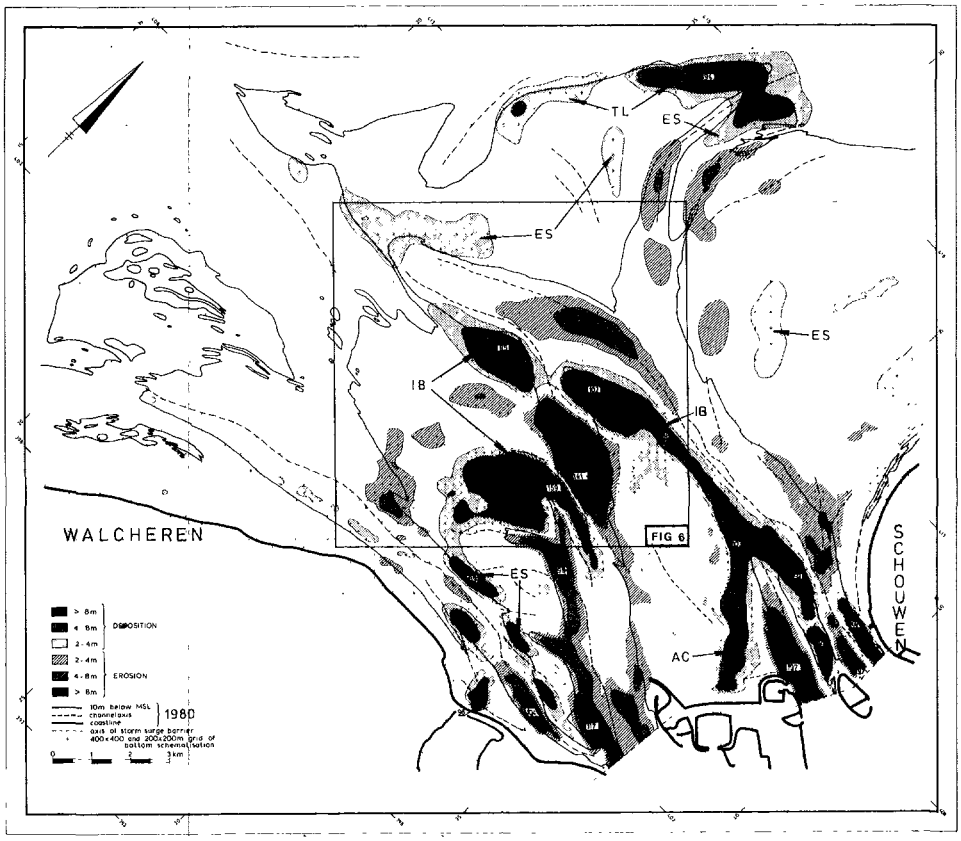

Fig. 2.7 Net deposition and erosion in the Oosterschelde tidal delta in the period 1960–1980. Nature of deposits: IB = Inner Bend of ebb channel; ES = Ebb Shield; TL = Terminal Lobe of ebb shield at the deltafront; AC = Abandoned Channel

The isallobath maps in Figure 2.7 are based on date of interpolated depths in the 200 × 200 m and 400 × 400 m schematization of the area. The figure underlines the dominating influence of the ebb tide in the morphodynamics of this area: a large part of the sediment eroded by the ebb current near the blind end of the Westgat ebb channel is deposited downcurrent in a horseshoe-shaped accumulation on the flat ebb shields of the channel. Although less evident, the same holds for the other expanding ebb channels.

It further emerges that two erosional processes played a role in breaching the sill between the Oude Roompot and Westgat channels:
– Firstly the seaward expansion of the Oude Roompot channel, which is predominantly achieved by channel bend erosion in the westernmost part of the channel. The fast erosion by the ebb current of the outside of the bend is compensated by deposition in the inner bend. It may be noted that similar

processes are taking place in secondary ebb channels branching off the SW bank of the Oude Roompot channel.
– Secondly the sill between the Oude Roompot and Westgat channels is eroded by currents that cross the bar. This is apparently caused mainly by the ebb current, since large amounts of sediment are deposited simultaneously just north of the sill.

After construction of the artificial islands and the damming of the Geul the total cross-sectional area below MSL of the Oosterschelde in the alignment of the Storm Surge Barrier was diminished by 17% (from 88.000 m^2 in 1968 to 73.000 m^2 in 1972). Therefore current velocities in the remaining channels have increased, resulting in erosion and deepening of an area extending several kms off the barrier alignment. This process was certainly enhanced by the increase in the tidal discharges after the damming of the Volkerak channel in 1969.
In accordance with the change in the distribution of the tidal discharge in the mouth after the damming of the Geul (Fig. 2.2) erosion in the Hammen channel was less than the remaining channels. The extent of the erosion is illustrated by an isallobath map covering the period 1960–1980 (Fig. 2.7).
Erosion was concentrated along the southern margin of the channels. This remarkable fact is connected to long-term processes of channel migration quoted before: rotation of the Schaar van Roggenplaat channel and southward bending of the Roompot channel (Fig. 2.2). Although considerable erosion occurred, the maximum depth of the channels did not change very much. Between 1968 and 1980 the maximum depth of the Roompot channel increased by 1 m to 34 m and the Schaar van Roggenplaat channel deepened from 19.5 to 21.5 m. The maximum depth of the Hammen channel even diminished by 1 m and became 28.5 m.
In spite of the southward migration of the left bank of the Oude Roompot channel, some erosion still occurred along the right (NW) bank of this channel, owing to a considerable widening process. Obviously this is related to the increase in tidal discharges through this channel caused by the Volkerak and Geul closures and to the coalescene of the Oude Roompot en Westgat channels.

The sand budget
Using the interpolated depth values per grid-square, the net erosion and sedimentation of the ebb tidal delta and parts of it over periods of 5 years have been calculated for the period 1960 to 1980. To discriminate between sedimentation processes in the different channels and between proximal and more distal parts of the tidal delta the area was divided according to flow areas of the major channels and proximity of the inlet (Fig. 2.4) Some of the results are shown in Figs. 2.8 and 2.9.

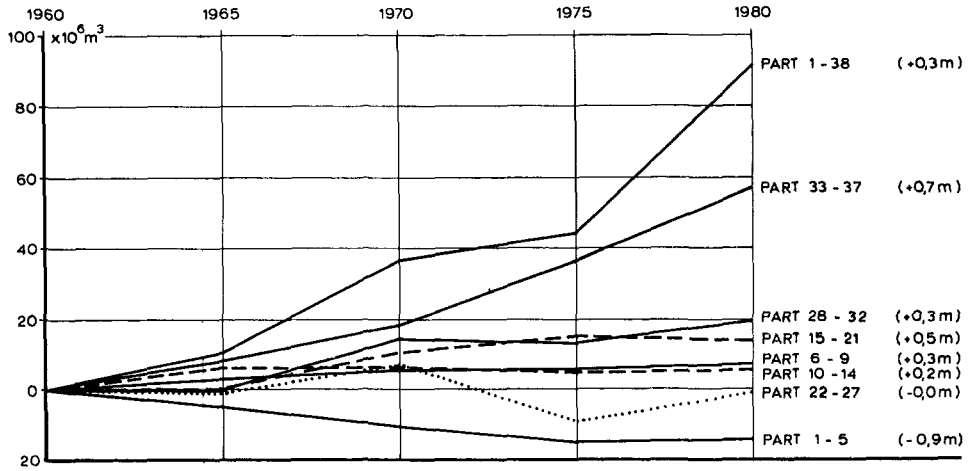

Fig. 2.8 Sediment budget of the tidal delta and parts of it in relation to proximity of the inlet entrance (1960–1980)

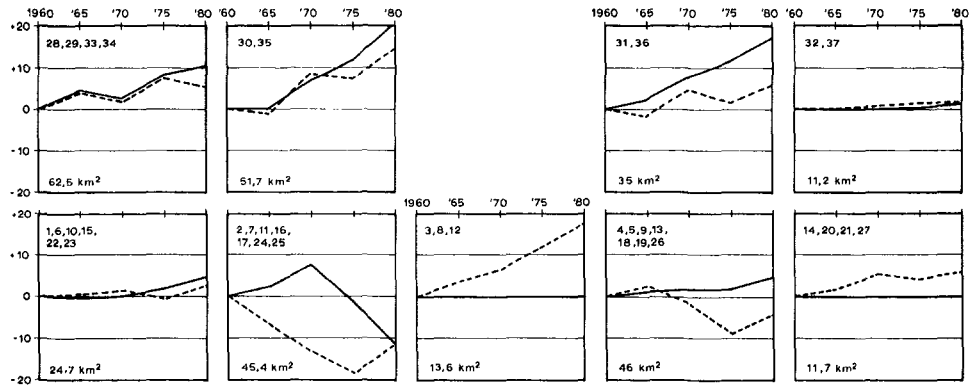

Fig. 2.9 Sediment budget of different flow areas in the tidal delta (1960–1980). Numbers refer to zones as indicated in figure 2.4. Amounts in 10^6 m^3 above (---) and below (—) the 10 m depth contour

One of the most remarkable results of the calculations is the large volume of sand deposited in the tidal delta in a period of only 20 years (0.9 10^8 m^3). Although accurate calculations of the erosion in the Oosterschelde have not yet been carried out is is certain that this is the main source area of the sediment. A source of minor importance, estimated at about 0.02 10^8 m^3, is found in the net loss of sand from beaches and dunes, especially along the Schouwen coastline, which locally retreated by 120 m in this period. The absence of a significant morphological change in the SW part of the tidal delta does not indicate a substantial sediment transfer from the Westerschelde region. Therefore, other sediment sources – if any – are considered negligible. Instead some loss of sand might be expected that accumulated in the Zeeland Ridges offshore

and along the coast farther north, as was the case in former periods. It is not obvious why the calculated total net deposition in the period 1975–1980 should have been more than in the preceding period of five years. The difference in the rate of deposition between the two periods seems too large to be ascribed to errors in the calculated sediment volumes caused by inaccuracies of the soundings. At least part of it must be explained, however, by a natural increase in the tidal discharge after the damming of the Volkerak channel, that was connected with a 18.61 year cyclic change in tidal range. This period represents the variation of the mean longitude of the ascending node of the lunar orbit.

The variation affects the tidal range. Along the coast of the SW Netherlands it causes a cyclic variation in the mean tidal range of about 3% (DE RONDE, 1983). As mentioned before, this leads to a variation in the tidal discharges of the Oosterschelde of about the same proportion.
By chance, the closure of the Volkerak took place at the tidal minimum of the cycle. Consequently, after the sudden increase of 8% of the tidal discharge of the Oosterschelde caused by the damming of the Volkerak channel, a further increase of 3% occurred till about 1978. This enhanced the erosion in the tidal basin which could at least partly explain the relatively high rate of deposition in the tidal delta in the period 1975–1980.

Implications for the study of fossil examples of ebb-tidal deltas

Although this investigation was focused on morphological changes some results bear interesting implications for the study of fossil ebb-tidal deltas which can not be disregarded. They will now be discussed briefly.
One of the most interesting aspects is the remarkable expansion of the tidal delta and the large sediment supply to it coming from the tidal basin in response to a rather small increase in tidal discharge through the inlet. In such a prograding ebb-tidal delta the expanding ebb channels are the most dynamic elements. Main depositional areas are the inner bends of these dynamic ebb channels, the major ebb shields and the terminal lobes of these shields at places where they form part of the underwater delta front (Fig. 2.7).
Echo soundings reveal that most of the ebb shield and inner channel bend environments is covered by a pattern of ebb-directed megaripples, indicating that deposits will consist mainly of ebb-directed cross-stratified sediments. A subrecent example of an inner bend deposit exposed in a construction pit of the storm surge barrier in the mouth of the Oosterschelde was described by VAN DEN BERG (1982). The terminal lobes of ebb shields at the delta front gradually encroach upon the innermost ridge of the system of sandwave-covered elongated sand ridges, known as the Zeeland Ridges, which run more

or less parallel to the present coast (Fig. 2.1: for a discussion on the origin stratigraphy of the Zeeland Ridges the reader is referred to LABAN & SCHÜTTENHELM, 1981). Prograding parts of the delta front show a concave upward seaward-facing ramp between 7 and 13 m below Mean Sea Level, with a maximum gradient of 4 to 12 degrees.

Information on bedforms on this slope is rather scanty. A side scan sonar survey revealed a relatively flat surface that passes abruptly into a megaripple field at the base of the slope. Above the 7 m depth contour a transition is found to a rather flat subtidal terrace. Strong wave action during periods of onshore gales inhibits these outermost shoal areas to shallow above 4 m below Mean Sea Level.

Data from shallow cores taken by the Geological Survey of the Netherlands suggest that sediments of the distal part of the ebb-tidal delta hardly contain mud laminae. This in a sharp contrast with deposits of the same age described from inshore subtidal environments in this area (TERWINDT, 1971, 1981; VAN DEN BERG, 1981, 1982; VISSER, 1980). This difference can partly be ascribed to a more intense wave agitation of bottom sediments in the offshore area. A more fundamental reason lies in the absence of short stand-still stages of the current, allowing mud to settle out of suspension. In the relatively narrow and elongate inlets and estuaries currents are laterally confined. Therefore at the transition from flood to ebb and vice versa the current direction changes drastically by about 180 degrees, implying a short slackwater period during which indeed fine-grained sediment can settle. Off the inlet entrance currents gradually become less channelized. Longshore components of the tide become more important and current vectors tend to describe a more elliptical to circular pattern (SIEGENTHALER, 1982). At the 'turn of the tide' current vectors gradually rotate and velocities remain strong enough to inhibit the settling and deposition of mud.

Conclusion

Owing to both natural and artificial influences the tidal volume of the Oosterschelde during the past century has shown an increase of about 25%. As a result, large amounts of sand have been eroded in the Oosterschelde. Also, in the proximal part of the ebb-tidal delta some large intertidal shoals have completely disappeared and major ebb channels have deepened and expanded in a seaward direction. Part of the eroded material has been incorporated in the distal part of the tidal delta, giving rise to a gradual seaward extension of the large ebb shields and part of the underwater delta front.

This paper shows that after 1969 the processes accelerated and illustrates how this was related to hydraulic changes induced by the damming of certain channels; as a consequence of the damming of the Volkerak in 1969 the tidal prism of the Oosterschelde increased by about 8%. The damming of the Geul in the mouth of the sea-arm cuased a further increase in tidal discharges through the Roompot and the Schaar van Roggenplaat channels.
It might have been reasonable to expect that the accelerated net sedimentation in the tidal delta and associated morphological trends in delta front progradation and ebb channel expansion would have slowed down some years after the sudden increase in the tidal prism that was caused by the damming of the Volkerak. No confirmation for this hypothesis could be found, however, in the results of calculations on the sand budget and the progress of the morphological changes. This could possibly be explained by a temporary further 3% increase in the tidal prism – after the initial 8% increase due to the damming of the Volkerak – related to the 18.61 year cyclic change in the tidal range. More certainly about this possibility will be obtained before long, as the calculations of the sand budget since 1960 are extended to the estuary and the coastal zone to the north.

Acknowledgements

I thank Poppe de Boer for some valuable suggestions improving the manuscript.

References

ANONYMOUS 1983. Het getijverschil te Yerseke na de voltooiing van de Oosterscheldewerken – Driemaandelijks Bericht Deltaweken 105: 247–250.
DE RONDE, J. G. 1983. Changes of relative mean sea-level and of mean tidal amplitude along the Dutch coast. In: Ritsema A. R. & A. Gürpinar (eds): Seismicity and seismic risk in the offshore North Sea-area: 131–142.
DRONKERS, J. J. 1969. Tidal computations for rivers, coastal areas and seas – ASCE, J. Hydr. Div. 95 (HYI): 29–77.
GOTTSCHALK, M. K. E. 1971. Stormvloeden en rivieroverstromingen in Nederland I: de periode vóór 1400 – Van Gorkum (Assen): 581 pp.
HARING, J. 1978. De geschiedenis van de ontwikkeling van de waterbeweging en van het profiel van de getijdewateren en zeegaten van het zuidelijk deltabekken en van het hierbij aansluitende gebied van de kust gedurende de perioden 1872–1933–1952–1968–1974 – Rijkswaterstaat, Delta Dept, nota K77MO31E: 41 pp.
LABAN, C. & R. T. E. SCHÜTTENHELM 1981. Some new evidence on the

origin of the Zeeland ridges. In: Nio, S. D., R. T. E. Schüttenhelm & Tj. C. E. van Weering (eds): Holocene marine sedimentation in the North Sea Basin – IAS Spec. Pub. 5 – Blackwell (Oxford): 239–245.
MORRA, R. H. J., H. M. OUDSHOORN, J. N. SVAŠEK & F. J. DE VOS 1961. The movement of sand in the tidal region of the southwestern part of the Netherlands – Rep Delta Comm. V: 328–380.
SIEGENTHALER, C. 1982. Tidal cross-strata and the sediment transport rate problem: a geologist's approach – Mar. Geol. 45: 227–240.
TERWINDT, J. H. J. 1971. Litho-facies of inshore estuarine and tidal inlet deposits – Geol. Mijnbouw 50: 515–526.
– 1973. Sand movement in the in- and offshore tidal area of the SW part of the Netherlands – Geol. Mijnbouw 52: 69–77.
– 1981. Origin and sequence of sedimentary structures in inshore mesotidal deposits of the North Sea. In: Nio, S. D., R. T. E. Schüttenhelm & Tj. C. E. van Weering (eds): Holocene marine Sedimentation in the North Sea Basin – IAS Spec. Pub. 5 – Blackwell (Oxford): 04–26.
VAN DEN BERG, J. H. 1981. Rhythmic seasonal layering in a mesotidal channel abandonment facies, Oosterschelde mouth, SW Netherlands. In: Nio, S. D., R. T. E. Schüttenhelm & Tj. C. E. van Weering (eds): Holocene marine sedimentation in the North Sea Basin – IAS Spec. Pub. 5 – Blackwell (Oxford): 147–159.
– 1982. Migration of large-scale bedforms and preservation of crossbedded sets in highly accretional parts of tidal channels in the Oosterschelde, SW Netherlands – Geol. Mijnbouw 61: 253–263.
VAN DEN BERG, J. H., P. L. DE BOER & M. J. VISSER 1980. Field course guidebook on clastic tidal deposits – Publ. Comparative Sedimentology Div. State Univ. of Utrecht: 67 pp.
VAN DE KREEKE, J. & J. HARING 1979. Equilibrium flow areas in the Rhine-Meuse Delta – Coast. Eng. 3: 97–111.
VAN RUMMELEN, F. F. F. E. 1978. Toelichting bij de Geologische kaart van Nederland 1: 50.000, Noord-Beveland – Rijks Geol. Dienst, Haarlem: 138 pp.
VISSER, M. J. 1980. Neap-spring cycles reflected in Holocene sub-tidal large-scale bedform deposits: a preliminary note – Geology 8: 543–546.
VOOGT, J. & A. ROOS 1980. The storm surge barrier and its effect on the estuary's tidal regime. In: Paape, A. J. Stuip & W. A. Venis (eds): Hydraulic aspects of coastal structures, I. – Delft Univ. Press (Delft): 59–72.
WILDEROM, M. H., 1964. Tussen afsluitdijken en deltadijken II: Noord-Zeeland – Littooy & Olthoff (Middelburg): 415 pp.

3. Migration of large-scale bedforms and preservation of cross-bedded sets in highly accretional parts of tidal channels in the Oosterschelde, SW Netherlands

Reproduced from Geologie & Mijnbouw vol. 61 (3), 1982, pages 253–263 by permission of the editors.

Abstract

Recent large-scale crossbedded sands have been studied in two construction pits of the 'Delta Project' in the Oosterschelde, The Netherlands. The deposits are formed by long crested megaripples of about two metres high at a depth of 4 to 17 metres below Mean Sea Level.

Crossbedded sets have been analysed for stand-still phases of megaripple migration during the subordinate tide (pause planes). An average lee side accretion rate of the dunes was calculated from the cyclic neap to neap tide change in thickness of the sand layers between successive pause planes.

Information on the morphodynamics of the environment of deposition and the rate of accumulation of the discussed units was acquired through some particular sedimentary structures and through the study of series of hydrographic charts of the area. The latter information also strongly suggests a wide occurrence of alike sedimentary units in the subsurface of shoals of the Oosterschelde mouth and outer delta. Finally the thickness and the number of the sets in relation to sandwave migration and rate of accumulation is discussed.

Introduction

Deep pits, dug at several locations in the tidal inlets of the SW Netherlands for the foundation of sluices and other heavy constructions, enable a detailed study of subrecent tidal deposits, laid down at depths as much as 15 m below Mean Sea Level. OOMKENS & TERWINDT (1960) and TERWINDT (1971) have described several lithologically and structurally different units which can also

be recognised in cores, and these authors have related them to conditions of flow. In a recent paper the latter author desbribed 7 lithofacies of assemblages of sedimentary structures and lithology, all reflecting a particular process or subenvironment (TERWINDT, 1981).
A paper by VISSER (1980) focused attention on the recognition of ebb/flood and spring/neap cyclus in x-bedded[1] sets; the occurrence of seasonal bedding in an abandoned channel fill has been reported by VAN DEN BERG (1981b).
The present paper is devoted to the origin of some unidirectionally x-stratified intervals built up in tabular sets with great set heights (up to 2.4 m) exposed in the 'Philipsdam' and 'Schaar' pits in the Oosterschelde tidal basin, SW Netherlands (for location, see Fig. 3.1).

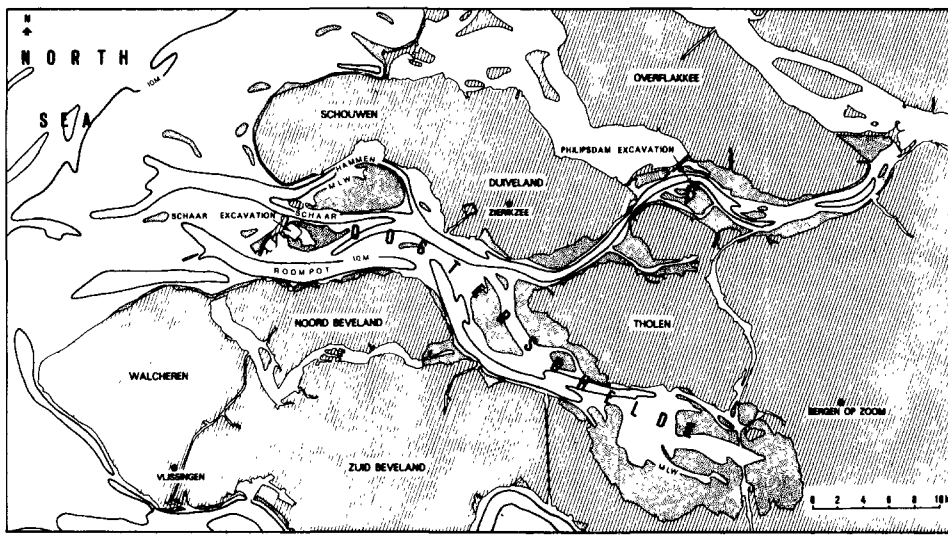

Fig. 3.1 Location of studied outcrops

The Philipsdam exposure

This exposure was situated in the southwestern part of the 'Philipsdam' pit at a depth of 3 to 9.5 m below Mean Sea Level.

Hydrographic background
The depositional history is well-documented by a series of sounding charts made by the 'Rijkswaterstaat' (the Governmental Board for Roads, Waterways and Harbours) of which annual editions are available from 1959 onwards. In the early years of this series of soundings the exposure was located at the southern bank of the Krammer channel (fig. 3.2).

[1] x-bedding in this paper refers to cross-stratification produced by migrating megaripples, while x-lamination is used for cross-stratification produced by small scale ripples.

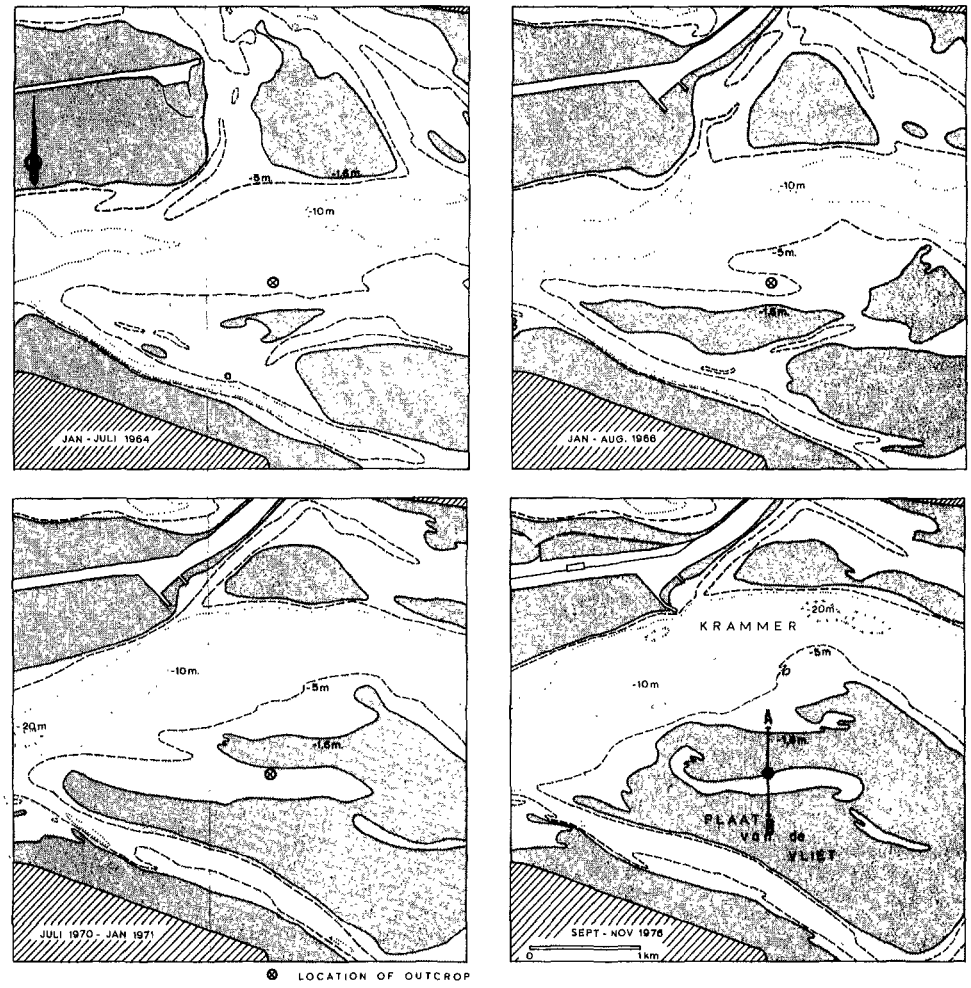

Fig. 3.2 Hydrography of the Krammer channel and adjacent shoals 1964–1976
A – B = cross section in Fig. 3.3

Originally the Krammer channel was part of a complicated net of tidal inlets east of the island of Schouwen-Duiveland.
With the construction of a dam accross this area (1962–1964) an artificial tidal watershed was established. As a consequence, the ebb discharge of the Krammer channel increased by about 25% (VAN DEN BERG, 1981a), initiating a rapid process of channel bending and deepening. Between 1965 and 1975 erosional retreat of the outer bank of the channel amounted locally to more than 600 m. Simultaneously considerable amounts of sand were deposited on the southern inner bend. The pattern and rate of accretion in this area were strongly influenced by the formation of a secondary flood channel, which in its most active stage – between the soundings of 1964 and 1965 – even resulted in

some erosion in its thalweg zone. At the site of the exposure this channel cut down to a depth of 9 m below M.S.L. After 1965 the flood channel silted up rapidly, and in 1973 it was abandoned because of the formation of a sill in its western connection with the Krammer main channel (Fig. 3.2). The exposure is a longitudinal section located in the midst of the channel fill. The process of silting up in this area in the course of some years, as revealed by sounding charts, is visualized by a transverse section of the channel fill (Fig. 3.3).

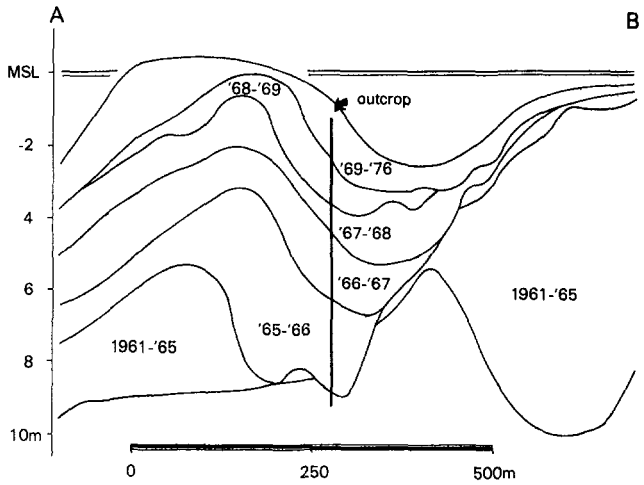

Fig. 3.3 Chronology of deposits in a cross section through the channel fill exposed in the Philipsdam pit, reconstructed on the basis of sounding charts (A – B in Fig. 3.2)

General description of the exposed sequence and its relation to hydrographic changes

The median grainsize of the deposit varies between 150 and 200 μm. The coarsest fraction consists of small to boulder size peat fragments derived from Holocene peat layers (Holland peat) which locally are exposed in channel banks. At about 9.0 m below M.S.L. the base of the channel fill is marked by a lag deposit consisting of somewhat coarser sand with many bivalve shells, shell debris and some artefacts like brick-bats. Sedimentary structures of the channel fill consist of easterly directed tabular x-bedding, passing upwards into an x-laminated unit (Fig. 3.4).

It is clear that this easterly directed x-bedding reflects the direction of the dominant flood current. The upward transition to an x-laminated unit expresses the decrease in current intensity, related to the gradual channel abandonment. The directions of the x-bedding correspond with the directions of the tidal currents, as inferred from sounding charts. In the following section the lower x-bedded interval will be dealt with in more detail.

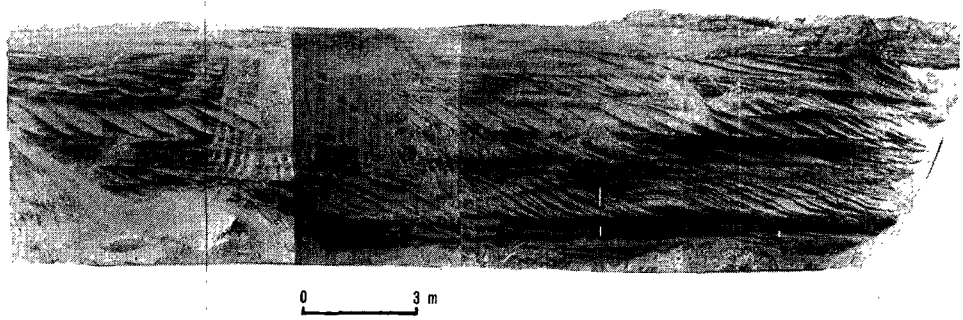

Fig. 3.4 The Philipsdam exposure

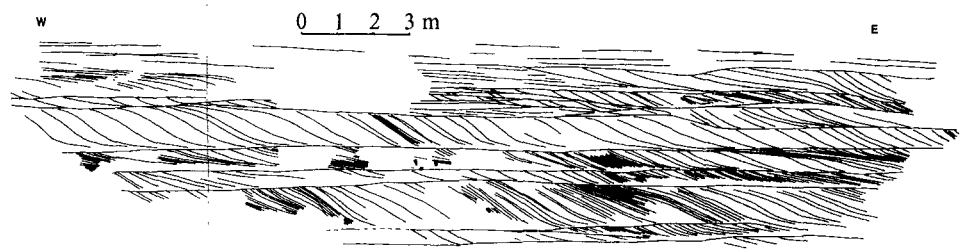

Fig. 3.5 Set boundaries and pause planes in the Philipsdam exposure

The coset of x-bedding

According to the classification of inshore tidal deposits by TERWINDT (1981) the lower x-bedded interval belongs to the lithofacies STRO CUR (strong currents) representing '.... a period of intensive transport in the form of mega-ripples ....'.

The lower 2.5 m of the coset was deposited in the period between the soundings of 1965 and 1966. The upper part was formed during the following two years (see Fig. 3.3). During deposition of this sequence, neap, mean and spring tidal ranges have been resp. 2.5, 3.1 and 3.5 m. The straight set boundaries in the exposed longitudinal section suggest deposition by straight long-crested bedforms. However, small sections perpendicular to the same outcrop revealed trough-shaped x-bedding. So lower set boundaries approach cylindrical forms and sets must have been produced by sinuous to cuspate bedforms. In order to produce the cylindrical set boundaries, scour pits in front of the crestlines must have migrated downstream together with the ripple bedforms.

The inferred ripple morphology corresponds with the ripple crest pattern visible at the bank of the channel on a contemporaneous aerial photograph (Fig. 3.6). The unidirectional foresets to the east are in agreement with the predominance of the flood current as expressed by channel geometry and megaripple asymmetry.

Within the foresets the cyclic tidal current reversal has resulted in the generation of 'tidal bundles' that are laterally enclosed between 'pause planes'. Such planes

are defined by TERWINDT (1981) as erosional or non-erosional surfaces representing the stand-still phase of megaripple migration during the subordinate tide. In fact a tidal bundle reflects the net ripple progradation during one tidal cycle.

Pause planes may be draped by one or two thin mud laminae representing slack water. Usually most of the slack water drape deposited on the ripple front directly after the dominant tide, is eroded. Only a mud drape laid down after the subordinate tide is preserved. In toesets some evidence could be found for the preservation of both high and low slack water periods which VISSER (1980) calls 'mud layer couplets', enclosing veneers of sand deposited by the subordinate current.
In wet sections pause planes could hardly be traced if non-erosional and not covered by a mud drape, which often is the case in the exposure. However, in case of absence of mud drapes, pause planes still became visible in drying sections. This is due to the fact that during slack water sand grain interstices in a thin layer below the pause planes, are partly filled with fine material. During dry weather conditions, these thin layers become slightly protrusive as they retain capillary water more easily and thus are less susceptible to erosion by dessication and wind. Set boundaries and pause planes in the exposed x-bedded sets are indicated in Fig. 3.5.

Bundles of sand vary in thickness from a few mm to more than 50 cm. The series of bundles in one set often show cyclic variations in thickness. This is (may be) attributed to properties of the tide (VISSER & DE BOER, 1982): periods of diurnal inequality of the tide, which produce an alternation of high and low velocities of the dominant tidal current, are reflected in series of alternating thick and thin bundles (Fig. 3.7). The 28 to 29 days neap-spring tide cycle, as described by VISSER (1980) is very clear; series of thin bundles are produced in the days around neap tide, whereas relatively thick bundles are generated around spring tide (see Fig. 3.5). Apart from the cyclic change in bundle thickness the neap to neap tide sequence of bundles manifests itself in a number of sedimentary features, summed up by TERWINDT (1981).

Several of these may be noted here briefly: thick toesets corresponding with thin bundles of the days around neap tide; erosive pause planes – especially in the upper part of sets – generated by stronger subordinate currents in the zone of thick bundles produced around spring tide.

Bedform preservation and set thickness
Maximum set heights of individual x-bedded units range from 0.2 to 1.5 m.

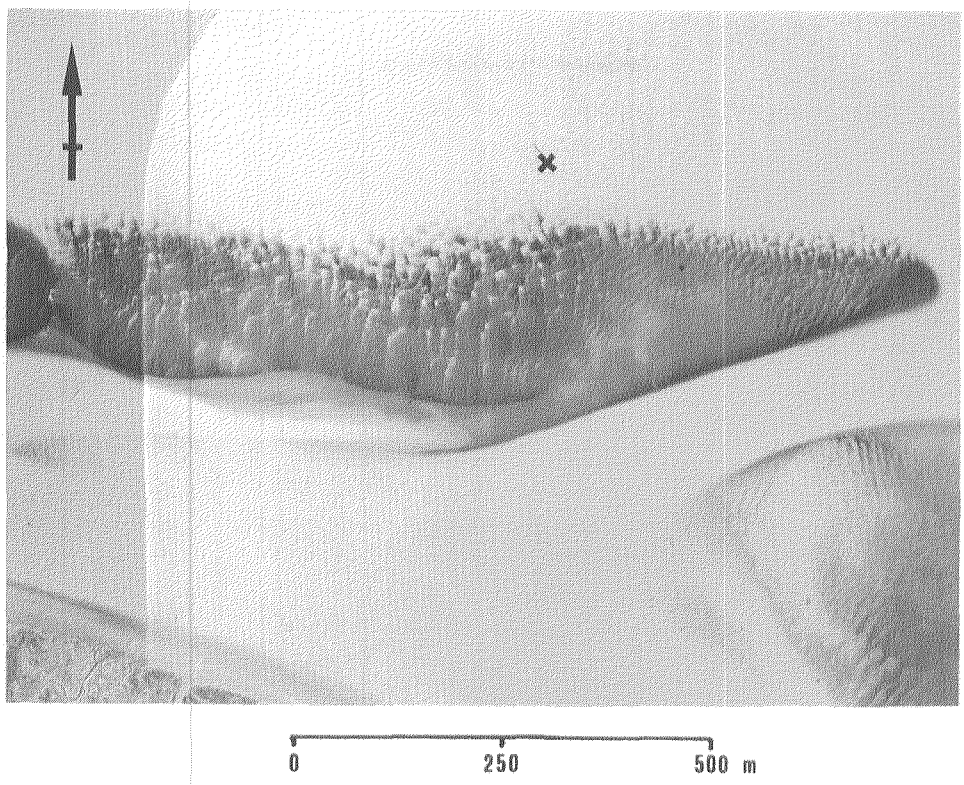

Fig. 3.6 Aerial photograph of the Krammer channel on May 12, 1966 at low tide (location of studied outcrop indicated by X)

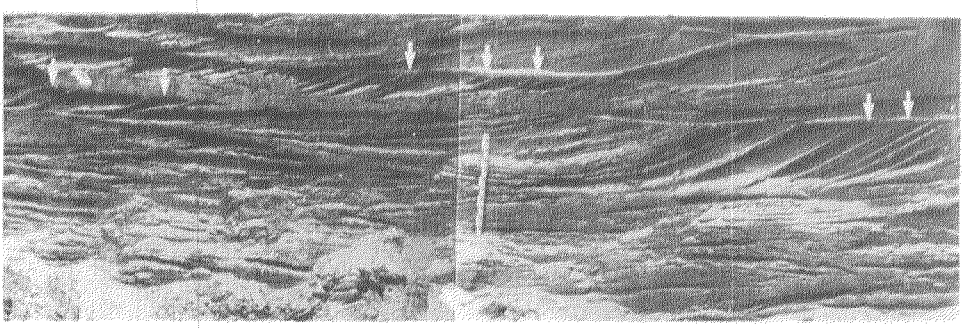

Fig. 3.7 Series of alternating thick and thin bundles of x-bedded sand (indicated by arrows) reflecting the diurnal inequality of the tide.
Length of graduated stick is 1 m

From the still available record of numerous soundings of the area, made in the period of rapid accumulation in the channel, a maximum ripple height of 1.5 m is deduced. The set heights measured in many places of the exposure point to an almost complete preservation of ripple front deposits, and therefore to an extremely high rate of sedimentation.

Unfortunately all sounding tracks run more or less perpendicularly to the direction of the channel axis and thus do not provide information in ripple spacing. However, this spacing can be estimated by comparing the rate of accumulation in the channel and the rate of migration of the set-producing bedforms.
In the time period between the sounding surveys of 1965 and 1966 – 357 days – the mean water depth of the area was reduced by 2.4 m (from approximately 9.0 to about 6.6 m, see Fig. 3.3). At the site of the exposure in this period 4 to 5 sets were preserved. An average migration rate of set-producing ripples in this interval of 12.8 m in a synodical month (29.53 days), or 155 m in the period between the soundings, can be deduced from the length of neap to neap bundle sequences.
Assuming that in this year of rapid sedimentation all bypassing ripples at the site of the exposure have contribited to deposition, an average ripple spacing of 31 to 39 m is calculated. Based on numerous soundings of ripple fields in thalwegs of tidal channels in the SW Netherlands, it was found, that ripples with a height of more than 1 m indeed do have spacings between 15 and 50 m (TERWINDT, 1971). Even in the case of a minimum of 15 m, still more than 40% of the bypassing ripples would have contributed to deposition.

This assumption, however, implies an irregular pattern of alternating rapid sedimentation and erosion which does not fit in a process of gradual channel abandonment. This consideration, together with the fact that on the photograph at the bank ripples show spacings of generally over 25 m, strongly indicates that in this lower part of the sequence most, if not all, bypassing ripples are represented in preserved sets.

The 'Schaar' exposure

This exposure is situated in the southwestern part of the 'Schaar' excavation in the mouth of the Oosterschelde (Fig. 3.1). A general impression of the whole outcrop may be obtained from Fig. 3.8. Seven lithostratigraphic units have been distinguished that are largely based on sedimentary structured (VAN DEN BERG ET AL, 1980). Here, attention is focussed on the lower two units (A en B).

Hydrographic background
Chronologically, the exposed deposits can be divided into two parts:

– from inspection of hydrographic charts, dating as far back as the beginning

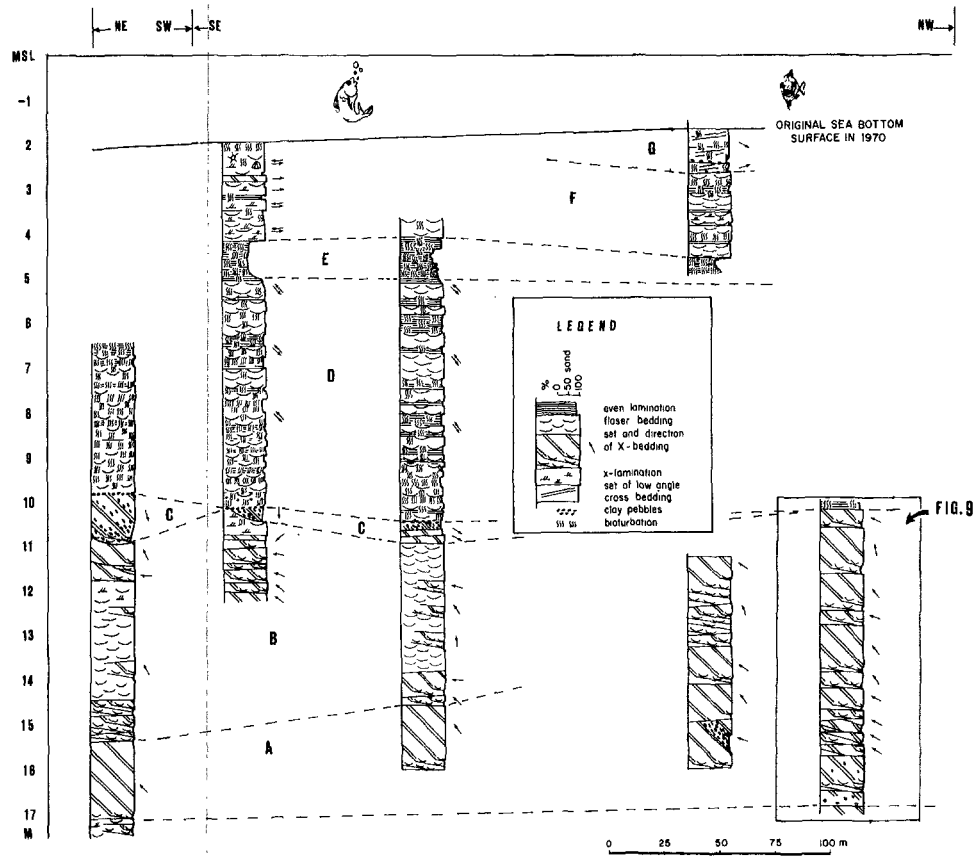

Fig. 3.8 General outline of the Schaar exposure

of the 19th Century, it follows that units A and B have been deposited at a depth which was not affected by tidal channels after the 18th Century.

It is established from the presence of juvenile specimens of Mya Arenaria (pers. comm. Dr. G. Spaink), a bivalve species imported by man from the Atlantic coast of North America at the end of the 16th Century (HESSLAND, 1946), that these deposits date from the 17th–18th Century. This means, that they are formed in an environment similar to that of the present or at least that of the 19th Century Oosterschelde mouth.

– according to hydrographic charts, sediments down to a depth of 11 m below Mean Sea Level (units C–G) have been deposited after A.D. 1860. Most of these were formed in the second and third decade of the 20th Century and consist of rhythmic seasonal bedding produced in an abandoned channel (VAN DEN BERG, 1981b).

In addition it may be remarked, that the depths at which the deposits are exposed can be considered as depositional depths and – because of their relative youth – those depths do not need to be corrected for a relative rise of the sea level, as is the case with older Holocene deposits.

General description of the sequence of large-scale cross-bedding

At the base of the 'Schaar' pit a dragline straightened and planed in steps nearly vertical exposures of adjacent parts of the excavated wall. After cleaning and smoothing with a shovel and trowel, photographs were taken of the walls and measurements were made.

In this way an exposure of a 70 m long and almost 5.8 m high section of unit A could be studied in detail. Like the Philipsdam example, this exposure represents a longitudinal section (parallel to the main current direction). An overall view of set boundaries and pause planes, drawn after photographs is given in Fig. 3.9

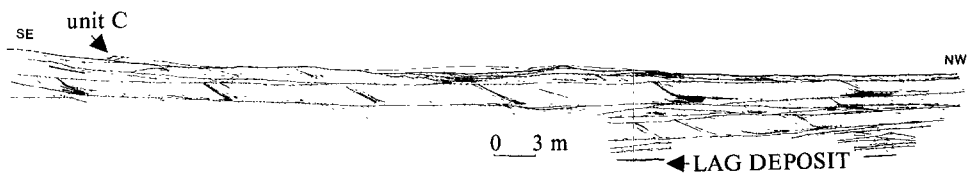

Fig. 3.9 Set boundaries and pause planes in the Schaar exposure (for location see Fig. 8)

Unit A consists of generally NW to N (ebb) directed x-stratification. Lower set boundaries are planar to weakly cylindrical. The more or less straight foresets merge into well-developed bottomset layers. Sets are up to 2.5 m high. Foresets reveal the same features as the tidal bundles described from the Philipsdam exposure with the exception that slack water mud drapes are much better developed. They may be up to 3 mm thick. The thickest mud drapes enclose the thin bundles that were produced in the days around neap tide and reflect the relatively long slack water period at that time. In toe- and bottomsets both high and low water slack periods are generally represented in mud layer couplets.

The base of the unit is formed by a lag deposit with similar characteristics as the channel lag at the base of the outcrop in the Philipsdam pit. To the SE in an upward direction, unit A passes gradually into unit B. The latter unit is characterised by mixed flaser bedding and ebb-oriented x-stratification. Flasers are formed on gently inclined slopes (predominantly at an angle of 5 to 10 degrees to the SW). Within the flaser beds solitary x-bedded sets occur which develop and disappear within short distances (see Fig. 3.10). The median grain size of both units varies between 150 and 210 microns.

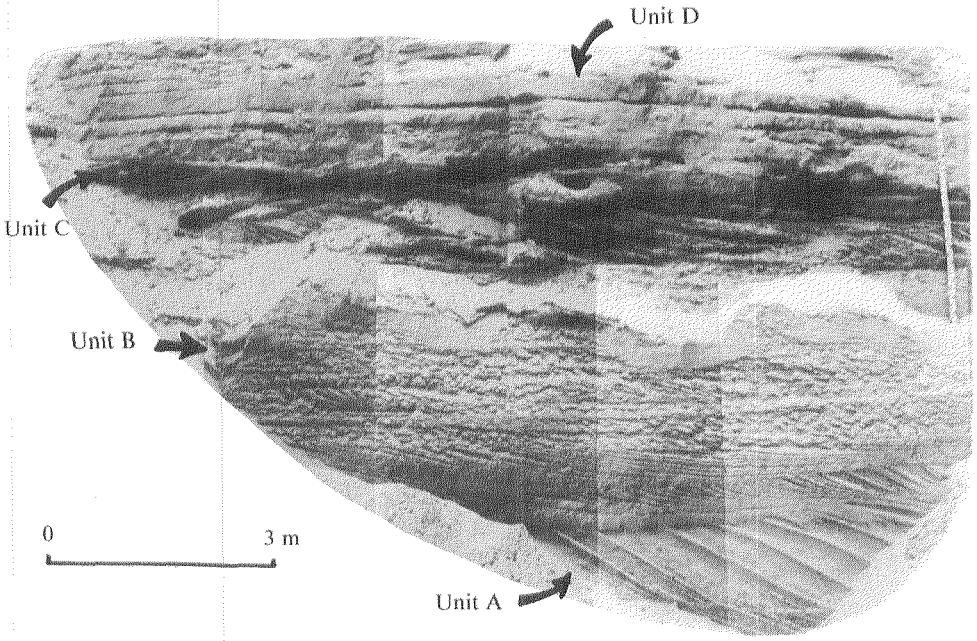

Fig. 3.10 The transition of unit A to unit B

Flood versus ebb current directions

Erosion of the steep lee-side of the megaripple (due to the subordinate flood current), is expressed in discontinuity planes between foreset strata. As might be expected most pronounced discontinuity planes coincide with thick bundles produced around spring tide. These erosional planes may contain a pattern of small-scale ripples generated by the subordinate tide. Such an occurrence was found in the two exposures which were studied, as well as in a number of previously described examples of recent and ancient tidal deposits. (TERWINDT, 1981 : NIO ET AL, 1980 ; DE RAAF & BOERSMA, 1971 ; BOERSMA, 1969; ALLEN & NARAYAN, 1964; HOMEWOOD, 1981). In the sequence discussed here, the presence of well-developed slack water mud drapes overlying these ripples allowed an examination of the small scale ripple pattern, which indicated that the ripples have straight to sinuous crestlines. Ripple crest alignments and deduced migration directions could be measured easily by cutting back exposed ripple cross-sections with a trowel.

After numerous measurements it appeared that the average migration direction of these ripples is not completely opposite to the x-bed direction but shows a remarkable deviation to the left (Fig. 3.11). This is not necessarily an indication of not-oppositely directed tidal currents. One might also think of a consistent deviation between ripple lee slope azimuth and dominant current direction as

a result of a lateral gradient in current velocity. Certainly, the feature points to a peculiar hydraulical and morphological situation which obviously continued during deposition of the whole sequence.

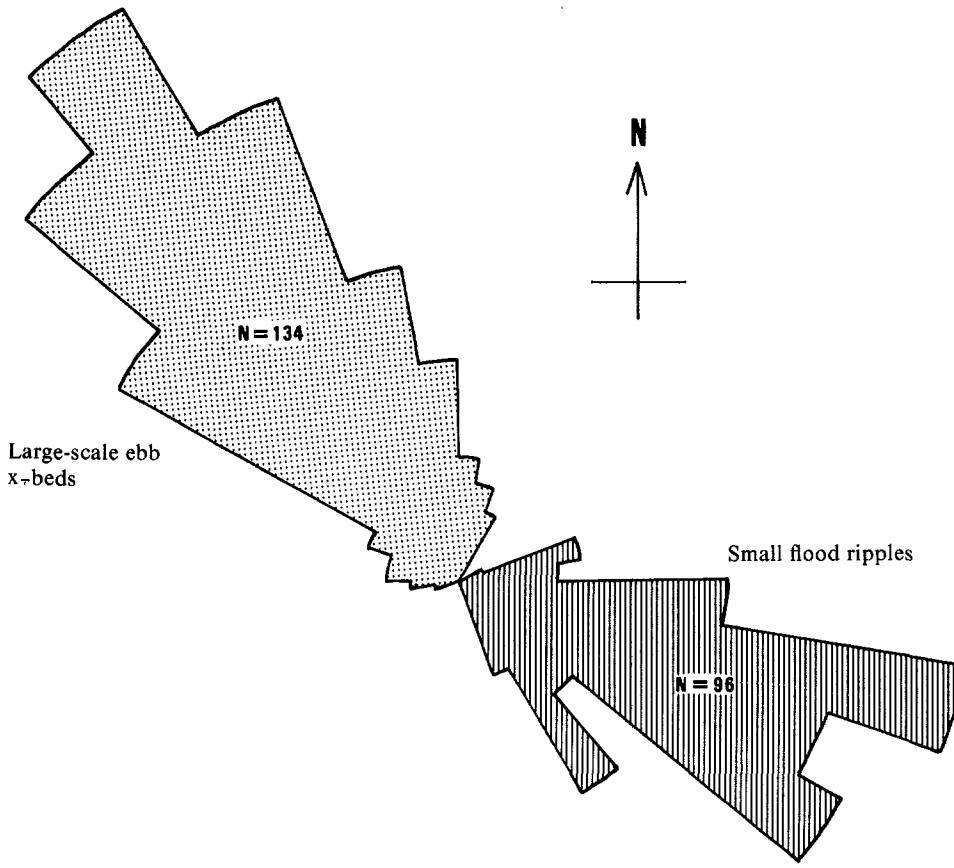

Fig. 3.11 Ebb x-bed azimuths and flood ripple migration directions

Bedform preservation and set height

In the 'Schaar' exposure the range of the maximum set heights is about the same as the one reported from the Philipsdam example. The fact, that at present ripple heights in the Oosterschelde rarely exceed 2 meters (TERWINDT, 1970) points to a comparable degree of preservation of ripples as was found in the Philipsdam pit. The presence of brinkpoint structures in the upper part of some of the thickest sets may further be mentioned as a significant indication of nearly complete preservation of ripple front deposits. A close-up of these structures is given in Fig. 3.12.

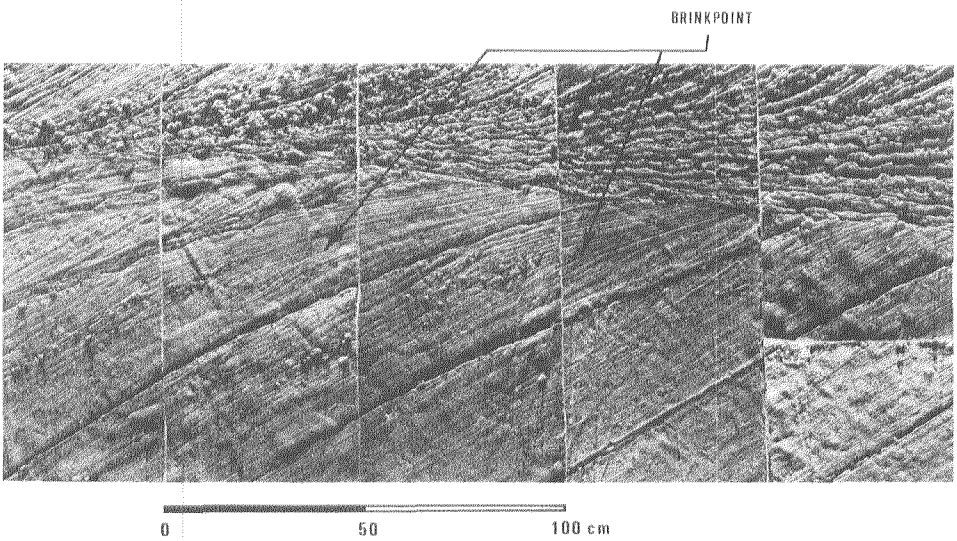

Fig. 3.12 Lacquer peels showing brinkpoint structures in the upper part of an x-bedded set

The depositional sequences of both the Schaar and the Philipsdam exposures have very much in common. Therefore it seems reasonable to base estimates of the rate of accumulation in this environment on the Philipsdam example. According to the length of the exposed neap to neap tide sequences, the average migration rate of the large scale bedforms was 278 m per year. If a preservation of all bypassing ripples and a minimal ripple spacing of 15 m is assumed, a maximum (vertical) accretion rate of 10.2 m in one year is calculated.

Depositional environment

The first reliable hydrographic chart covering the Oosterschelde area is the 'Carte réduite des côtes des Pays-bas', made and published by the famous French cartographer Beautemps-Beaupré in 1817. Since then the area was surveyed repeatedly by the Dutch Hydrographic Service. From the available editions of the 19th and the beginning of the 20th Century, 6 maps have been selected and have been adjusted to a standard way of presentation (Fig. 3.13).

Although the discussed sequence was deposited before the first reliable map of the area was made, the series of charts provide an important indication of the probable depositional environment. The maps show a rapid change of a complex pattern of channels and shoals. The channels can be divided into ebb, flood and continuous channels, according to their topography (VAN VEEN, 1950). Two major channels can be distinguished, separated by a broad shoal area intersected by a number of roughly NW–SE directed ebb and flood channels.

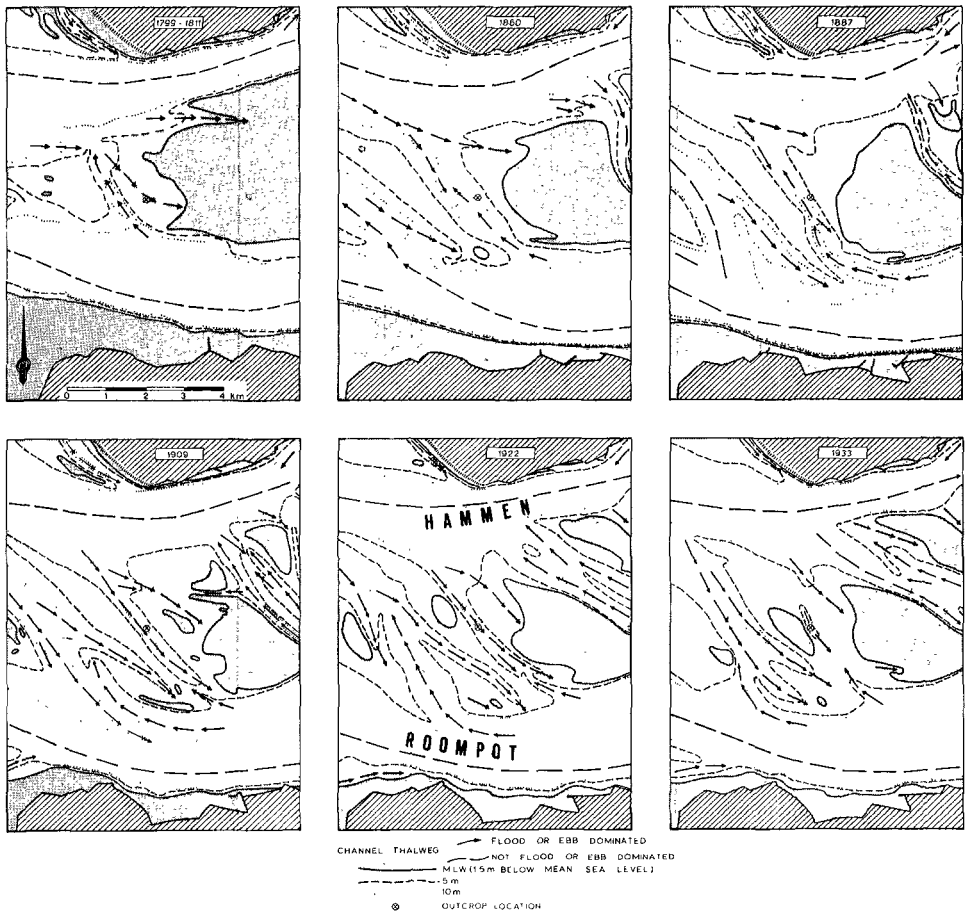

Fig. 3.13 Hydrography of the Oosterschelde mouth between 1800 and 1933

The distribution of ebb and flood channels points to systematic temporal differences in water elevation between the northern and southern margin of the shoal area during the tidal cycle; all flood channels were connected with the northern major channel (Hammen), whereas all ebb channels originated from the southern major channel (Roompot). This means, that during flood the net transport of water was from the northern into the southern major channel. During ebb water flowed in an opposite direction. The tidal currents from the major channels were diverted into the smaller ebb and flood channels. As in river meander loops, this resulted in erosion of the outer bends of the channels, whereas deposition took place in the inner bends. This caused an eastward lateral shift of the flood channels which were connected with the northern major channel. The ebb channels on the contrary (which were connected with the southern major channel) migrated westward.

The lateral migration was sometimes very fast: e.g. an ebb channel south of the location of the construction pit shifted 2 km to the west in the period from 1887 to 1922. From the history of the Oosterschelde entrance (DE BRUIN & WILDEROM, 1961; WILDEROM, 1964; VAN DEN BERG ET AL, 1980) it can be deduced, that the 19th century morphodynamic system began to evolve in the 18th Century. Since the northern rim of the Roompot channel at that time was situated more to the north and closer to the pit, it is likely that one or more ebb channels migrated across the location of the pit. The possibility that the sequence under discussion was produced at the passage of such a channel – for instance in an early stage of the ebb channel which was present near the location of the pit in the beginning of the 19th century – is supported by the following considerations:

- The 19th century ebb channels eroded to a maximum depth of 15–20 m; the channel lag at the base of the exposure was found at a similar depth of 16–17 m.
- The rapid shift of ebb channels involves rapid accretion on the inner banks. This is in agreement with the postulated high sedimentation rate of the x-bedded sequence.
- The gradual upward transition to the flaser beds of unit B could very well reflect a decrease in current intensity in connection with a lateral shift of an ebb channel (OOMKENS & TERWINDT, 1960).
- The direction and angle of inclination of most of the flaser beds closely corresponds with slope characteristics of accretional banks of 19th century ebb channels.

Conclusions

The sequences studied in the Philipsdam and Schaar excavations have been built up rapidly in a channel which was dominated by one of the tidal currents. They represent respectively a stable channel which was abandoned by the tidal currents, and an actively migrating channel environment. The high rate of accumulation is manifested by large set heights in comparison with the amplitude of the original bedforms. These bedforms were straight to sinusoidal megaripples, with a maximum height of about 2 metres, and migrated in the direction of the dominant current at a speed of 5 to 15 metres in a neap to neap tide cycle. During this accretion most or all of the dunes which passed by probably contributed to the sedimentary record.

High accretion areas make up only a small part of the Oosterschelde sea arm. They are generally confined to channel banks of rapidly migrating channel systems. The Philipsdam example may be considered an exception to this rule. Despite the rather scanty occurrence of recent high accretion areas in the

environment, their fossil deposits should have a wide occurrence in the subsurface: in the past two centuries a large portion of the shoal complexes of the Oosterschelde mouth and outer delta have been reworked by such dynamic channels down to a depth of 10 to 20 metres. Most deposits of these channels represent rapidly built-up accretional bank units, in which sequences like those described in this paper presumably have a great preservation potential.

Acknowledgements

I express my appreciation to the engineering staff of Rijkswaterstaat at the 'Schaar' construction pit for arranging appropriate sections. The manuscript has benefited from critical reviews by Carola Romein, André van Gelder and Poppe de Boer. I gratefully acknowledge their contributions.

References

ALLEN, J. R. L. & J. NARAYAN 1964 Cross-stratified units, some with silt bands, in the Folkstone beds (Lower Greensand) of southeast England – Geol. Mijnbouw 43: 451–461.
BOERSMA, J. R. 1969 Internal structure of some tidal mega-ripples on a shoal in the Westerschelde. Report of a preliminary investigation – Geol. Mijnbouw 48: 409–414.
BOERSMA, J. R. & J. H. J. TERWINDT 1981 Neap-spring tide sequence of intertidal shoal deposits in a mesotidal estuary – Sedimentology 28: 151–170.
DE BRUIN, M. P. & M. H. WILDEROM 1961 Tussen afsluitdijken en deltadijken – Noord-Beveland, geschiedenis van strijd, nederlaag en overwinning op het water – Littooy & Olthoff (Middelburg): 304 pp.
DE RAAF, J. F. M. & J. R. BOERSMA 1971 Tidal deposits and their sedimentary structures – Geol. Mijnbouw 50: 479–504.
HESSLAND, J. 1964 On the Quaternary Mya Period in Europe – Arkiv för Zoologi 37A: 01–51.
HOMEWOOD, P. 1981 Facies et environnements de dépôt de la Molasse de Fribourg – Eclogae Geol. Hel. 74: 29–36.
NIO, S. D., J. H. VAN DEN BERG, M. GOESTEN & F. SMULDERS 1980 Dynamics and sequential analysis of a mesotidal shoal and intershoal channel complex in the Eastern Scheldt (southwestern Netherlands) – Sed. Geol. 26: 263–279.
OOMKENS, E. & J. H. J. TERWINDT 1971 Inshore estuarine sediments in the Haringvliet – Geol. Mijnbouw 39: 701–710.
TERWINDT, J. H. J. 1970 Observation on submerged sand ripples with heights

ranging from 30 to 200 cm occurring in tidal channels of SW Netherlands – Geol. Mijnbouw 49: 489–501.
– 1971 Litho-facies of inshore estuarine and tidal inlet deposits – Geol. Mijnbouw 50: 515–526.
– 1981 Origin and sequences of sedimentary structures in inshore mesotidal deposits of the North Sea. In: Nio S. D., R. T. E. Schüttenhelm & Tj. C. E. van Weering (eds): Holocene Marine Sedimentation in the North Sea Basin. IAS Spec. Publ. 5 – Blackwell (Oxford); 04-26.
VAN DEN BERG, J. H. 1981a Morfologische ontwikkeling van het Krammer en het Slaak tijdens de aanleg van de Philipsdam – Nota DDWT 81.024 Rijkswaterstaat: 38 pp.
– 1981b Rhythmic seasonal layering in a mesotidal channel abandonment facies, Oosterschelde mouth, SW Netherlands. In: Nio, S. D., R. T. E. Schüttenhelm & Tj. C. E. van Weering (eds): Holocene Marine Sedimentation in the North Sea Basin. IAS Spec. Publ. 5 – Blackwell (Oxford): 147–159.
VAN DEN BERG, J. H., P. L. DE BOER & M. J. VISSER 1980 Field course guidebook on clastic tidal deposits – Publ. Comparative Sedimentology Division. State University of Utrecht: 67 pp.
VAN VEEN, J. 1950 Eb- en vloedschaar-systemen in de Nederlandse getijwateren – Tijdschrift Kon. Aardrijksk. Gen. 2e reeks 67: 303–325.
VISSER, M. J. 1980 Neap-spring cycles reflected in Holocene sub-tidal large-scale bedform deposits: a preliminary note – Geology 8: 543–546.
VISSER, M. J. & P. L. DE BOER 1982 The effect of the diurnal inequality on tidal sediments: a tool in the recognition of tidal influences – IAS 3rd Eur. Mtg. Copenhagen 1982. Abstr.: 88–90.
WILDEROM, M. H. 1964 Tussen afsluitdijken en deltawerken II: Noord-Zeeland – Littooy & Olthoff (Middelburg): 415 pp.

4. Rhythmic seasonal layering in a mesotidal fill sequence, Oosterschelde mouth, the Netherlands

Reproduced from Special Publication 5 of the international Association of Sedimentologists, 1981, pages 147–159 by permission of Blackwell Scientific Publications.

Abstract

Sedimentary features of a subrecent channel fill sequence produced during abandonment of a 12 m deep tidal channel are described. The history of channel abandonment and subsequent infill is documented by detailed hydrographic charts. The sequence contains a 5 m thick layer composed of a rhythmic alternation of two facies. Evidence for a seasonal origin of this rhythmic bedding is provided by: the relationship between the thickness of individual couplets of winter and summer layers, and the annual rate of accumulation as interpreted from hydrographic charts; the growth and mortality pattern of some frequently occurring bivalve species (*Macoma balthica, Cerastoderma edule, Abra alba, Spisula subtruncata);* the different degrees of bioturbation between the two members of each couplet; the occasionally perceptible increase in diameter of internal traces (press structures) of the heart urchin *(Echinocardium cordatum)* in upward direction. Inorganic primary sedimentary structures point to remarkable low-energy conditions during deposition of the rhythmic beds. The summer facies consist of interlaminated mud, silt and fine sands. The winter layers are composed of flaser bedding. The transition from summer to following winter layer is slightly erosional, whereas a more gradual transition occurs from winter to summer layers. The thickness of individual winter-summer couplets ranges between 20 and 60 cm. Individual couplets may continue for hundreds of metres, especially in sections parallel to the axis of the channel.

Introduction

Thinly interlayered bedding caused by rhythmic seasonal changes is known

from many lake deposits, both recent and ancient. Seasonal rhythmites have also been described for several recent and ancient marine stagnant and evaporite basins. In general we are dealing with thin annual couplets consisting of two members of different lithological composition. This paper documents a rather different type of thick seasonal bedding that originated in a dynamic mesotidal environment (mean spring and neap tidal ranges are 3.5 and 2.3 m respectively).
The sequence is exposed in an excavation made in the mouth of the Oosterschelde tidal inlet (location see Fig. 4.1). A general impression of the studied outcrop may be obtained from Fig. 4.2. Seven lithostratigraphic units have been distinguished, based largely on sedimentary structures. The sequence of rhythmic beds (unit D in Fig. 4.2), located at a depth of 5 to 10 m below mean sea-level, was formed in an abandoned tidal channel during the second and third decade of this century (Fig. 4.3).
Data in this paper were collected from two exposures, described as outcrops A and B respectively (see Fig. 4.1).

General characteristics of the rhythmic beds

The rhythmic beds consist of fine sand (median grain size 110 μm) with an admixture of 5-20% mud. Following TERWINDT (1967, 1977) 'mud' includes all material having a fall velocity in water less than that of a quartz grain 50 μm in diameter. The primary sedimentary structures consist of an alternation of flasers and parallel laminated layers. The laminated layers generally have a higher mud content. A gradual transition from the flasers into the parallel laminated layers can be observed. The transition from parallel laminated layers into flaser layers, however, is sharp because it is slightly erosional.
A lithology of the rhythmic beds, observed in outcrop A, is given in Fig. 4.4.
The sequence of rhythmic layers is laterally persistent. It can be found throughout the exposed wall of the pit, a length of more than 200 m. The strike of the exposed wall is more or less parallel with the axis of the abandoned channel. All individual couplets can be traced laterally without any structural and lithological change.
The thickness of the individual couplets may show slight variation, however; this variation is probably related to differences of the depositional depth.
The lower part of the sequence shows more bioturbation, caused by 'press' structures of *Echinocardium cordatum* (SCHÄFER, 1962; REINECK & SINGH, 1973) and the dwelling traces of various polychaete worms. The transition from laminated into flaser layers within this lower part if often marked by a population of bivalve shells which are almost completely composed of doublets. These populations are mostly dominated by specimens of one

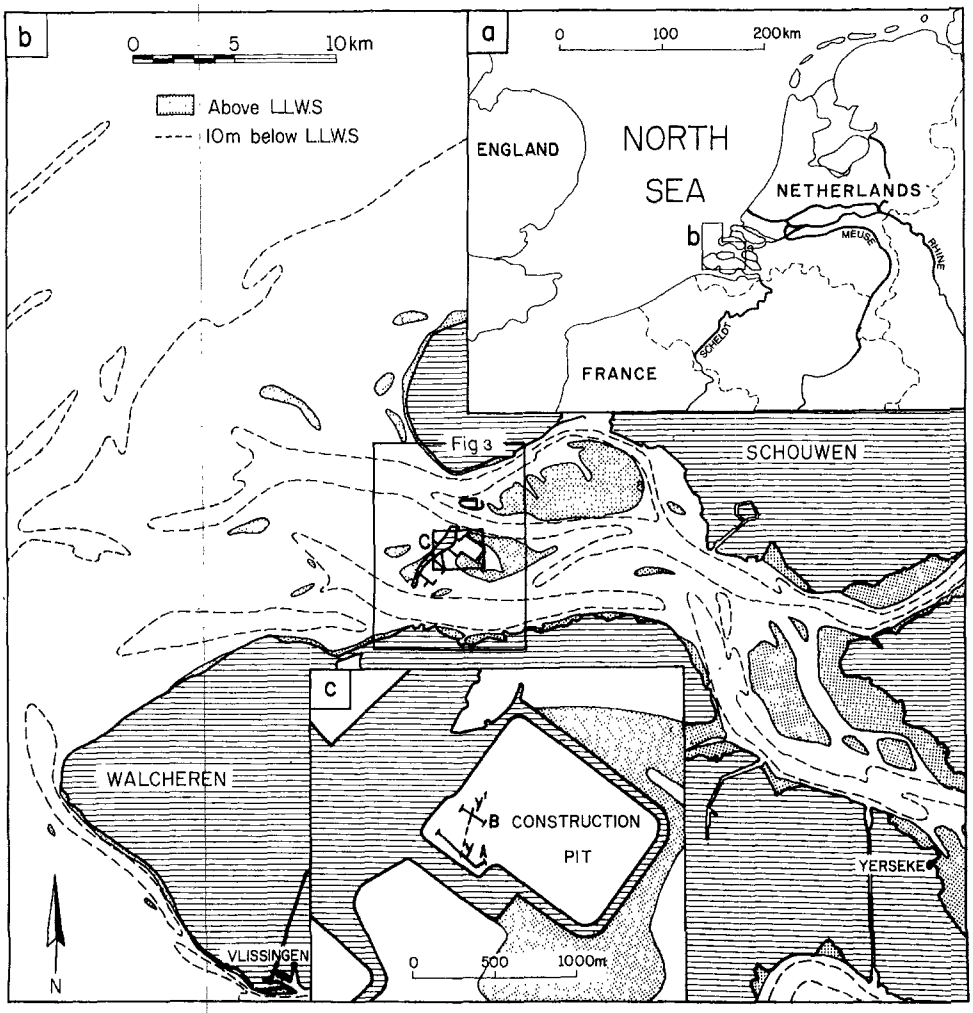

Fig. 4.1 Location of study area. Outcrop sites are indicated by A and B.
Y-Y¹: correlation line in Fig. 4.5

species which died at the same age (one year class). Apart from bivalve shells body fossils of the echinoderm *Echinocardium cordatum* and *Ophiura texturata* are common. Also present are the dwelling tubes of the polychaete *Pectinaria koreni.* They can be found in large quantities within the lower part of the sequence preserved in 'life position' or washed together in small heaps.

Evidence for a seasonal origin of the rhythmic beds

The agreement between the thickness of individual couplets and the annual rate of sedimentation as interpreted from hydrographic maps.

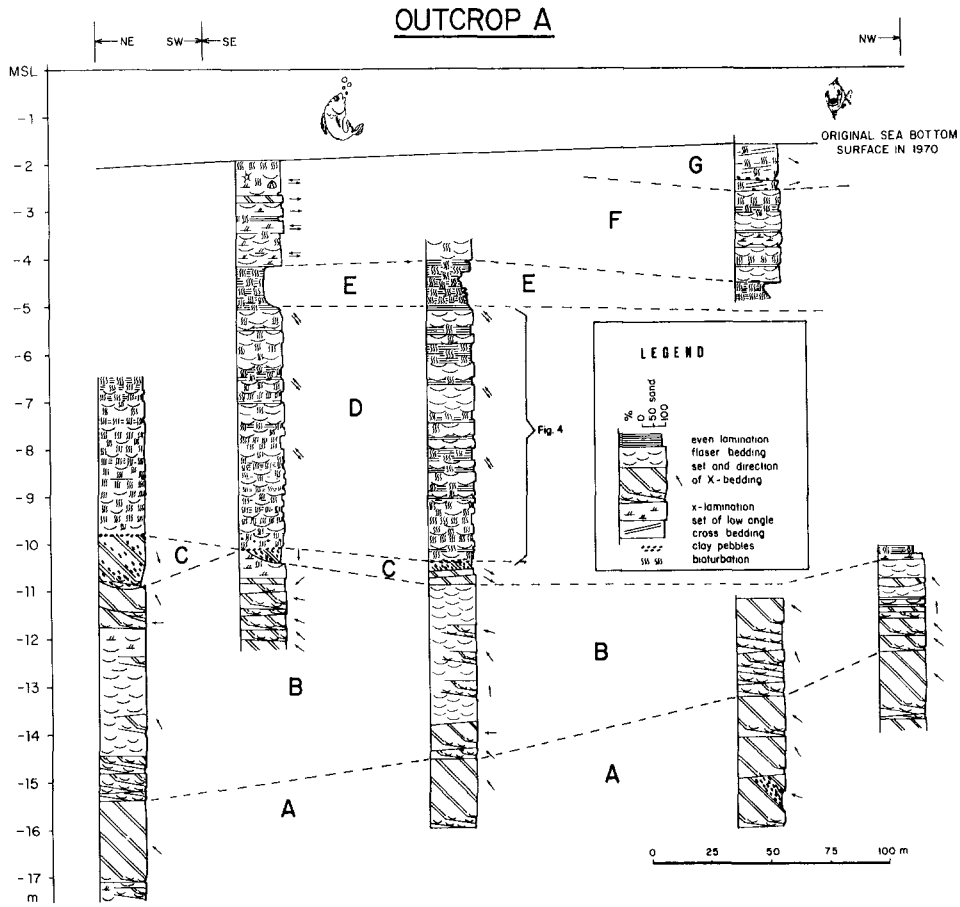

Fig. 4.2 General Outline of outcrop A. For location see Fig. 4.1

The depositional history of the rhythmic beds is documented by a series of hydrographic maps (see Fig. 4.3). According to these maps, the water depth at the site of outcrop A was reduced from more than 9 m to about 5 m within a period of 12 years, between 1922 and 1933. A similar number of couplets can be observed between 9.8 and 5.0 m below sea-level, and this already suggests an annual origin of these couplets. In an upward direction, an increase in thickness of the rhythmic beds is noticeable.

There are several indications that this increase resulted from a higher rate of annual accumulation. Although the channel was largely abandoned by the tidal flow during the deposition of the rhythmic beds, its lateral migration to the north-east continued (Fig. 4.3).

According to the hydrographic maps, the channel axis must have crossed the site of outcrop A in the shallowing period between 1922 and 1933, or within

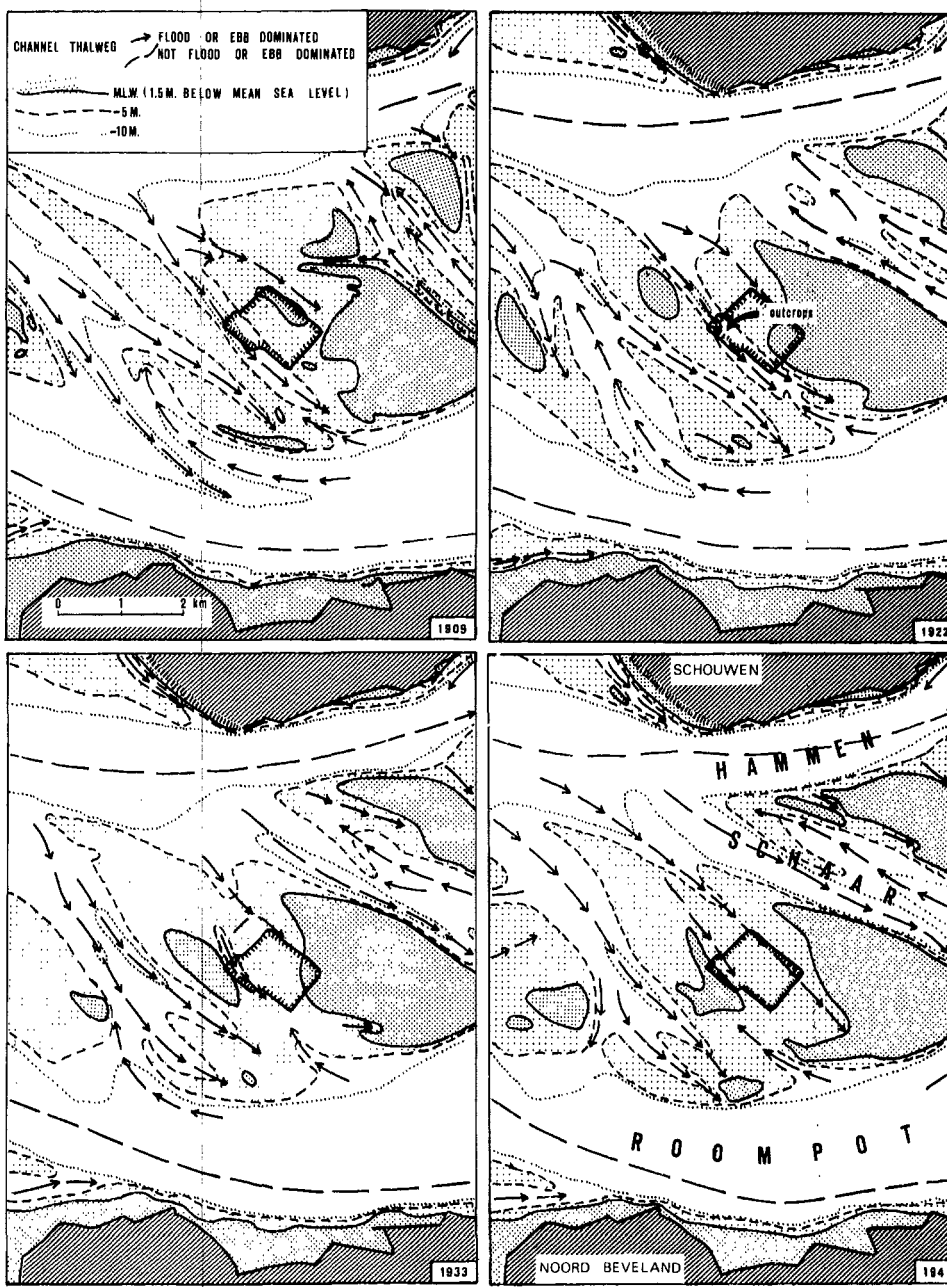

Fig. 4.3 Hydrography of the Oosterschelde mouth between 1909 and 1948

the period when the rhythmic bedding was formed. Thus the upward increase in thickness of the individual layers could reflect the passage of the thalweg

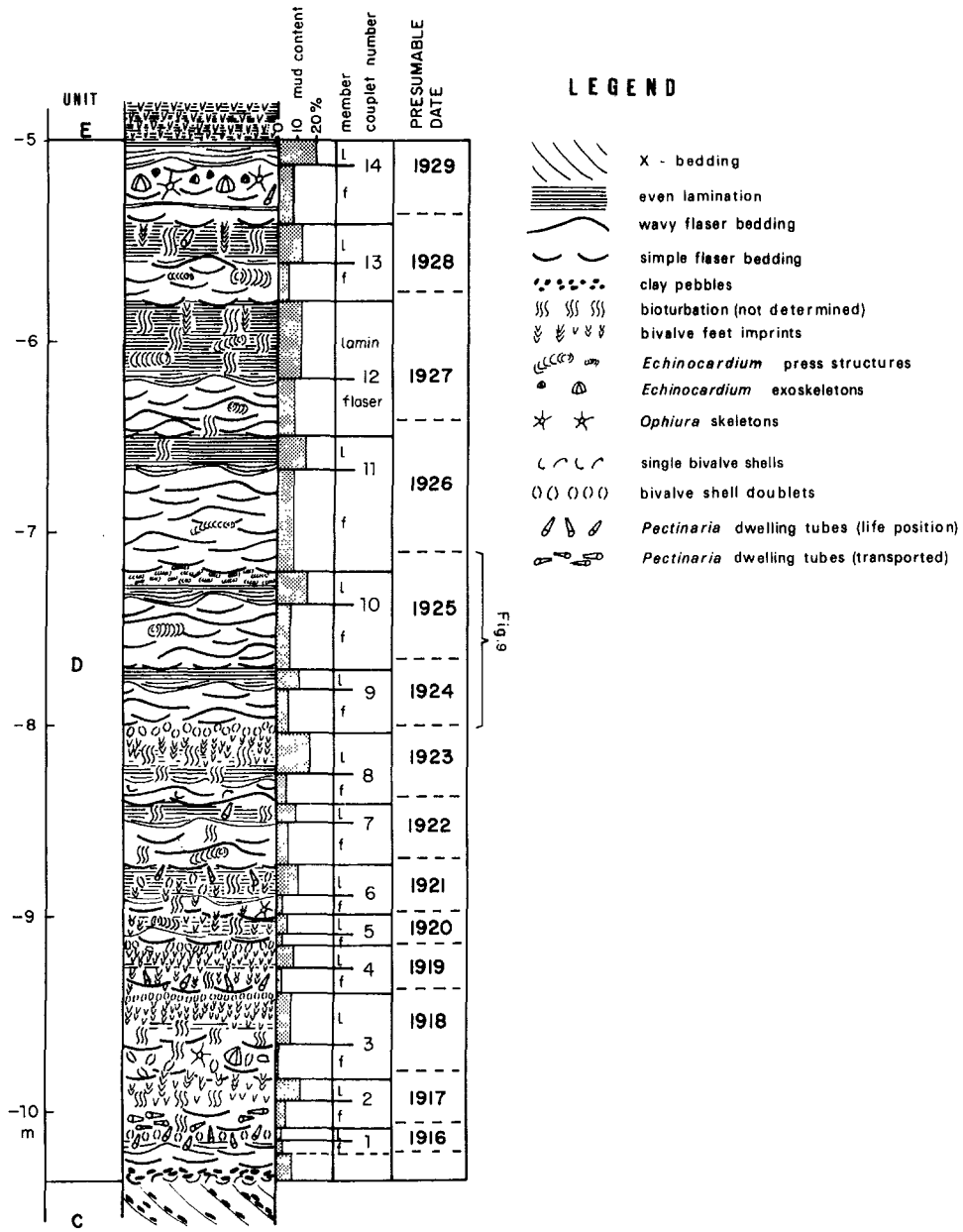

Fig. 4.4 Detailed log of the rhythmic beds in outcrop A. For location see Fig. 4.2

zone. Evidence for this suggestion was found by a detailed correlation of outcrops A and B, which was possible by several key beds of echinoderms and bivalves. The correlation on the basis of the number of couplets and these key beds allows a lateral connection of the individual seasonal layers. This corre-

lation is given in Fig. 4.5, clearly demonstrating the gradual inversion of the slope between both outcrop locations, caused by the passage of the deepest part of the channel.

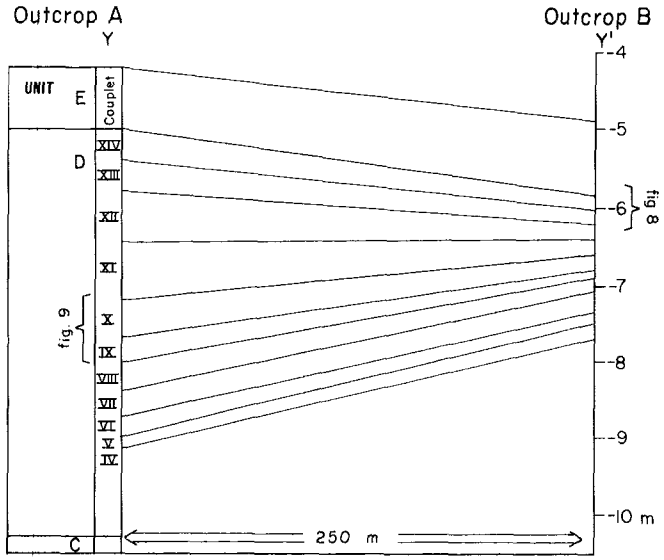

Fig. 4.5 Correlation of the rhythmic beds between the two outcrops. For location of Y-Y' see Fig. 4.1

Growth and mortality pattern of some bivalve species through successive layers. The rhythmic beds contain many bivalve remains, especially in the lower part of the sequence. The preserved shells are clearly autochthonous; they are almost always preserved as double-valved specimens, often still in life position. In shells of *Spisula subtruncata* the tender periostracum is still retained completely. In four of the five common species, year classes could be distinguished by the fact that specimens show distinct size groups, e.g. the *Abra alba* population of couplet number 3 consists of three size classes of about 4, 10 and 18 mm shell length, interpreted as specimens in their first, second and third years of life respectively (Fig. 4.6).

The winter growth ring patterns locally developed in adult specimens of *Abra alba* and *Spisula subtruncata* support this conclusion. Separate year classes could be followed easily throughout the succession. They show a gradual growth through successive couplets. The growth of year classes from any couplet to the overlying one corresponds exactly with the annual growth increment. This proves again that the rhythmic cycles are annual couplets. The regular growth pattern of separate year classes through successive rhythmic beds confirms the above-mentioned continuity of deposition, without any breaks or conditions of intermittent erosion.

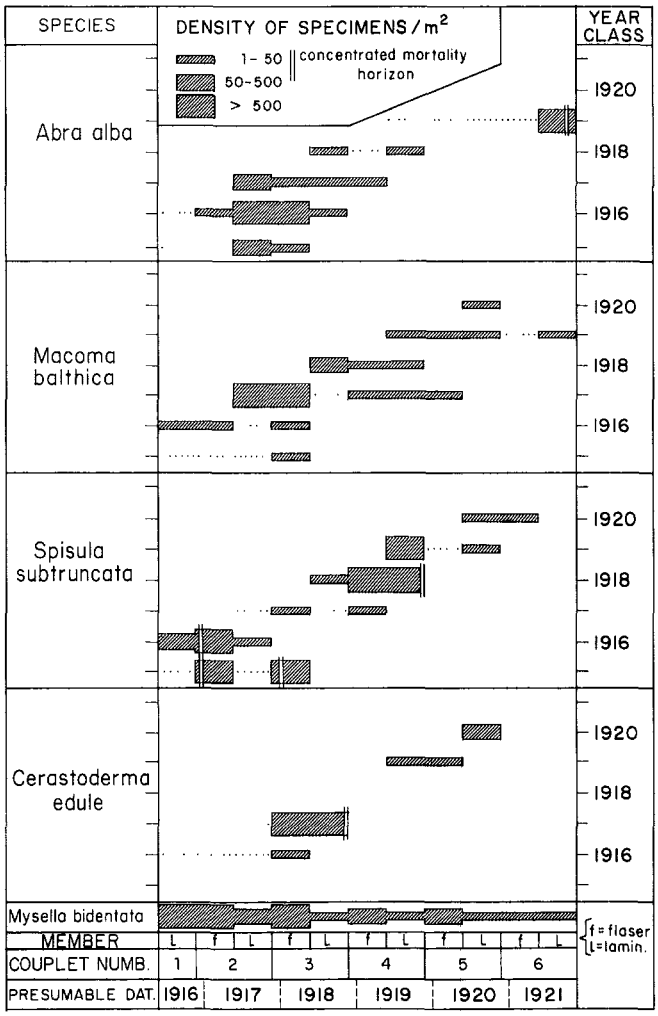

Fig. 4.6 Year classes and densities of specimens of some bivalve species in the lower part of the rhythmic beds (no year classes are distinguished in specimens of *Mysella bidentata*). Two valves are considered as one specimen

The transition from laminated to flaser beds is repeatedly marked by a mortality horizon, a concentration of double-valved specimens of *Spisula subtruncata* or *Cerastoderma edule* (see also Fig. 4.4). This horizon indicates a nearly total extermination of the year classes involved. Since couplets are annual layers it is likely that each laminated and each flaser layer represent particular parts of the year. Several considerations lead us to the conclusion that the above-mentioned mortality horizons mark the change to low water temperatures during the winter season.

Water temperature measurements by Rijkswaterstaat (the Governmental Board

for Ways, Waterways and Harbours) near the location of the pit in the period 1972-9 give minimum winter temperatures ranging between 0.9 and 4.9°C. Unfortunately little is known about the effects of low water temperatures on the muscular activity of bivalves, in particular their ability to escape burial during deposition.
According to KRISTENSEN (1957) *Cerastoderma edule* is not capable of digging itself into the sand at temperatures below 2.5°C. It will probably also fail to dig itself out when covered by a sediment layer. Since the habitat of the bivalve populations in the abandoned channel was subjected to continuous sedimentation, such failure is precisely what might be expected during relatively cold winter periods.
During a cold spell the inactive bivalves would be buried and normal siphonal respiration processes would become impossible. Although no data are available about the survival time under anaerobic and low-water-temperature conditions, it seems likely that a long cold spell could be lethal.

In addition to the dense horizons of *Spisula* and *Cerastoderma* a less concentrated mortality layer of *Abra alba* is found in the laminated (summer) layer of couplet 6 (see Fig. 4.4). The different nature of this mortality layer can be explained as follows: *Spisula subtruncata* and *Cerastoderma edule* have short siphons and live near the surface, so that mass mortality in winter gives rise to a concentrated shell layer at the transition to or at the base of the flaser (winter) layer.
On the other hand *Abra alba* possess long siphons and live more dispersed in a relatively thick layer below the sediment surface. Thus, when the animals become sluggish and eventually die of asphyxia during winter, they may still be found dispersed through the summer layer. *Mysella bidentata* grows very slowly and therefore does not form distinct size classes. Since winter growth rings could not be discerned, no year classes could be distinguished; only mortality densities are given in Fig. 4.6. This small bivalve lives near the surface and, as could be expected, a high mortality is found in the flaser (winter) layers.
Thanks to a remarkable and continuous mortality horizon of heart urchins (*Echinocardium cordatum*) together with brittlestars (*Ophiura texturata*) present in the winter member of couplet 14, of which the probable date of origin can be established, it is possible to label all cycles with their successive years of formation.
In outcrop A mainly adult sea urchins are found in couplet 14 (30 mm test length), whereas in outcrop B together with this size class a dense population of rather juvenile specimens is present (16 mm test length). Generally many spines are still attached to the *Echinocardium* exoskeletons. The fragile skeletons of the brittlestars are also complete; this indicates that after succumbing

the specimens were hardly transported. The autochtonous position of the echinoderm fauna is further confirmed by the fact that the size of the internal traces of *Echinocardium cordatum* preserved directly below the mortality horizon corresponds with the size of the body fossils. Since body and trace fossils of the heart urchin are generally found scattered at random throughout the sequence of seasonal layers, the occurrence of only horizon of heavy mortality points to exceptional conditions. Severe mortality of heart urchins in subtidal habitats has been reported only for the extremely cold winter of 1962–3. During this winter a long period of low water temperatures resulted in a mass mortality of many marine organisms including the heart urchin in the southern North Sea (WOODHEAD, 1964; ZIEGELMEIER, 1964).

Heaviest mortalities are recorded from the coldest parts of the North Sea, such as along the southeast coast of Britain (CRISP ET AL., 1964) and the German Bight (ZIEGELMEIER, 1964; REINECK, GUTMAN & HERTWECK, 1967). According to the series of hydrographic maps, the rhythmic beds must have been deposited between about 1922 and 1933. This period includes the severe winter of 1928–9. Temperature conditions and effects on marine life (fish mortality) of this winter in the southern North Sea were comparable to those of the cold spell of 1962–3 (LUMBY & ATKINSON, 1929; WOODHEAD, 1964; RIJKSWATERSTAAT, 1966; ANONYMOUS, 1968). Floating ice was reported for 31 days in the eastern part of the Oosterschelde (KORRINGA, 1940) and was even reported during a couple of days at the lightvessel Schouwenbank, 20 km offshore (DORRESTEIN, 1964).
Thus conditions in the entrance must have been lethal to most, if not all heart urchins. Unfortunately no temperature measurements of the Oosterschelde entrance exist from this period. Approximate water temperatures can be calculated by taking into account the delayed transmission of air temperature to water masses. Results with such converted air temperatures at Flushing according to the equation below show a reasonable correlation with water temperatures measured in the Oosterschelde entrance (P. T. C. VAN DER HOEVEN, Royal Dutch Meteorological Institute, personal communication):

$$W_o = (8A_o + 4A_1 + 2A_2 + A_3)/15$$

In this equation W_o and A_o are mean 'delayed' air temperature and measured air temperature of the same month respectively; A_1, A_2 and A_3 are mean air temperatures of the first, second and third months before the month of A_o. Since a long period of low water temperatures together with continuous sedimentation is postulated as the main cause of heavy bivalve mortalities, the minimum values of monthly means of winter water temperatures in the Oosterschelde mouth are compared with the position of mortality layers (Fig. 4.7). Also, water

temperatures measured 20 km off shore at the lightvessel Schouwenbank are mentioned. It must be stressed here that no definite conclusions can be made on de influence of small fluctuations between lowest winter temperatures on the mortality amongst bivalve species, since the number of mortality horizons is too small. Furthermore the calculations can give only an approximation of the real water temperatures. Nevertheless some interesting remarks can be made.

Couplet number	Member l = laminated f = flaser	Mortality horizon Species	Density m²	Lowest monthly mean of winter temperature (°C) Vlissingen*	Schouwenbank†	Date of winter
14	l					
	f	2 and 4 summer heart urchins	—	−0·8	1·3	1928/29
13	l					
	f			3·8	3·8	27/28
12	l					
	f			4·2	4·4	26/27
11	l					
	f			3·9	4·9	25/26
10	l					
	f			4·7	5·8	24/25
9	l					
	f			1·9	3·2	23/24
8	l	1 summer *Cerastoderma edule*	10200			
	f			5·4	5·4	22/23
7	l					
	f			3·2	3·1	21/22
6	l	3 summer *Abra alba*	600			
	f			5·4	5·6	20/21
5	l					
	f			5·3	4·9	19/20
4	l	2 summer *Spisula subtruncata*	20600			
	f			2·8	3·6	18/19
3	l	1 summer *Cerastoderma edule*	7200			
	f	3 summer *Spisula subtruncata*	1100	3·9	2·9	17/18
2	l					
	f	1 and 2 summer *Spisula subtruncata*	3200	0·1	1·2	16/17
1	l					
	f			5·1	5·2	15/16

Fig. 4.7 The relationship between horizons of heavy mortality and presumably lowest winter temperatures. * 'Delayed' air temperatures; † water temperatures

As can be seen in Fig. 4.7 the mortality horizons of *Cerastoderma edule* are connected with relatively cold winter periods. Calculated temperatures are below 3°C, which is in fair accordance with the value of 2.5°C at which the digging activity stops according to KRISTENSEN (1957). The same is valid for the *Abra alba* population, which survived the relatively warm winters of the couplets 5 and 6 and finally perished in the somewhat colder winter spell of 1921–2. The pattern of Spisula mortality seems not to be influenced by differences in winter cold. Some survived the cold winter of 1916–17 and died in

relatively warm winter seasons. Obviously some unknown factor influenced their ability to survive the winter periode.

The upward growth of a dense population of heart urchins through successive rhythmic beds.

Traces and body remains of the heart urchin (*Echinocardium cordatum*) are found distributed throughout the whole sequence of rhythmic beds. Spines are found everywhere in fairly large quantities. Apart from their frequent occurrence in the mortality layer of couplet 14 exoskeletons are uniformly distributed, although slightly more are found in the flaser layers, indicating a somewhat higher mortality in winter. On the other hand, the internal traces are more concentrated in the laminated layers, which is in accordance with the higher activity of the animals during summer. In some places laminations have been completely destroyed by the burrowing activity of the heart urchins, particularly in outcrop B (Fig. 4.8). In general it was hard to distinguish size or year classes in the population of trace and body fossils. An exception is formed by a successful settlement in the upper member of couplet 10 (S in Fig. 4.9).

Internal traces of press structures of numerous juvenile specimens impart a mottled structure to the upper part of this summer layer (Fig. 4.9). In a large part of outcrop A the traces of a dense population are no longer present in the overlying winter layer. In the southwestern part of the outcrop, however, a dense population continues to be present until its extermination in the mortality horizon of couplet 14.

Figure 4.10 shows the average test length through successive couplets, as estimated from the curvature of the press structures. Comparison with data on the annual growth increment given by BUCHANAN (1966) for two heart urchin populations along the Northumberland coast strongly supports the annual origin of the deposits.

The difference in growth rate between the two populations studied by Buchanan was considered to be mainly the result of differences in mud content between the two habitats; a silty substratum would inhibit the animal's passage through the sediment and thus its food uptake, resulting in a slow growth rate. Therefore it is suggested that an increase in mud content results in a slowing down of the growth rate. The latter reasoning is in agreement with the annual growth increment of the heart urchins as measured in the rhythmic beds of the Oosterschelde, for both the mud content as well as the growth rate of the studied population in this environment is intermediate between the values in the habitats studied by Buchanan.

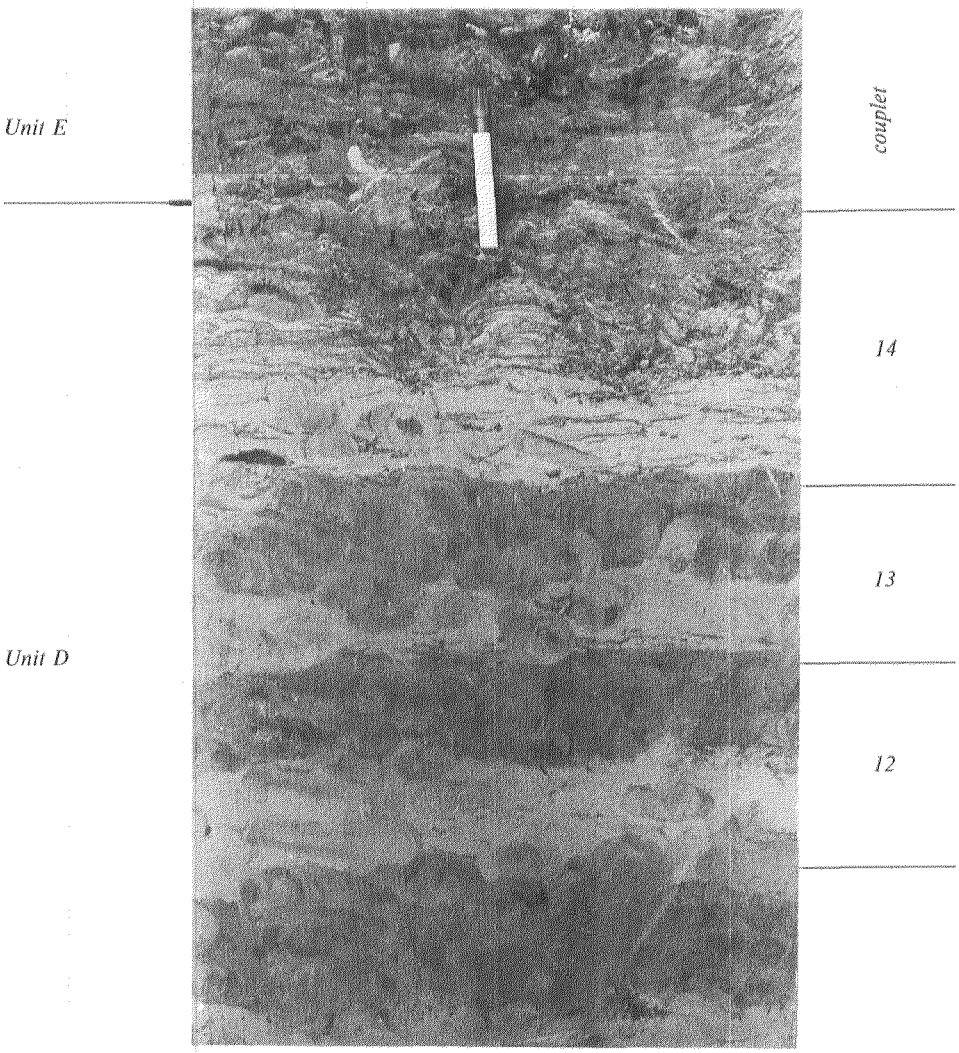

Fig. 4.8 Rhythmic bedding in outcrop B. Original physical sedimentary structures have almost completely disappeared due to the burrowing activity of heart urchins; only a repetition of light and dark layers remains, denoting small differences in mud content. Length of the pen is 14 cm

The origin of the rhythmic change in physical structures

The flaser and laminated members within the annual rhythmic cycles represent a winter and a summer layer respectively. The interlaminated mud and fine sand of the summer member represent conditions of accumulation from suspended sediment on flat bottoms, periods during which wave and current activity are

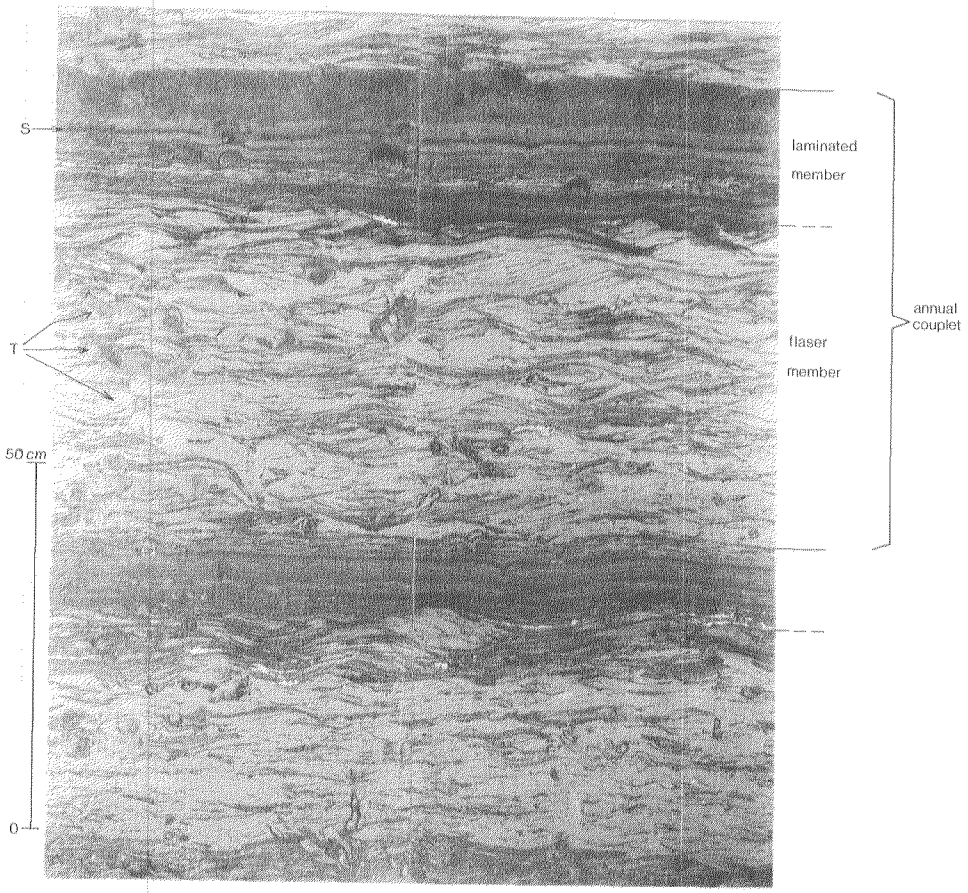

Fig. 4.9 Characteristic sequence of structures within annual couplets: photograph of a wet lacquer peel (wet, the mud has a dark colour by which it can be distinguished more easily from the sand). T = *Echinocardium* press structures; S = settlement of juvenile heart urchins. For locations of the lacquer peel see Fig. 4.4

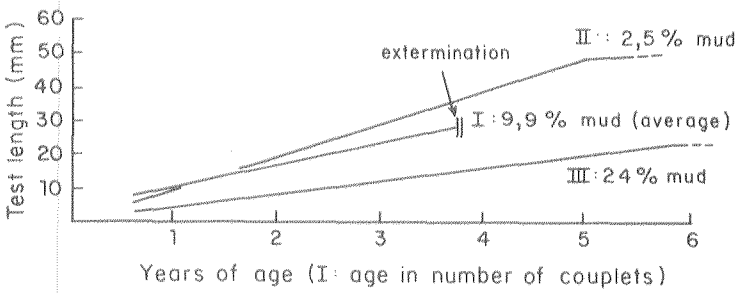

Fig. 4.10 Comparison of test length between the discussed population of *Echinocardium cordatum* in the rhythmic beds of the Oosterschelde (I) and at two Northumberland localities (II = intertidal, III = offshore, 40 m deep)

too low to produce ripples. Most of the flaser bedding belongs to the wavy flaser type (REINECK & WUNDERLICH, 1968). Their formation can be explained by the occurrence of currents which only partially erode the crest of previously formed ripples (REINECK & SINGH, 1973).

Cross-laminations contain partings of faecal pellets and fine organic matter; these features indicate that cross-laminations are produced under relatively low energy conditions. Cross-laminations show a bipolar orientation parallel to the axis of the abandoned channel in which they are formed, indicating that the ripples migrated under the influence of the reversing currents. Cross-laminated sets may be covered by multiple mud flasers infilling ripple troughs and draping ripple crests. The latter features reflect prolonged periods in which wave agitation or tidal current velocity was too low to intiniate appreciable movement of grains. It is plausible to suggest that the seasonal variation in primary structures is due to temperature, for this affects the density and viscosity of the water which, in turn, involves some change in flow pattern and flow regime. For example, HARMS & FAHNESTOCK (1965) found a transition to a higher flow regime and related bedforms (from dunes to upper flat bed) after a drop in temperature of 17.5°C in the Rio Grande river, U.S.A.

However, flume experiments suggest that the influence of temperature on the threshold for the initiation of grain movement and the formation of ripples is rather small (MIDDLETON, 1978). It is difficult to extrapolate the value of data from the extremely narrow range of flow depths in flume experiments to natural deep flows, the more so as they are all restricted to steady currents and do not take into account any superimposed wave oscillation, which in our case may be important.
It does not seem likely that a change in temperature can be held responsible for the rather drastic seasonal change in physical structures. It may be stated that in general the presence of inorganic mud particles between sand grains imparts some cohesion to the sediment. The fact that the laminated layers on the average contain more mud could therefore mean that in summer somewhat higher current velocities would be required for the formation of ripples. Although it cannot be denied that this factor might be of some importance it cannot be the main cause, since some of the flasers and laminated layers contain about the same amounts of mud (see Fig. 4.4). Presumably the initial organic content of the deposits is of more importance to the seasonal change in the sedimentary structures. Most of the organic matter in settling mud is of planktonic origin. In spring, during the major bloom of phytoplankton, 50–75% of the mud is of organic origin (TERWINDT, 1977). A secondary maximum may be present in summer during the development of a second but less important plankton bloom (DRINKWAARD, 1958, 1959).

In the remaining part of the year amounts gradually drop to a minimum of about 10% in winter (J. H. B. W. ELGERSHUIZEN, personal communication). It can be imagined that the high organic content of the mud in summer influences the physical properties of the sediment, in such a way that it could support the cohesive forces between the grains. Also grains might glue together during bacterial mineralization of the organic matter. If so, this could mean that flow velocities in summer did not cross the threshold necessary for the initiation of grain movement and the formation of ripples, so that a laminated facies was produced. At this moment these assumptions are only speculation. Future research must prove their validity.

When returning to winter conditions the flat bottom changed into a rippled morphology, attended by some slight erosion of the laminated summer layer by the ripple troughs. This resulted in a sharp boundary, which is in contrast with the gradual non-erosional transition from flaser to a laminated layer.

Conclusions

The development of seasonal layering is not restricted to low energy environments, but may also occur in a highly dynamic area of tidal channels and shoals. The described seasonal layering will probably not represent a large part of the sequential complex of deposits produced in the Oosterschelde mouth. Accretional patterns caused by channel migration will play a more important role when compared with the occurence of channel abandonment. The development of seasonal beds within these abandoned channels will be favoured by weak tidal currents and wave action together with a relatively high rate of sedimentation. Future studies must decide whether the present example should be considered as a rare exception, or that seasonal beds are produced more frequently in other areas with comparable conditions of sedimentation. For example in some delta-front environments.

Acknowledgements

I wish to express my gratitude to mr J.G.M. Raven for placing his internal report on the distribution of bivalves at my disposal. I am greatly indebted to Dr. S. D. Nio, Dr. C. Siegenthaler and Dr. A. van Gelder for critically reading the manuscript and Dr. J. H. J. Terwindt for some fruitful discussions at the exposure.

References

ANONYMOUS. 1968. Monthly Means of Surface Temperatures and Salinity

for Areas of the North Sea and the North-eastern North Atlantic in 1963. International council for the exploration of the sea, Service Hydrographique Charlottenlund, Copenhagen, Denmark.
BUCHANAN, J. B. 1966. The biology of Echinocardium cordatum (Echinodermata: Spatangoidea) from different habitats. J. mar. biol. Ass. U.K. 46: 97–114.
CRISP, D. J., MOISE, J. & NELSON-SMITH, A. 1964) General conclusions. In: The effects of the severe winter of 1962–63 on marine life in Britain (Ed. by D. J. Crisp), J. Anim. Ecol. 33: 202–210.
DORRESTEIN, R. 1964. Drijfijswaarnemingen van Nederlandse lichtschepen in Januari–Maart 1963, De Zee, 83: 202–210.
DRINKWAARD, A. C. 1958. The quality of oysters in relation to environmental conditions in the Oosterschelde in 1958. Ann. biol. Copenh. 16: 255–261.
DRINKWAARD, A. C. 1959. The quality of oysters in relation to environmental conditions in the Oosterschelde in 1959. Ann. biol. Copenh. 16: 255–261.
HARMS, J. C. & FAHNESTOCK, R. K. 1965. Stratification, bed forms, and flow phenomena (with an example from the Rio Grande). In: Primary Sedimentary Structures and their Hydrodynamic Interpretation (Ed. by G. V. Middleton). Spec. Publ. Soc. econ. Paleont. Miner., Tulsa, 12: 84–115.
KORRINGA, P. 1940. Experiments and observations on swarming, pelagic lif and settling in the European flat oyster *Ostrea edulis L.* Doctoral thesis, University of Amsterdam: 249 pp.
KRISTENSEN, I. 1957. Differences in density and growth in a cockle population in the Dutch Wadden Sea. Archs nèerl. Zool. 12: 351–453.
LUMBY, J. R. & ATKINSON, G. T. 1929. On the unusual mortality amongst fish during March and April 1929 in the North Sea. J. Cons. int. Explor. Mer, 4: 309–332.
MIDDLETON, G. V. 1978. Mechanics of Sediment Movement. S. E. P. M. Short Course 3: 27 pp.
REINECK, H. E. & SINGH, I. B. 1973. Depositional Sedimentary Environments – with Reference to Terrigenous Clastics, Springer-Verlag, Berlin: 349 pp.
REINECK, H. E., GUTMAN, W. F. & HERTWECK, G. 1967. Das Schlickgebiet südlich Helgoland als Beispiel recenter Schelfablagerungen. Senckenberg. Leth. 48: 219–275.
REINECK, H. E. & WUNDERLICH, F. 1968. Classification and origin of flaser and lenticular bedding. Sedimentology, 11: 99–104.
RIJKSWATERSTAAT 1966. IJsverslag Winter 1962–1963, Staatsuitgeverij, Den Haag: 85 pp.
SCHÄFER, W. 1962. Aktuo-Paläontologie nach Studien in der Nordsee. Kramer, Frankfurt: 666 pp.
TERWINDT, J. H. J. 1977. Mud transport in the Dutch delta area and along the adjacent coastline. Neth. J. Sea Res. 3: 505–531.

TERWINDT, J. H. J. 1967. Mud transport in the Dutch delta area. Geol. Mijnb. 56 : 203–210.
WOODHEAD, P.M.J. 1964. The death of fish and sublittoral fauna in the North Sea and the English Channel during the winter of 1962–1963. In: The effects of the severe winter of 1962–63 on marine life in Britain (Ed. by D. J. Crisp). J. Anim. Ecol. 33 : 165–210.
ZIEGELMEIER, E. 1964. Einwirkungen des kalten Winters 1962/63 auf das Makrobenthos im ostteil der Deutschen Bucht. Helgoländer wiss. Meeresunters. 10 : 272–282.

5. Bedform migration and bed-load transport in some rivers and tidal environments

Submitted to Sedimentology

Abstract

Reliable field data obtained by directly measuring bed-load transport of fine to coarse grained bed material are extremely scarce, mainly because of the difficulty of sampling accurately. Therefore the verification of bed-load transport formulae is largely based on flume experiments, which refer to unrealistic shallow water conditions. In this study some bed-load transport formulae were tested against data from natural environments. As an alternative to ascertaining the bed-load transport rate by sampling the bed-load, the transport rate was deduced from data on bedform height and bedform celerity. For this purpose, 43 sets of data from rivers, representing a wide range of bed material, bedform dimensions and hydraulic conditions were collected as were some sets of data from tidal settings. Two formulae were used for the prediction of the bed-load transport: the formula of VAN RIJN (1981) and the KALINSKE (1947) formula as approximated by ELZERMAN & FRIJLINK (1951) (and, in the present study slightly modified for application to tidal waters).
Both the bed-load function of Van Rijn and the modified formula of Kalinske-Frijlink require data which is easily obtained and that can be measured accurately.
At those stages of the flow when bed-load transport was high the Van Rijn function tended to overestimate that transport. For flow stages when bed-load transport was low the opposite was true. The modified Kalinske-Frijlink function gave consistently good results: 86% of the transport rates predicted using the river data were within 0.5 – 2.0 times the values actually measured.

Introduction

Bed-load transport is defined as the transport of sediment particles by rolling,

sliding and saltation. The thickness of the bed-load transport layer is determined by the saltation height of the sediment particles, which rarely exceeds 10 particle diameters (VAN RIJN, 1984). Direct measurement of the bed-load transport rate is generally done using conventional sand-traps placed on the bottom. But when fine sands predominate such measurements are not reliable because unknown amounts of suspended particles will also be trapped. There is an alternative way of ascertaining bed-load transport rates: subtracting measured rates of suspended load transport from the measured rates of total load transport. Although currently used in laboratory studies, in natural environments this method meets with serious logistic and instrumental problems, that cannot be satisfactory solved and that impede the collection of reliable results. A second indirect way to measure bed-load transport rate is to compute the sediment volume involved in bedform migration, using bed profile records obtained by diver measurements or echo sounding.
Generally, the sediment transport involved in ripple or dune migration (S_c) is assumed to represent the bed-load transport (S_b). This is certainly true if bed-load consists of medium- to coarse-grained sands. However, if the bed material is composed of fine sands and most of the load is carried in suspension, this assumption is suspect: part of the suspended load is deposited in the troughs behind the bedforms and so contributes to the lee-side accumulation and hence the migration of the bedforms. On the other hand near the brinkpoint of dunes, where there is an area of turbulent flow separation, part of the bed-load material becomes suspended instead of being spread in avalanches along the steep lee-side slope of the dune.

This paper tests the assumption that a reliable estimate of the bed-load transport can be obtained by using data on the height and celerity of bedforms. As a closely related problem, the reliability of certain bed-load transport formulae in natural conditions is also investigated. For this purpose data obtained by measuring bedform migration and hydraulic conditions simultaneously in a number of river and tidal areas were used. The reliability of three formulae was assessed: a deterministic bed-load transport formula originally proposed by BAGNOLD (1963) as modified and calibrated by STERNBERG (1972) and GADD ET AL. (1978); a stochastic formula developed by KALINSKE (1947), as modified and calibrated by ELZERMAN & FRIJLINK (1951), and a deterministic bed-load transport formula recently developed at the Delft Hydraulics Laboratory (VAN RIJN, 1981; 1984).
Like many other bed-load transport formulae the Kalinske-Elzerman & Frijlink formula contains a bedform factor eliminating that part of bed-shear stress related to form drag that does not contribute to the bed-load transport.
As will be shown, it is preferable to avoid the explicit use of a bedform factor (μ) in a bed-load transport formula when applied to non-steady conditions such

as found in tidal environments. For this reason, a further modification of the Kalinske-Elzerman & Frijlink formula will be discussed in this paper; this modification is based on a method of directly relating mean current velocity to the shear stress associated with grain resistance.
The available information on the bedforms in the locations discussed in this paper is generally restricted to their height, length and celerity. Therefore, no attempt was made to classify the bedforms according to their three-dimensional shape, such as proposed by HARMS ET AL. (1975) or DALRYMPLE ET AL. (1978), but instead, for practical reasons, they were classified on the basis of their size: bedforms with an amplitude of several centimetres are called ripples, larger bedforms are denoted as dunes and very large forms whose wavelength exceeds 100 m are termed sandwaves.

Bed-load transport as a function of bedform height and celerity
The volumetric sediment transport rate involved with the celerity of bedforms per unit width and time including the voids (S_c) is equal to the product of dune cross-sectional area (A) and dune celerity (U_c) divided by the dune length (λ). If dunes are assumed to be triangular in cross-section, the following equation holds:

$$S_c = \frac{U_c}{\lambda} \cdot A = \frac{U_c}{\lambda} \cdot \tfrac{1}{2}\lambda H = \tfrac{1}{2}U_c H \quad [m^2 s^{-1}] \tag{1}$$

in which H = bedform height. (For an explanation of the notation used in this and subsequent equations, and in the text, see Appendix I).
Expressed in terms of the dry weight of the sediment involved, equation (1) can be written as follows:

$$S_c = \tfrac{1}{2}\varrho_s(1 - \varepsilon)U_c H \qquad [kgm^{-1}s^{-1}] \tag{2}$$

in which ϱ_s = sediment density
ε = porosity

When applying the latter formula to describe the bed-load transport rate – as is common practice in recent literature – it should be realised that some inaccuracies are introduced, because:
– in reality the bedform profile may deviate considerably from a triangular shape;
– as stressed by Engel and Lau (1980), in the area below the wake behind dunes net bed-load transport is negligible. Therefore only that part of the dune cross-sectional area above the point of flow reattachment should be considered when calculating the bed-load transport;

– for reasons already mentioned, the migration of dunes might also be influenced by processes of suspension of bed-load at the dune front and settling of suspended matter in the wake behind the dune.

Therefore, equation (2) is modified by replacing S_c by S_b (the bed-load transport per unit width ($ML^{-1}T^{-1}$)), and to account for the deviation resulting this replacement a bedform coefficient β is introduced:

$$S_b = \varrho_s(1 - \varepsilon)\beta U_c H \qquad (3)$$

In the present study, the values chosen for β and ε in the equation were obtained from literature. MARDJIKOEN (1966) studied bed-load transport data, obtained by sampling from different sources: flume data (with sand of 180 μm and 800 μm) obtained by ZNAMENSKAYA (1963) and date from the Hii river, Japan, reported by SHINOHARA & TSUBAKI (1959). He compared these measured values for bed-load transport with the values obtained by using equation (3), and found $\beta = 0.6 \pm 0.21$. Similarly data from the Skive-Karup river, Denmark, presented by HANSEN (1966) yield a β-value of 0.49, whereas data from the IJssel river, the Netherlands, reported by HAVINGA (1982), yield a β-value of 0.6. SIMONS ET AL. (1965) compared 101 flume experiments with ripple and dune bedforms and proposed $\beta = 0.5$. However from the graph presented by these authors it becomes clear that a better agreement is obtained if β 0.6. In all these cases a porosity $\varepsilon = 0.4$ was assumed.
None of these results challenges Mardjikoen's findings, and therefore, in this study a shape factor $\beta = 0.6$ and a porosity $\varepsilon = 0.4$ will be assumed.

The bed-load transport formulae assessed in this study
The literature contains many bed-load transport formulae (YALIN, 1972). Most of the commonly used theories, such as the bed-load formula of EINSTEIN (1950) and that of MEYER-PETER & MÜLLER (1948) have been evaluated by WHITE ET AL. (1973; 1975), who showed that the predictive value of these formulae was poor, especially when bed material was fine.
As mentioned earlier, in this paper the efficacy of three theories is assessed: two versions of a bed-load transport formula devised by BAGNOLD (1963); a modified version of the bed-load transport function of KALINSKE (1947) and a bed-load transport formula that has recently been developed at the Delft Hydraulics Laboratory (VAN RIJN, 1981; 1984).

During the past decade the bed-load transport concept outlined by BAGNOLD (1963) has become increasingly popular among marine geologists. Since some

of the parameters of the original equation cannot be measured, for application some assumptions and simplifications are necessary before it can be applied. Such modifications have been proposed by STERNBERG (1972) and GADD ET AL. (1978):

STERNBERG (1972) gives $$S_b = K_1 \frac{\varrho u_*^3}{\Delta g} \quad (4)$$

and GADD ET AL. (1978) $$S_b = K_2(u_{1.0} - u_{1.0,cr})^3 \quad (5)$$

in which: K_1 and K_2 are dimensional coefficients, $u_{1.0}$ average current velocity at 1.0 m above the bottom, u_* is the bed-shear velocity, $\Delta = (\varrho_s - \varrho)/\varrho$ is the specific density and ϱ_s and ϱ are the sediment and fluid density respectively.

K_1 was calibrated by Sternberg against flume data from GUY ET AL. (1966) with median grain sizes of 190 μm, 280 μm, 450 μm and 930 μm. The results indicate that K_1 depends on grain size and on excess shear stress

$(\tau - \tau_{cr})/\tau_{cr}$

(with τ = bed shear stress and τ_{cr} = critical value of bed shear stress for the initiation of motion).
It should be noted that in Eq. (4) the bed-load transport rate is considered to be a function of the total bottom shear stress, whereas it is well-known that such a function may only be valid when the bottom is flat. If bedforms are present, the total bottom shear has to be reduced by the shear related to the loss of energy expended to overcome the form resistance imparted by the ripples or dunes. As demonstrated by BROOKS (1958) and ENGELUND & HANSEN (1967), a large and variable part of the total bed-shear stress may be related to form drag. It is therefore unlikely that the bed-load transport rate can be predicted reliably unless the bed-shear is reduced to the pure frictional drag.

GADD ET AL. (1978) restructured Eq. (4) by replacing the shear velocity parameters by the current velocity at 1 m above the bed and removing the dependence of K on excess shear. When they calibrated the equation against a selection of the above mentioned flume data, GADD ET AL. (1978) found K_2 = 7.22 kg m^{-4}s^2 for D_{50} = 190 μm and K_2 = 1.73 kg m^{-4}s^2 for D_{50} = 450 μm. Using data from GUY ET AL. (1966) from D_{50} = 320 μm, LANGHORNE (1981) found K_2 = 0.94 kg m^{-4}s^2.

Independently from earlier calibrations, TEYSSEN (1984) calibrated the formula with a set of data from the same series of flume experiments that Gadd et al. had used and concluded that the value of K_2 not only depended on grain size but also on current velocity. With increasing flow velocities a sharp decrease in K_2 was found. From a graph presented by Teyssen, at an average flow velocity of 0.5 ms^{-1} values of $K_2 = 2$ kg $m^{-4}s^2$ for $D_{50} = 190$ μm, and $K_2 = 15$ kg $m^{-4}s^2$ for $D_{50} = 450$ μm can be obtained. At flow velocities above 0.8 ms^{-1} K_2 approaches unity.
In all these studies the depth mean flow velocity in the flume was assumed to be equal to that expected at 1.0 m above the bed.
Since the average flow depth was in the order of 0.1 – 0.3 m it is obvious that this assumption leads to a significant and variable underestimation of the $u_{1.0}$ values, the extent of which depend on the flow depth and the vertical velocity gradient.
The discrepancy between the calibration results obtained by GADD ET AL. (1978) and those obtained by TEYSSEN (1984) may be attributed to data selection. The former authors only used data with flow velocities less than 0.55 ms^{-1}, whereas Teyssen considered data in the flow range of 0.4 – 1.0 ms^{-1}. Also, differences in the determination of threshold current velocities will have contributed to the discrepancy.

Note that in none of the studies mentioned above is the relationship of K with grain size precisely defined. Therefore K values obtained by calibration might only be reliable for a narrow range of grain sizes around the grain size considered in the calibration. At present, it is generally accepted that the effective bed-shear stress is related to a roughness height of Nikuradse (k'_s) determined by the coarse tail of the grain size distribution. In most bed-load transport equations this relation is taken into account. The fact that the versions of Bagnold's equation examined do not incorporate a relation with a parameter for the coarse tail of the grain distribution must be regarded as somewhat of a shortcoming, which casts further doubt on the reliability of the formulae.
Although both the Bagnold formulae have been applied to a number of field situations (for a review, see ALLEN & HOMEWOOD, 1984) no verification study based on reliable data from a wide range of flume and field conditions has ever been done. Given the mentioned shortcomings and doubts about the proper values of K as a function of grain size and flow velocity, this study did not attempt such a verification. Note that, in the case of the version proposed by GADD ET AL. (1978), such a verification would only be possible if the parameters of the near bottom current were replaced by parameters of mean flow. Difficulties may arise, when large-scale bedforms are present. For example a current meter positioned at 1 m above the bed will usually lie within an internal boundary layer of the flow, within which the flow structure is directly

related to the bedform morphology. Reliable averages of the current velocity can only be obtained above this boundary layer, which extends above the crest of the bedform for a distance of two to three times the bedform height (DYER, 1980).

KALINSKE (1947) designed a bed-load transport formula that is principally based on observations concerning the critical shear stress for the initiation of grain movement and on a formulation involving the turbulent velocity fluctuations near to the bed, which were assumed to be normally distributed. In the original formula the influence of form drag was ignored.
The complicated formula was simplified by an approximation proposed by ELZERMAN & FRIJLINK (1951). The latter authors also introduced a ripple factor for reducing the bottom shear stress by the shear related to form resistance. They recalibrated the equation using flume and river data. In this paper following BIJKER (1967) this modified equation will be designated as the Kalinske-Frijlink formula.

Recently, the Delft Hydraulics Laboratory presented a method enabling the bed-load transport to be computed as the product of separately derived functions describing the saltation height, the particle velocity and the bed-load concentration (VAN RIJN, 1981; 1984).
A verification study by VAN RIJN (1983), based on a large number of experimental results and data from some shallow rivers, with particle sizes in the range 190-1500 μm, indicated that the Kalinske-Frijlink and the Van Rijn formulae have about the same overall reliability: the inaccuracy of the bed-load transport rate predicted with the formulae, i.e. that measured by sampling was given in terms of a discrepancy ratio, defined as

$$r = \frac{S_{b,\,\text{predicted}}}{S_{b,\,\text{measured}}}$$

In the discrepancy range 0.5–2.0 the two equations showed a similar score (62%), which is a good result for a sediment transport theory (WHITE ET AL., 1975). Therefore these two formulae seem to be the most appropriate for application to situations with bed material in the range of fine to coarse sand.

Van Rijn (1981; 1984) bed-load equation
Van Rijn derived separate functions to predict the thickness of the bed-load layer and the particle velocity and sediment concentration within this layer. As

a product of these functions a bed-load transport formula was established, which can be written as

$$S_b = 0.0351 \varrho_s D_{50} D_*^{-0.3} T^{1.5} u'_* \left\{ 9 + 2.6 \log D_* - 8 \left(\frac{\theta'_{cr}}{\theta'} \right)^{0.5} \right\} \tag{6}$$

in which D_{50} = median particle size, D_* = dimensionless particle parameter, u'_* = bed-shear velocity related to grains, θ' = particle mobility parameter, θ'_{cr} = critical value of the latter parameter according to Shields, T = transport stage parameter, defined as:

$$T = \frac{\theta' - \theta'_{cr}}{\theta'_{cr}}$$

In the Shield's diagram the initiation of collective motion of sediment particles along a plane bed is given as a relationship between a particle mobility parameter θ' and the grain Reynolds number $\bar{R}e_*$:

$$\theta' = \frac{(u'_*)^2}{g \Delta D_{50}} = \frac{\tau'}{\varrho g \Delta D_{50}} \quad ; \quad Re_* = \frac{u'_* D_{50}}{\upsilon}$$
$$\theta'_{cr} = f(Re_*) \tag{8}$$

in which g = acceleration of gravity, τ' = grain-shear stress, υ = kinematic viscosity coefficient.
The original Shield's diagram is not practical, because the critical shear velocity $u_{*,cr}$ can only be ascertained by successive iterations. A more convenient form was proposed by WHITE ET AL.(1973) and YALIN (1972) by replacing the grain Reynolds number by a dimensionless particle parameter D_*:

$$D_* = \left\{ \frac{(Re_*)^2}{\theta'_{cr}} \right\}^{1/3} = D_{50} \left(\frac{\Delta g}{\upsilon^2} \right)^{1/3} \tag{9}$$

The Shields diagram was approximated by VAN RIJN (1981) by the following curves:

$$\begin{aligned}
D_* &< 4 \quad , \quad \theta'_{cr} = 0.24 (D_*)^{-1.0} \\
4 < D_* &\leq 10 \quad , \quad \theta'_{cr} = 0.14 (D_*)^{-0.64} \\
10 < D_* &\leq 20 \quad , \quad \theta'_{cr} = 0.04 (D_*)^{-0.10} \\
20 < D_* &\leq 150 , \quad \theta'_{cr} = 0.013 (D_*)^{0.29} \\
D_* &> 150 , \quad \theta'_{cr} = 0.055
\end{aligned} \tag{10}$$

The shear stress related to grain roughness or effective grain-shear stress (τ') is defined as

$$\tau' = \frac{\varrho g \bar{u}^2}{(C')^2} = \mu\tau \tag{11}$$

in which C' = Chézy coefficient related to grains, μ = bedform factor, $\bar{u}$ = depth mean flow velocity.
When bed forms are present it is assumed that τ' represents the average shear stress at the stoss side of the bed forms.

The Chézy coefficient related to surface roughness is defined as

$$C' = 18 \log \frac{12R}{k_s'} \tag{12}$$

with R = hydraulic radius and k_s' = equivalent grain roughness height of Nikuradse related to a plane bed. The value of k_s' can be ascertained by applying the Kármán-Prandl logarithmic velocity law to experimental data on near-bottom current profiles under plane bed conditions:

$$\frac{u}{u_*} = \frac{1}{\varkappa} \ln \frac{30z}{k_s'} \tag{13}$$

in which $\varkappa$ = constant of Von Kármán, z = height above the bed. Generally, it is implied that the value of k_s' is governed by the coarse tail of the grain size distribution. However, there is little agreement about the nature of this relation. Proposed values for the equivalent grain size range from $k_s' = 1.23\ D_{35}$ (ACKERS & WHITE, 1973) to $k_s' = 5.1\ D_{84}$ (MAHMOOD, 1971). This disagreement at least partly results from the fact that computed values for k'_s always show considerable scatter. The choice of a proper grain diameter therefore remains somewhat arbitrary. In his bed-load transport relation van Rijn chose a value of $k_s' = 3\ D_{90}$, which is the mean value of a large number of flume and field data obtained under approximate plane bed conditions (VAN RIJN, 1982). In addition, it should be noted that the value of C' is not very sensitive to the choice of k_s', especially in the case of natural deep-water fluvial or tidal systems. To determine the grain-shear velocity (u_*') Eq. (11) is transformed to:

$$u'_* = \frac{\bar{u}\sqrt{g}}{C'} \tag{14}$$

Kalinske-Frijlink bed-load equation (1951)
This formula can be written as follows:

$$S_b = 5\varrho_s D_{50}\sqrt{D_{50} g \Delta \mu \theta} \cdot e^{\frac{-0.27}{\mu\theta}} \tag{15}$$

in which:

$$\theta = \frac{Ri}{\Delta D_{50}} = \frac{\tau}{\varrho g \Delta D_{50}} \quad = \text{Shield's entrainment parameter} \tag{16}$$

$$\mu = \left(\frac{C}{C'}\right)^{\alpha} \quad = \text{bedform factor} \tag{17}$$

with C′ according to Eq. (12), $k'_s = D_{90}$,

$$\text{and } C = \frac{\bar{u}}{\sqrt{Ri}} \quad = \text{overall Chézy coefficient} \tag{18}$$

in which i = energy gradient $\simeq$ surface slope
The definition of the bedform factor μ (Eq. 11) implies an exponent $\alpha = 2$. Instead of taking this value ELZERMAN & FRIJLINK (1951) followed MEYER-PETER & MÜLLER (1948), who found that their formula agreed better with experimental results when the value of the exponent $\alpha = 1.5$.

Modification of the Kalinske-Frijlink equation.
Under field conditions the energy gradient (i) is generally not an appropriate parameter for computing the overall Chézy coefficient, because of nonequilibrium phenomena (rising and falling stages of the flow) and problems of accurate measurement.

An alternative way of estimating the value of the Chézy coefficient (C) is to apply Eq. (12) to parameters related to overall roughness:

$$C = 18 \log \frac{12R}{k'_s + k''_s} \tag{19}$$

In which k_s'' = hydraulic roughness caused by bed forms; this parameter can be estimated using empirical functions relating it to bedform height and length such as those proposed by SHINOHARA & TSUBAKI (1959) and VAN RIJN (1984).

A practical difficulty of this alternative is that it is hard to establish an average or representative value for the bedform parameters, especially if several dimensions of superimposed (large-scale) bedforms are present, as is often the case in large rivers and tidal environments.
A further objection to the use of these empirical formulae arises from the fact that they are derived for situations in which the bedforms and flow are in equilibrium. In reality such conditions are hard to find. Form drag is related to the transformation of energy into turbulence in the zone of vortices behind ripples and dunes. When bedforms have not adjusted to the existing flow regime it is to be expected that vortex development will deviate from the equilibrium situation, and it is doubtful whether the hydraulic roughness can still be predicted sufficiently accurately. Because of the large amount of material incorporated in dunes and other large scale bedform the adjustment to changing flow conditions is generally a slow process. In tidal channels therefore, equilibrium is the exception rather than a rule, but in rivers bedform adjustment may also lag far behind change in discharge (ALLEN & COLLINSON, 1979). As demonstrated by BOERSMA & TERWINDT (1981) in tidal environments flow detachment behind dunes may only be well-developed at the time of the maximum velocity of the dominant tidal current. During the subordinate tide, flow separation may be absent.

An attractive alternative for overcoming the objections related to the use of a bedform factor would seem to be replacing the overall shear stress (τ) in Eq. (16) by the shear stress related to grain roughness (τ'). By doing this, the bedform factor (μ) can be left out of the bed-load equation. It is therefore suggested that the particle mobility parameter θ' (as defined in the Van Rijn bed-load equation), with $k_s' = 3D_{90}$ be substituted for the term $\mu\theta$ in Eq (15):

$$S_b = 5\varrho_s D_{50}\sqrt{D_{50} g \Delta\theta'} \cdot e^{\frac{-0.27}{\theta'}} \qquad (20)$$

Note that the definition of the particle mobility parameter (θ'; Eq. 8 and 11) implies a bedform factor (μ) with an exponent $\alpha = 2$, which agrees with the theoretical value, but does not agree with the value of α employed in the original formula of Kalinske-Frijlink (Eq.15). Also, the value chosen for k'_s in Eq. (20) differs from that in Eq. (15). Therefore the formula could not be modified as

proposed above in Eq. (20) until the values of the calibration coefficients (5 and -0.27 in the original version) had been checked. To do this, experimental results from tests in a 45 m long, 2.5 m wide flume at Fort Collins executed by SIMONS & RICHARDSON and published by GUY ET AL. (1966) were used. In these experiments the bed-load transport (S_b) was determined as the difference between the total load transport and the suspended load transport.
For some of their tests Simons & Richardson also gave values for the bedform parameters U_c and H. For the present study these data were used to calculate the bed-load transport in an alternative way, using Eq. (3) and assuming a bedform coefficient $\beta = 0.6$ and a porosity $\varepsilon = 0.4$.

For the calculations done in the present study only those experiments in which the flow depth exceeded 0.1 m and from which the bed-load transport rate could be computed with both methods, were used. The bed-load transport rate was predicted with the original Kalinske-Frijlink function (Eq. 15) and the suggested modification of it (Eq. 20). In total 62 tests were available. In 14 of these tests the median grain size of the sediment was 190 μm, in 11 it was 270 μm, in 17 it was 280 μm, in 2 it was 470 μm and in the remaining 18 it was 930 μm. In table I the results are summarised in terms of the discrepancy ratio (r) as defined on page 97.

Table I Predictive ability of the original Kalinske-Frijlink equation and the proposed modification of it vis- à -vis measured bed-load transport using flume data published by GUY ET AL. (1966).

Bed-load transport formula	Method of bed-load transport measurement	Discrepancy ratio 0,75–1,5	0,5–2	0,33–3		
Kalinske-Frijlink (Eq. 15)	total-susp. load data	37.1	61.3	80.7	%	Scores of predicted bed-load transport
	data U_c and H (Eq. 3)	32.3	71.0	85.5	%	
Modified Kalinske-Frijlink (Eq. 20)	total-susp. load data	40.3	71.0	82.3	%	
	data U_c and H (Eq. 3)	33.9	69.4	88.7	%	

The checks indicated that the proposed modifications to the Kalinske-Frijlink formula did not reduce the predictive ability of the formula. Therefore it did not seem necessary to adjust the calibration coefficients.
Moreover it was also observed that the score of predicted versus measured bed-load transport was hardly affected by the method chosen to ascertain the bed-load transport rate.

The applicability of the Van Rijn and the modified Kalinske-Frijlink functions, as revealed by flume tests

Van Rijn verified his bed-load transport formula with data from flumes and shallow rivers in which the particle size of the bed-load particles ranged from 190–1500 μm (VAN RIJN, 1981; 1983). To date, the only tests on the predictive ability of the modified Kalinske-Frijlink formula have been done with a smaller range in grain sizes (see table I). Therefore, in this study and in order to further evaluate the influence of grain size and flow parameters for a wider range of conditions, it was decided to use a series of flume experiments using fine sand (FALKNER, 1935; GUY ET AL.,1966), coarse sand (ZNAMENSKAYA, 1963; GUY ET AL.,1966) and fine gravel (HO, 1939; LIU AND CASEY, 1935, mentioned by JOHNSON, 1943). In the experiments mentioned by GUY ET AL. (1966) the bed-load transport was ascertained by substracting the suspended load transport from the total load transport. In the other experiments the bed-load transport was measured by a sand trap at the downstream end of the flume. Only experiments with a flow depth exceeding 0.1 m and a Froude number below 0.9 were considered.

Fig. 5.1 gives the resulting discrepancy ratios of predicted versus measured bed-load transport (r) as a function of transport stage (T) for the modified Kalinske-Frijlink formula. Fig. 5.2 does the same for the Van Rijn formula.

For the modified Kalinske-Frijlink equation the results (Fig. 5.1) show a general trend from overestimation at low transport stages to a slight underestimation of measured bed-load transport at high transport stages. For the Van Rijn function no such general trend is present (Fig. 5.2); however, for the experiments with fine sand there is a tendency for bed-load transport to be underestimated at lower transport stages.

Comparison of measured and predicted bed-load transport rate in some rivers and tidal environments.

Description of field data used in the present study.

Published field data on simultaneously measured bedform celerity, bedform height and current velocity are extremely scarce. Only two sets of reliable published data could be traced: for the Hii river in Japan (SHINOHARA & TSUBAKI, 1959) and for the Skive-Karup river in Denmark (HANSEN, 1966). In addition to this, data from some unpublished reports, on rivers and tidal areas in the Netherlands will be considered here: measurements reported by OTTE (1982), for the Pannerden Canal and by HAVINGA (1982) for the IJssel river, both of which are distributaries of the Rhine river; data of the Dommel river (VAN ALPHEN ET AL., 1983), a small distributary of the Meuse river; and three sets of the data from a tidal setting: two locations on a shoal in the

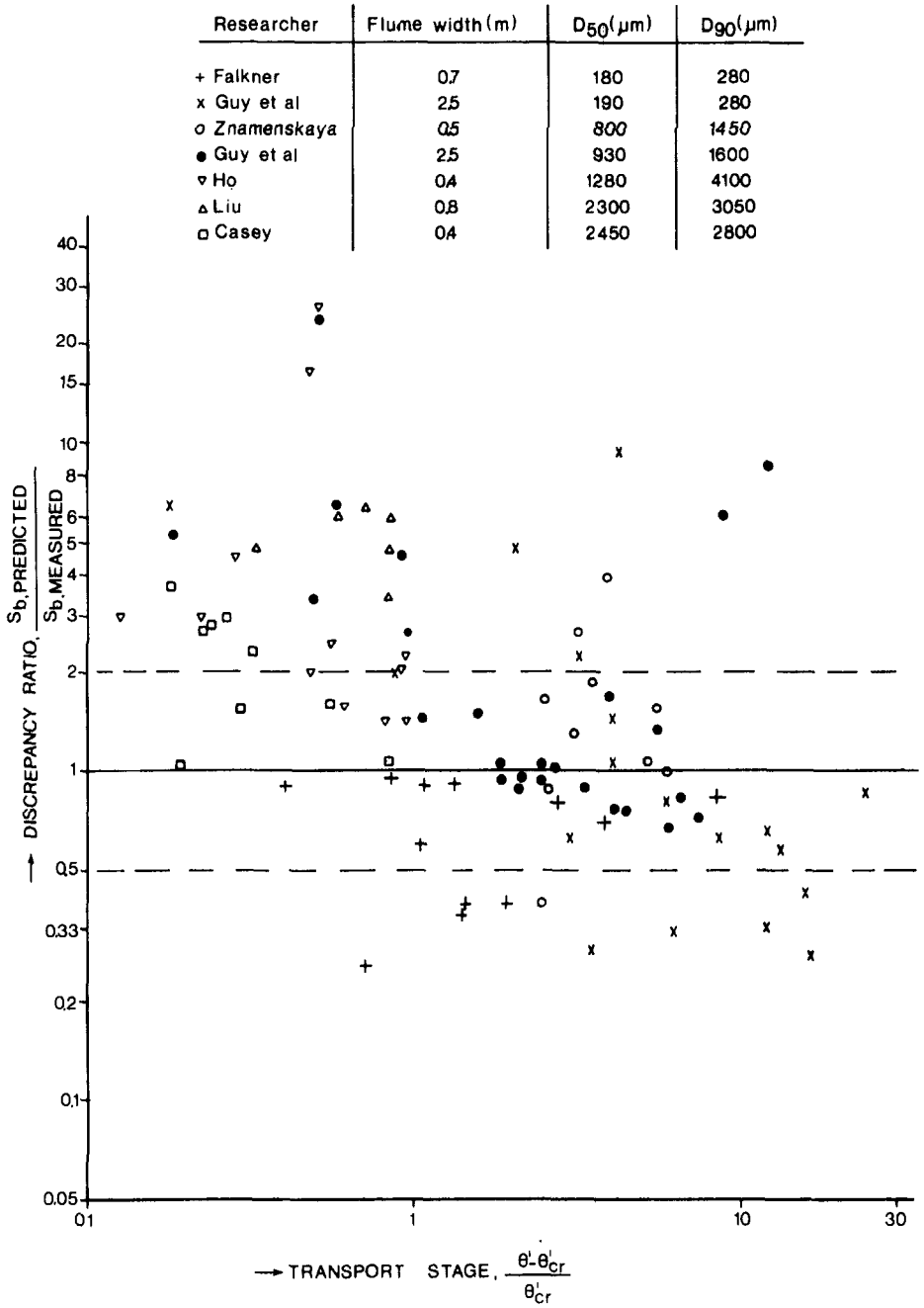

Fig. 5.1 Discrepancy ratio of bed-load transport as a function of transport stage, using the modified Kalinske-Frijlink bed-load formula and flume data

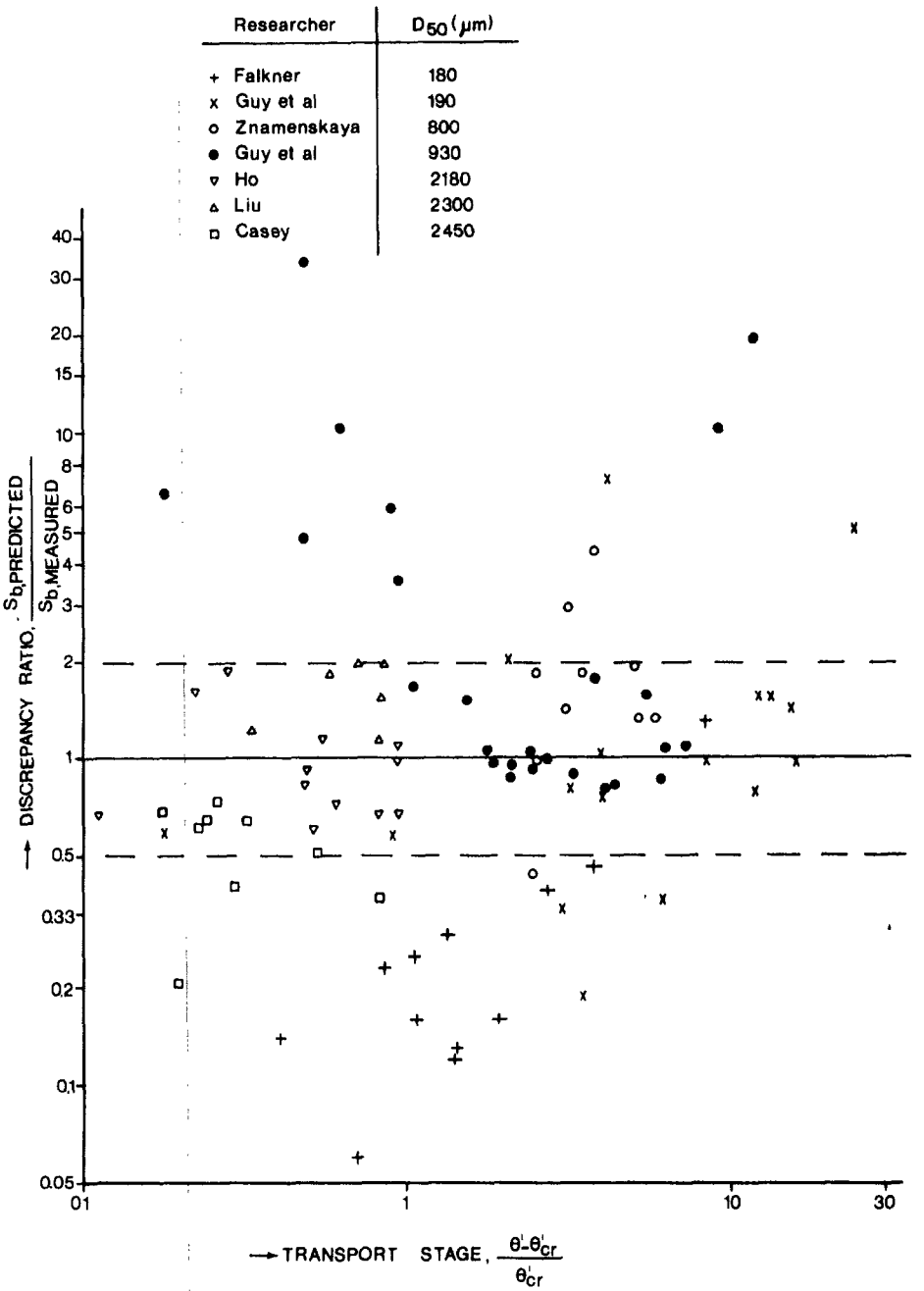

Fig. 5.2 Discrepancy ratio of bed-load transport as a function of transport stage, using the Van Rijn bed-load transport formula and flume data

Westerschelde (BERBEN ET AL., 1978) and some data from a tidal channel in the Oosterschelde (VAN DEN BERG, 1985); some other unpublished data sets from locations in the Rhine river and its southernmost distributary, the Waal river, in the Netherlands were also used (pers. comm. H. Havinga, Rijkswaterstaat, Arnhem).
The geographical locations of the unpublished studies are indicated in Fig. 5.3. Table II gives the range of average values of some characteristic parameters measured during these studies.
Some information on measuring procedures and results of the unpublished work is given in the following sections.

Location 1–5
In the large Dutch rivers (location 1–5 in Fig. 5.3) data on bedform parameters have been collected using a digital sounding system. Soundings were carried out at distances of 15 to 30 m apart along a number of longitudinal transects.

To ascertain the dune dimensions and propagation speed, erroneous small-scale undulations and bed level fluctuations related to very long and flat sandwaves on which the dunes were sometimes superimposed, were discarded, using a filtering procedure described by HAVINGA, (1982). For instance, at location 5, bedforms with a wavelength greater than 100 m and smaller than 7 m were ignored.

Current velocity and river discharge were measured with shipboard operated Ott-type propellor current meters at a number of locations in the river cross-section. Then the relation between the mean current velocities computed for the central part of the river and the mean dune height and celerity computed from sounding data covering the central part of the river over a distance of several hundreds of metres upstream and downstream from the measuring site was ascertained. An exception is formed by the study done at location 1. Here, the sounded river stretch was 500–900 m upstream from the site where the current was measured. All the studied examples of the Rhine and its distributaries refer to straight stretches of river. This means that the flow structure was little influenced by channel curvature and probably did not vary greatly over the study area. Therefore, the measured current velocity data were regarded as being representative of the river stretches studied.

The measurements were all carried out at periods of high river discharge, mostly in the spring at the time that snow melts in the upper reaches of the Rhine river. During some of the investigations, river discharge changed dramatically. For instance, at location 1 within a measuring period of 6 days the discharge fell

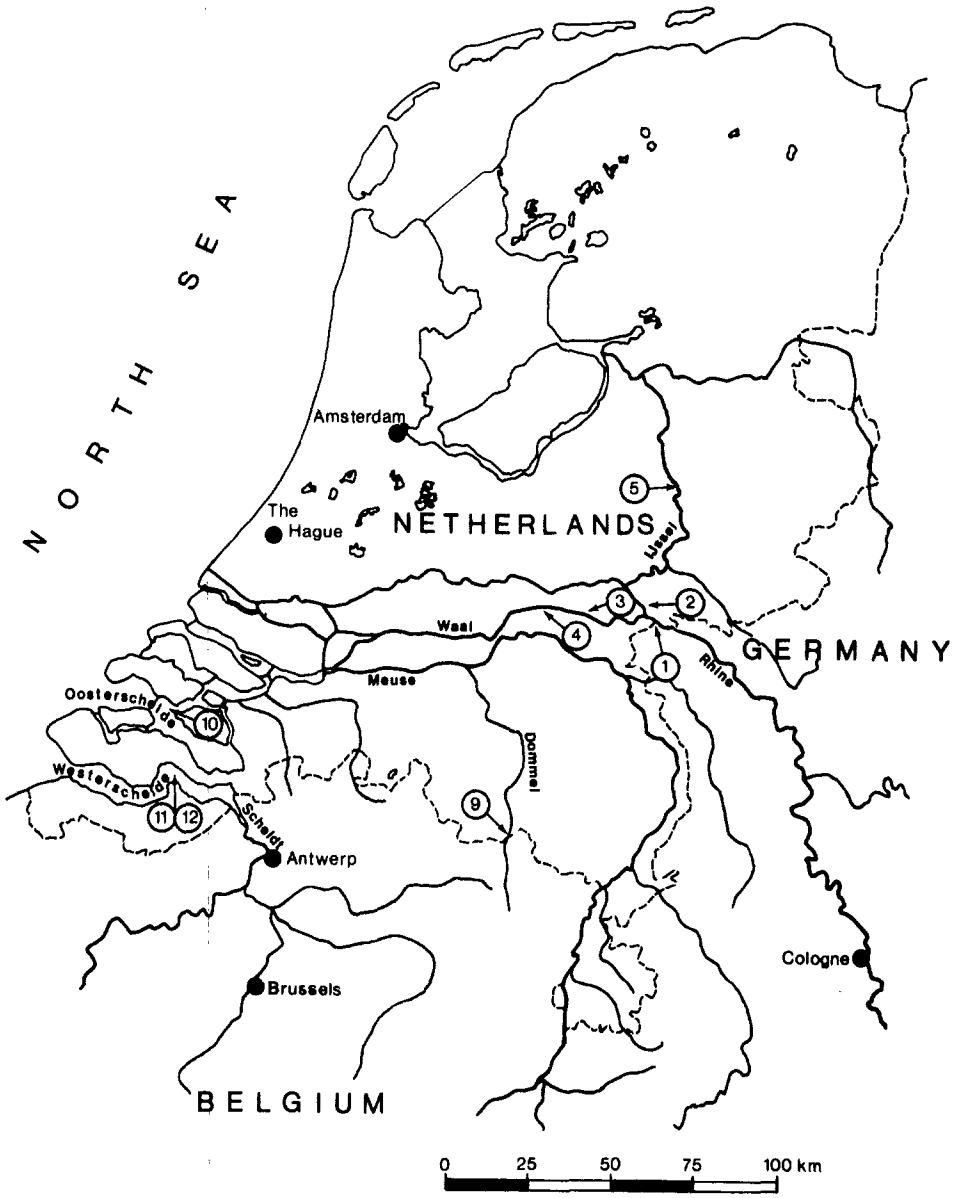

Fig. 5.3 Location of study areas (unpublished investigations)

from 8100 m^3s^{-1} to 4500 m^3s^{-1}. Despite that, mean dune height was hardly affected, diminishing by only 10%.

At peak discharge the mean rate of dune migration was approximately 14.5 m per day. However, remodelling of dune shape continued to take place at a slow rate. Monitoring of specific morphological features indicated that individual dunes were easily recognizable on consecutive daily echograms (see Fig. 5.4).

The data on grain size shown in table II refer to means of large numbers of samples of the riverbed taken in the different river stretches during a sampling campaign in 1974–1976 by the Rijkswaterstaat, Arnhem. But the river measurements that yielded the values for grain parameters used in the present study were all carried out in the period 1979–1983. There is, therefore, a chance that these parameters may deviate from those obtained by the earlier samplings. However, occasional sampling during the past few years does not indicate that the grain size characteristics have changed significantly at these locations (pers. comm. H. Havinga).

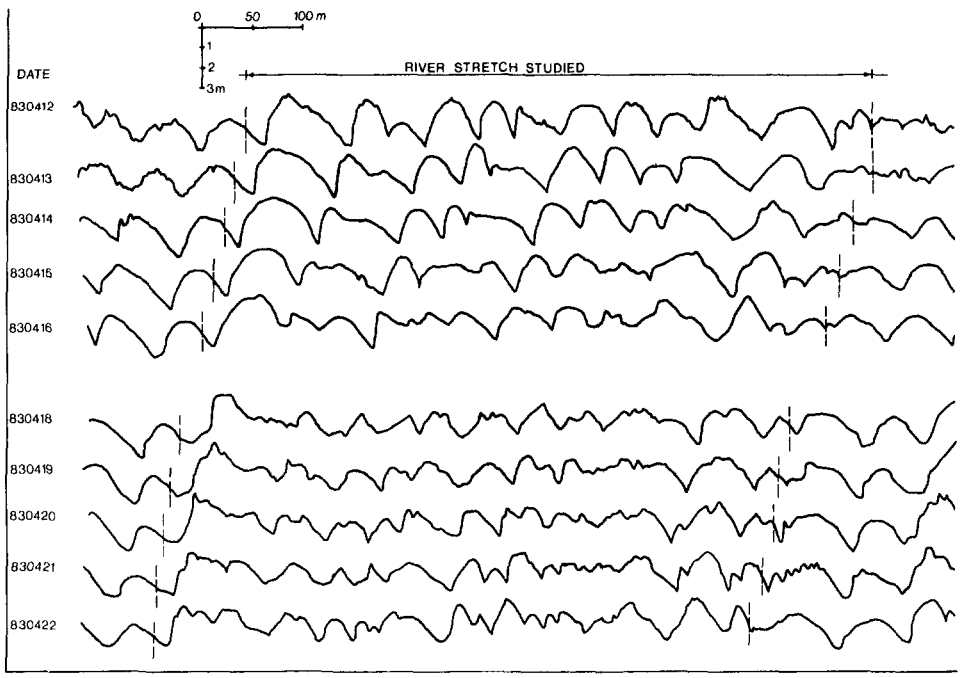

Fig. 5.4 Dune migration on daily echograms of the Waal, location 3

Table II Summary of field data

Setting	Location	Source	River discharge ($m^3.s^{-1}$)	h (m)	$\bar{u}$ ($m.s^{-1}$)	D_{50} (μm)	D_{90} (μm)	Temp (°C)	H (m)
Large rivers (Rhine and its distributaries)	1 Rhine	This paper	4500–8100	8.9–10.4	1.47–1.60	3600	14500	1–2	1.4–1.6
	2 Pannerden canal	Otte (1982)	1530–2280	8.0–9.4	1.55–1.78	3800	5000	7	no data
	3 Waal	This paper	3490–6080	8.6–10.0	1.34–1.65	1050	1750	9–11	1.0–1.3
	4 Waal	This paper	1630–2750	9.0–10.0	1.10–1.20	950	1550	9–10	0.8–1.2
	5 IJssel	Havinga (1982)	370–410	5.0–5.3	0.49–0.57	690	1270	7	0.5–0.6
Small rivers	6 Hii	Shinohara & Tsubaki (1959)	no data	0.59–0.73	0.74–0.93	1440	4000	no data	0.08–0.14
	7 Hii			0.71–1.03	0.79–0.90	1110	2700		0.18–0.25
	8 Skive Karup	Hansen (1966)	6.45	1.0	0.6	460	1260	10	0.09
	9 Dommel	v. Alphen et al. ('83)	1.11–1.36	0.66–0.80	0.43–0.60	370–452	750–780	16	0.02–0.05
Tidal environments	10 Oosterschelde (channel)	v.d. Berg (1985)		6.7–9.8	0 –1.15	208	307	11–18	0.9
	11 Westerschelde (shoal)	Berben et al. (1978)		0 –2.1	0 –0.82	170	250	20	0.13–0.18
	12 Westerschelde (shoal)	Berben et al. (1978)		0 –3.1	0 –1.00	170	250	20	0.17–0.38

Location 9
In the Dommel river bed profiles were measured using a sounding system moving along a rail of a rigid construction placed on the riverbed. In this way a series of longitudinal transects, each of 4 m length was measured at several locations. Simultaneously samples of the bed material were taken and current velocities were measured with a number of current meters mounted at different heights above the bed in a frame placed near to the sounding bridge.

Location 10–12
These locations are found in two tidal settings in the Southwestern part of the Netherlands. Tides in these areas are semidiurnal. In the vicinity of the study areas in the Oosterschelde and Westerschelde mean tidal ranges during spring tide were 3.4 m and 4.9 m respectively. At neap tide tidal ranges were 2.7 m and 3.5 m.

Both settings may thus be classified as mesotidal (DAVIES, 1964). The Westerschelde forms the estuarine lower course of the Scheldt River. The Oosterschelde, which lost its estuarine connection with the Scheldt River in the 19th century, might be described as an abandoned estuary or tidal sea-arm (VAN DEN BERG, 1980). In the central part of the Oosterschelde sea-arm (location 10), migration of dunes was studied in a strongly flood-dominated part of a tidal channel. Attention has focused on an area measuring 160 × 160 m, lying 7.5 to 9.0 m below Mean Sea Level. Over a period of two spring-neap tidal cycles current velocity and current direction were measured 4 metres above the bottom by means of an automated propeller current meter (Flachsee). Data on current parameters for 10-minute periods were averaged, and stored on tape. In addition current velocity was measured simultaneously at different heights above the bed throughout a tidal cycle. To prevent undesired effects of large-scale turbulence, average current values were read over periods of 300 s. In this way, 10 velocity profiles per hour were measured. In a period around slack water, current velocity distribution was dominated by inertial forces. However it was found that at average flow velocities above 0.35 ms^{-1} frictional forces were dominant and the velocity profile appeared to take a logarithmic distribution resembling steady river flow conditions. In the study area the threshold for the collective motion of sand particles along the bed was found according to the Shield's criterion (θ'_{cr}) to occur at an average current velocity of $\bar{u} = 0.4$ ms^{-1} (Eqs. 8, 9, 10, 11 and 12).
This, is may be assumed that bed-load transport only start after the velocity profile had adjusted to a logarithmic form. This would also be true for the locations studied in the Westerschelde. This means that the hydraulic relations in the bed-load equations used could also be applied to the tidal settings studied.

In the Oosterschelde study area, depth mean flow velocities computed from the measured current profiles were related to the long-term current measurement at 4 m above the bottom. By so doing, an array of 10 minute values of mean flow velocity over a period of 4 weeks was produced. According to this data set, maximum flow velocities at flood tide were 0.67 ms^{-1} and 0.93 ms^{-1} at neap and spring tides, respectively. At ebb tide the flow velocity reached a value of 0.42 ms^{-1} at neap tide and 0.50 ms^{-1} at spring tide. Thus, if the critical current for sediment motion is 0.4 ms^{-1} it is obvious that bed-load transport in the Oosterschelde study area almost exclusively took place at flood tide.
In the Oosterschelde sea-arm, migration of dunes was followed over six months using Side-Looking Sonar images. (Klein, hydroscan 500, 500 KHz). Data were processed to eliminate lateral scale distortions. The direction of the Sonar tracks was parallel to the main direction of the dune crestlines, in order to ascertain the maximum reflection and resolution of the sideways transmitted sound pulses of the Sonar fish on the steep dune fronts facing the Sonar device. In this way sonograms were obtained showing the dune fronts as dark tones, on one side sharply limited by the top of the avalanche slope (brinkpoint). Dune migration was ascertained measuring the distance of the sharply defined brink-point on the Sonar images from marks representing Sonar reflectors that were firmly moored on the bottom. The bedforms consisted of dunes with sinuous crestlines. Average wavelength was 22 m and dune amplitude measured 0.9 m. These values barely fluctuated during the research period. Bedforms with a wavelength of less than 10 m were ignored. The dunes appeared to migrate in the same direction as the flood current at a rate of about 4.5 m over a month time.

Finally, data from two locations in the Westerschelde estuary were considered. The locations were situated on a shoal, one at a height of about 0.5 m above mean sea level and the other at 0.5 m below mean sea level.
The vertical velocity profile was measured at 10 min. intervals throughout a number of tidal cycles over a period of two neap/spring cycles. Dune height and celerity were also measured. The latter data were obtained from 27 m long flow parallel seabed profiles obtained at low tide.
For the present study, very low migration rates (indicating a bed-load transport less than 10 kg $m^{-1}tide^{-1}$) were discarded. 27 sets of data covering complete tidal cycles remained available for computations. Both sites were located in flood dominated areas.
At locations 11 and 12, measured averages of flow velocity during the flood tide ranged between 0.6–0.8 ms^{-1} and 0.5–1.0 ms^{-1}, respectively.
For the ebb, the corresponding maximum flow ranges were 0.3–0.5 ms^{-1} and 0.3–0.6 ms^{-1}.
At location 12 dune height showed a cyclic change related to the neap/spring

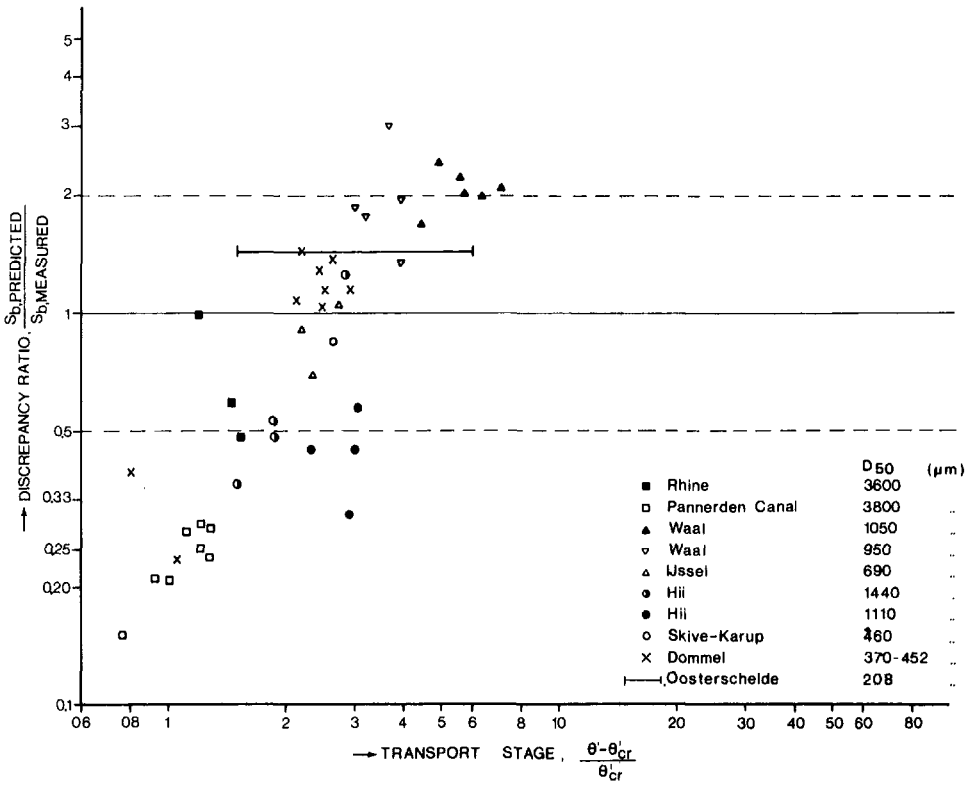

Fig. 5.5 Discrepancy ratio of bed-load transport as a function of transport stage, using the Van Rijn bed-load transport formula and data of rivers and the Oosterschelde

cycle. Dune height increased gradually from about 0.2 m at neap to 0.4 m at spring tide. At location 11 this relation was less obvious. For a more detailed description of measuring procedures, hydraulic conditions and bedform morphology on the shoal during this investigation the reader is referred to TERWINDT & BROUWER (1986).

Additional information on the data used for predicting the bed-load transport

The river data used to test the applicability of the bed-load transport formulae are given in appendix II. Only data obtained from a flow depth larger than 0.5 m were used.

For the tidal locations considered in this study the formulae were applied to the 10-min. arrays of average flow velocity values. In the case of the Oosterschelde study area calculations were carried out assuming a constant water depth of 9.5 m. This is about the water depth at which the flood current velocity reached its maximum (1 hour before high water). Because of the great water-depth the transport formulae are not very sensitive to changes in the flow depth,

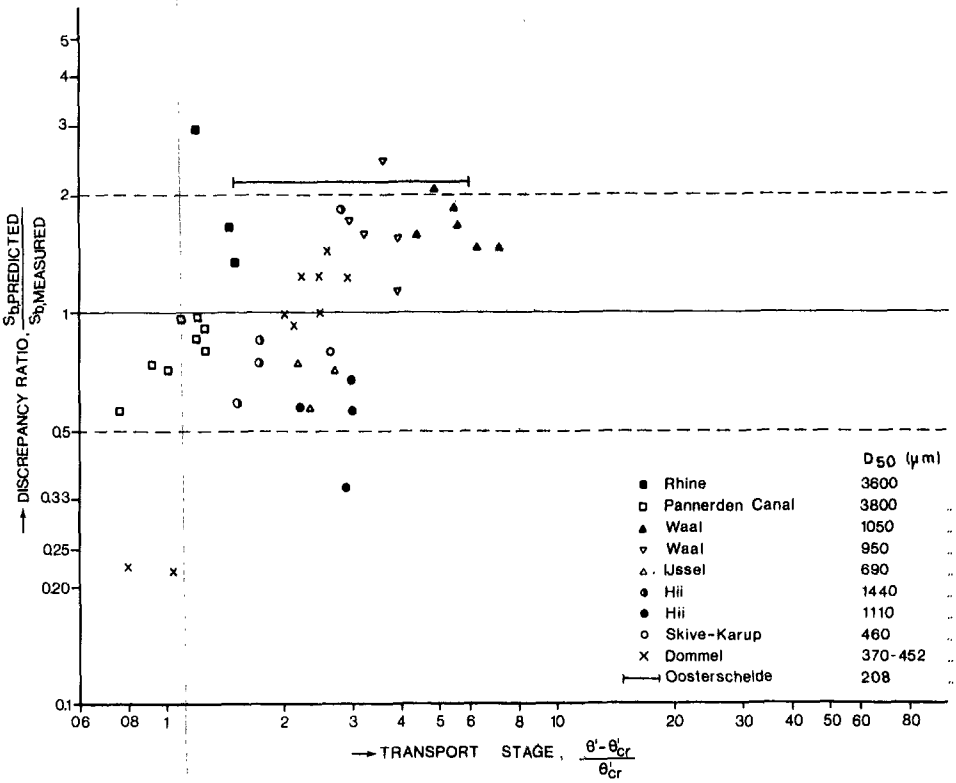

Fig. 5.6 Discrepancy ratio of bed-load transport as a function of transport stage, using the modified Kalinske-Frijlink bed-load transport formula and data of rivers and the Oosterschelde

which justifies this simplification: a 10% systematic error in the assumed representative depth would account for a deviation of about 5% in the bed-load transport predicted by the Van Rijn formula. In the case of the modified Kalinske-Frijlink equation this deviation would be even less: about 3%.
These errors are small compared with errors in the computed flow velocity. For instance, a plausible 3% systematic error of this kind at current velocities of 0.8 ms^{-1} would result in deviations in the computational results 17% in the Van Rijn formula and 10% in the modified Kalinske-Frijlink formula.

Results

In Figs. 5.5 and 5.6 the discrepancy ratios (r) of bed-load transport as deduced from bedform parameters (Eq. 3) and predicted with the bed-load transport formulae (Eqs. 6 and 20) are given as a function of transport stage (T). The river data used for these figures are given in Appendix II. For the Oosterschelde study, the final results for the whole measurement period (175 days) are presented; within this period 4 sidescan sonar surveys were used to ascertain

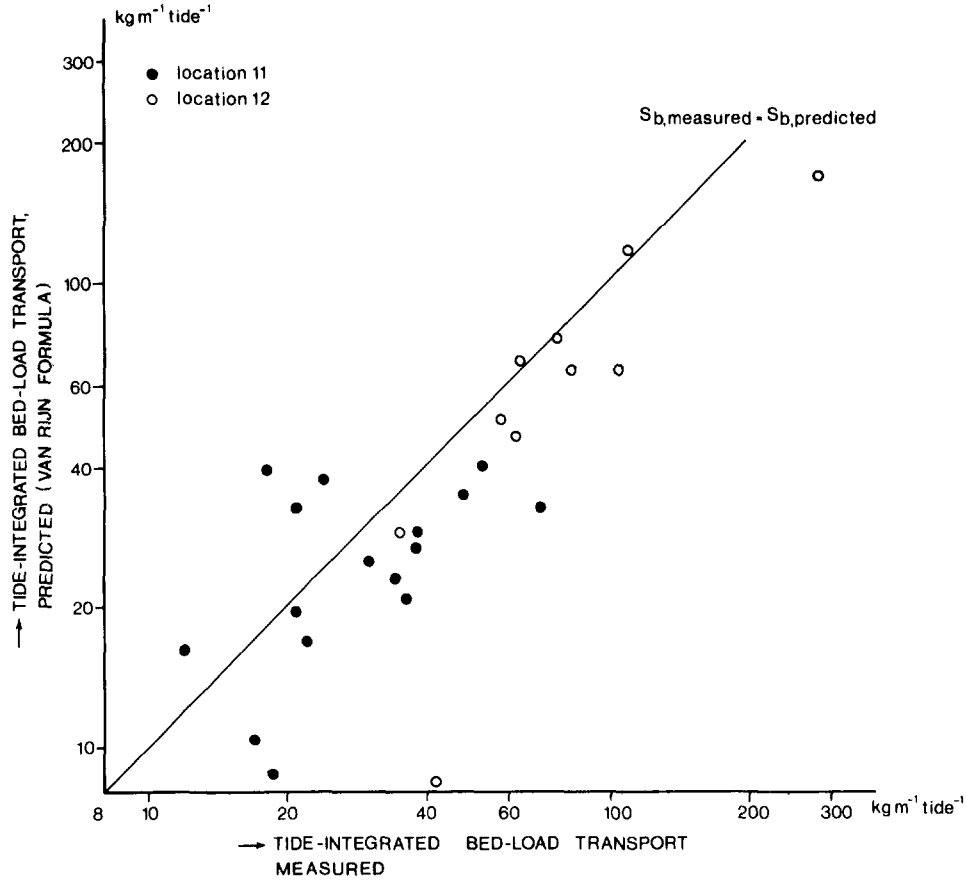

Fig. 5.7 Tide-integrated bed-load transport on the Ossenisse Shoal locations measured by dune migration (Eq. 3) and predicted by the Van Rijn formula (Eq. 6)

dune migration. The discrepancy ratios computed for the periods between the successive sonar surveys do not deviate more than 12% from the final results. Representative transport stages for this tidal setting range between 1.5 and 6.0. At transport stages (T) below 1.5, the frequency distributions of measured flood and ebb flow velocity suggest that the total ebb and flood bed-load transports equalize each other.

The results for Van Rijn's bed-load theory (Fig. 5.5) show that at relatively high transport stages bed-load transport is systematically overestimated, whereas at low transport stages it is systematically underestimated. A similar trend of increase in the discrepancy ratio with transport stage can be observed in the verification results presented by VAN RIJN (1981) for some of the series of flume experiments he used, and the tests with fine sands presented in Fig. 5.2.

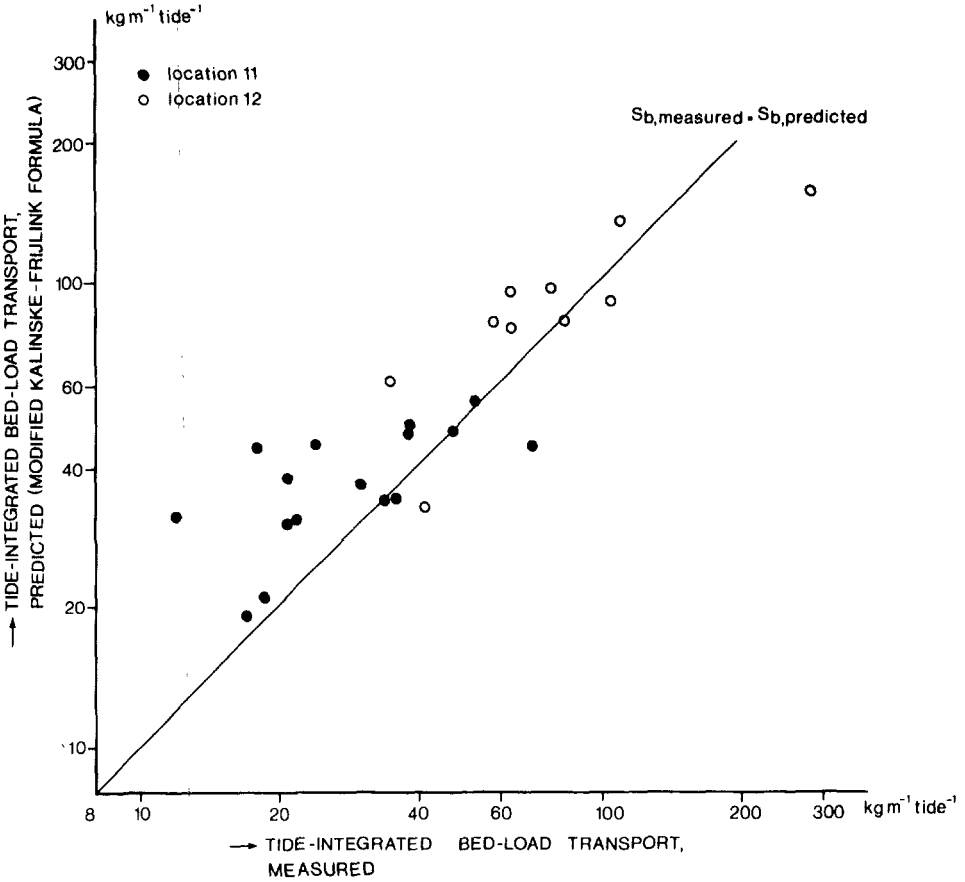

Fig. 5.8 Tide-integrated bed-load transport on the Ossenisse Shoal locations measured by dune migration (Eq. 3) and predicted by the modified Kalinske-Frijlink formula (Eq. 20)

The results for the modified Kalinske-Frijlink equation (Fig. 5.6) show a better agreement between the observed and predicted bed-load transport rates. Contrary to the findings from flume tests (Fig. 5.1) there was no tendancy to overestimate bed-load transport at low transport stages. Instead, for values of the transport stage (T) larger than 3, the predicted bed-load transport was somewhat too high. As can be observed in Figs. 5.5 and 5.6, neither of the formulae show systematic deviations related to the particle diameter.

The results of a comparison between of predicted and observed net bed-load transport rates per tide at the shoal locations in the Westerschelde are presented in Figs. 5.7 and 5.8.

Both the predictions by the Van Rijn formula and by the modified Kalinske-Frijlink formula give a reasonable estimate of the bed-load transport as deduced

from bedform parameters: the greater the bed-load, the more reliable the estimate. When small amounts of material are transported the modified Kalinske-Frijlink equation slightly overestimates the measured amounts.
Given that the bed material in the Westerschelde is fine-grained, the agreement between predicted and measured bed-load transport is remarkable, since local differences in the balance between lift into suspension and settling from suspension along the bed may significantly influence the bedform migration: detailed examination of the internal sedimentary structure in cross-sections of dunes on the Westerschelde shoal location by BOERSMA & TERWINDT (1981) and KOHSIEK & TERWINDT (1981) revealed, that significant volumes of sand may settle from suspension on the dune lee-side, especially during accelerating and decelerating stages of the dominant tidal current. On the other hand, at full vortex stage of dune migration similar quantities might be lifted into suspension in the area of vigorous turbulence near the brinkpoint of the dunes.
If this process is important, the sediment transport involved in dune migration will be smaller than the bed-load transport. But if the process of settling from suspension on the dune front dominates, the opposite will be true. The correspondence found suggests that in the Westerschelde cases both processes are not very important or balance each other. In the case of the Oosterschelde tidal channel, the process of 'bursting' might account for an overestimation of predicted values of bed-load transport: according to MATTHES (1947) bursting processes resulting from the development of vertical eddies or kolks behind dunes would be more strongly developed in deep waters, thus enhancing the take-up of bed-load material into suspension.

Conclusions

The main aim of this study was to investigate the assumption that a reliable estimate of the bed-load transport, defined as the sediment transport in the saltation layer, could be obtained using data on bedform height and bedform celerity. A second aim was to check the ability of some bed-load transport formulae to predict the bed-load transport as deduced from bedform migration in natural environments with bed material ranging from fine to coarse grained sand.

The main conclusions of this study are:
– An analysis of flume experiments and some river data indicated that a reasonable estimate of the bed-load transport rate can be obtained by using data on the height and celerity of bedforms.

– It was found that some simplified versions of the Bagnold bed-load theory,

which enjoy a certain popularity amongst marine geologists, do not satisfactorily represent the physical parameters involved. Therefore, the reliability of these formulae is suspect.

– Results of a verification study using field data showed that the Van Rijn bed-load function overestimates the bed-load transport at relatively high transport stages and underestimates it at low transport stages.

– The above mentioned trend was not obvious in the results obtained using a slightly modified version of the Kalinske-Frijlink formula. This function gave a reliable estimate of the bed-load transport: of the 43 sets of river data 86% of the predicted transport rates were found to be within 0.5–2.0 times the measured values.

– When verifying the bed-load transport formulae using flume data against results using field data with a greater water depth, there were some discrepancies. Therefore it may be generally stated that an evaluation of a transport formula using flume data is not conclusive and should always be followed by a verification in the field.

Acknowledgments

I would like to thank Mr. L. C. Van Rijn, senior engineer, Delft Hydraulics Laboratory, and Mr. E. A. Collard, Svasek Engineering Consultants, for some useful comments and suggestions at an early stage of the study. Prof. Dr. J. H. J. Terwindt, Utrecht University, and my fellow colleagues Messrs. L. H. M. Kohsiek, F. M. L. Berben, T. Louters and P. Van Vessem are thanked for their careful and critical reviews. I am also grateful to Mr. Havinga, Rijkswaterstaat, Arnhem and Mr. Kohsiek, for placing measuring data at my disposal.

References

ACKERS, P. & W. WHITE, 1973. Sediment transport: new approach and analysis. Journal of the Hydraulics Division, ASCE, HY 11: 2041–2060.
ALLEN, J. R. L. & J. D. COLLINSON, 1974. The superposition and classification of dunes formed by unidirectional aquous flows. Sedimentary Geology, 12: 169–178.
ALLEN, P. A. & P. HOMEWOOD, 1984. Evolution and mechanics of a Miocene tidal sandwave. Sedimentology, 31: 63–81.
BAGNOLD, R. A., 1963. Mechanics of marine sedimentation. In: Hill, M. N. (ed.). The Sea: Ideas and Observations. vol. III. Interscience, New York.
BERBEN, F. M. L., M. J. N. BROUWER, L. H. M. KOHSIEK, J. C. A.

LEMKES & F. H. I. M. STEYAERT 1978. Ribbelvormen, waterbeweging en hun onderlinge samenhang in een getijdengebied (Plaat van Ossenisse, Westerschelde). Geografisch Instituut, Rijksuniversiteit Utrecht: 214 pp (unpublished).
BIJKER, E. W., 1967. Some consideration about scales for coastal models with movable bed. Delft Hydraulics Laboratory, Publication No. 50: 142 pp.
BOERSMA, J. R. & J. H. J. TERWINDT, 1981. Neap-spring tide sequences of intertidal shoal deposits in a mesotidal estuary. Sedimentology, 28: 151–170.
BROOKS, N. H., 1958. Mechanics of streams with movable beds of fine sand. Transactions ASCE, 123: 526–549.
CASEY, H. J., 1935, Über Geschiebebewegung. Mitt. der Preuss. Versuchanst. Wasserbau und Schiffbau, 19, Berlin: 86 pp.
DALRYMPLE, R. W., KNIGHT, R. J. & J. J. LAMBIASE 1978. Bedforms and their hydraulic stability relationships in a tidal environment, Bay of Fundy, Canada. Nature, 275: 100–104.
DAVIES, J. L. 1964. A morphogenetic approach to world shorelines. Zeitschrift für Geomorphologie, 8: 127–142.
DYER, K. R., 1980. Velocity profiles over a rippled bed and the threshold of movement of sand. Estuarine and Coastal Marine Science 10: 181–199.
EINSTEIN, H. A., 1950. The bed load function for sediment transportation in open channel flows. Soil conservation service. U.S. Department of Agriculture, Washington D.C., Technical BulletinNo. 1026: 25 pp.
ELZERMAN, J. J. & H. C. FRIJLINK, 1951. Present state of the investigation on bed load movement in Holland. IXth Assembly of the International Union of Geodesy and Geophysics, Brussels: 100–106.
ENGEL, P. & Y. LAM LAU, 1981. Bed load discharge coefficient. Journal of the Hydraulics Division ASCE No. HY 11: 1445–1453.
ENGELUND, F. & E. HANSEN, 1967. A monograph on sediment transport in alluvial streams. Teknisk Forlag, Copenhagen.
FALKNER, H., 1935. Studies of river bed materials and their movement with special reference to the lower Mississippi river. Paper 17, U.S. Waterways Exp. Station, Vicksburg.
GADD, P. E., J. W. LAVELLE & D. J. SWIFT, 1978. Estimates of sand transport on the New York Shelf using nearbottom current meter observations. Journal of Sedimentary Petrology, 48; 239–252.
GUY, H. P., D. B. SIMONS & E. V. RICHARDSON, 1966. Summary of alluvial channel date from flume experiments 1955–1961. Prof. paper U.S. Geological Survey, 4621; 92 pp.
HANSEN, E., 1966. Bed–load investigations in Skive–Karup river. Technical University of Denmark, Bull. no. 12: 1–8.
HARMS, J. C., J. B. SOUTHARD, D. R. SPEARING & R. G. WALKER, 1975. Depositional environments as interpreted from primary sedimentary structures

and stratification sequences. Lecture Notes Soc. Econ. Paleont. Miner. Short Course 2. Dalles, Texas: 161 pp.
HAVINGA, H. 1982. Bed load determination by dune tracking. Rijkswaterstaat, Directie Waterhuishouding en Waterbeweging, District Zuidoost, Nota 82.3: 15 pp.
HO, PANG YUNG, 1939. Abhängigkeit der Geschiebebewegung von der Kornform und der Temperature. Mitt. der Preuss. Versuchsans. Wasserbau und Schiffbau, Berlin: 43 pp.
JOHNSON, J. W., 1943. Laboratory investigations on bed-load transportation and bed roughness; a compilation of published and unpublished data. Paper SCS-TP-50, U.S. Dept. of Agriculture, Washington D.C.: 116 pp.
KALINSKE, A. A., 1974. Movement of sediment as bed load in rivers. Transactions American Geophysical Union, 28: 615–620.
KOHSIEK, L. H. M. and J. H. J. TERWINDT, 1981. Characteristics of foreset and topset bedding in megaripples related to hydrodynamic conditons in an intertidal shoal. In: Nio, S-D, R. T. E. Schüttenhelm & Tj. C. E. van Weering (eds.); Holocene Marine Sedimentation in the North Sea Basin. Special Publication I.A.S., 5, Blackwell, Oxford: 27–37.
LANGHORNE, D. N., 1981. An Evaluation of Bagnold's dimensionless coefficient of proportionality using measurements of sandwave movement. Marine Geology, 43: 49–64.
MAHMOOD, K., 1971. Flow in sand bed channels. Water management technical report 11, Colorado State University, Fort Collins.
MARDJIKOEN, P. 1966. Some characteristics of sandwaves in open channels with movable bed. Delft Hydraulics Laboratory; Report R. 7, Delft, The Netherlands, 17 pp.
MATTHES, G. H.,1947. Macroturbulence in natural stream flow. Transactions, American Geophysical Union, 28: 255–262.
MEYER-PETER, E. & R. MÜLLER, 1948. Formulas for bed load transport. Proceedings second congress IAHR Stockholm, Sweden, Paper No. 2, 39–64.
OTTE, F. J., 1982. Bodemtransport en duinen: vooruitgang? Deel 2: theorie en nauwkeurigheid. TH Delft, 166 pp (unpublished).
SHINOHARA, K. & T. TSUBAKI, 1959. On the characteristics of sand waves formed upon the beds of the open channels and rivers. Reports of Research Institute for applied mechanics, Kyushu University.: 15–45.
SIMONS, D. B., E. V. RICHARDSON & C. F. NORDIN, 1965. Unsteady movement of ripples and dunes related to bed-load transport. Proceedings I.A.H.R. congress Leningrad, 3.29.: 1–8.
STERNBERG, R. W., 1972. Prediction of initial motion and bedload transport of sediment particles in the shallow marine environment. In: Swift, D. J. P., Duane & O. H. Pilkey (eds.) Shelf sediment transport: process and pattern. Dowden, Hutchinson & Ross; Stroudsburg; 61–82.

TERWINDT, J. H. J. & M. J. N. BROUWER, 1986. The behaviour of intertidal sandwaves during neap-spring side cycles and the relevance for palaeo-flow reconstructions. Sedimentology, 33:1–31.
TEYSSEN, T., 1984. Physical model and fortran IV program to estimate paleotidal flow velocities from features of sand waves. Computers & Geosciences 10: 237–244.
VAN ALPHEN, J., P. BLOKS & P. HOEKSTRA, 1983. Onderzoek naar de waterbeweging, morfologie en sedimentaire strukturen in de meanderende rivier de Dommel. Geografisch Instituut Rijksuniversiteit Utrecht, 419 pp (unpublished).
VAN DEN BERG, J. H., 1980. Field Course Guidebook on Clastic Tidal Deposits, Comparative Sedimentology Division, Institute of Earth Sciences Rijksuniversiteit Utrecht: 63 pp.
VAN DEN BERG, J. H., 1985. Meting en berekening van bodemtransport in een megaribbelveld ten noorden van de Galgeplaat, Oosterschelde. Nota DDWT 85.023, Rijkswaterstaat.
VAN RIJN, L. C., 1984. Sediment transport, part I: bed–load transport. Journal of Hydraulics Engineering, 110: 1431–1456.
Netherlands, 43 pp.
VAN RIJN, L. C., 1982. Equivalent roughness of alluvial bed. Journal of the Hydraulics Divisions, ASCE, HY 10:
VAN RIJN, L. C., 1983. Siltation in dredged trenches: Entrainment of fine sediment particles; sediment pick–up functions; Delft Hydraulics Laboratory; Report Investigation M1531 part IV, Delft, The Netherlands, 29 pp.
VAN RIJN, L. C.,1984. Sediment transport, part I: bed-load transport. Journal of Hydraulics Engineering, 110: 1431–1456.
VAN RIJN, L. C., 1984. Sediment transport, part III: bed forms and alluvial roughness. Journal of Hydraulic Engineering, 110: 1733–1754.
WHITE, W. R., H. MILLI & A. D. CRABBE, 1973. Sediment transport: an appraisal of available methods, vol. 2, performance of theoretical method when applied to flume and field data. Report INT 119 Hydraulic Research Station, Wallingford, England.
WHITE, W. R., H. MILLI & A. D. CRABBE, 1975. Sediment transport theories: a review. Proceedings Institution of Civil Engineers, Part 2; 265–292.
YALIN, M. S., 1972. Mechanics of Sediment Transport. Pergamon Press, New York: 298 pp.
ZNAMENSKAYA, N. S., 1963. Experimental study of the dune movement of sediment. Soviet Hydrology selected papers, no. 3.: 253–275.

Appendix I – Notation

The following symbols are used in this paper:

A	area (L^2);
C	Chézy-coefficient ($L^{0.5}T^{-1}$);
D_{50}	median particle diameter of the bed material (L);
D_{35}	35% of the bed material is finer than this particle diameter (L);
D_*	particle parameter (–);
g	acceleration of gravity (LT^{-2});
H	bedform height (L);
h	flow depth (L);
i	slope (–);
K	coefficient formula Bagnold ($ML^{-4}T^2$);
k_s	equivalent roughness height of Nikuradse (L);
R	hydraulic radius (L);
Re_*	grain Reynold's number (–);
r	discrepancy ratio = $S_{b,}$ predicted/$S_{b,}$ measured (–);
S_b	bed-load transport per unit width ($ML^{-1}T^{-1}$);
S_c	sediment transport per unit width involved in bedform migration ($ML^{-1}T^{-1}$);
T	$(\theta' - \theta'_{cr})/\theta'_{cr}$ = transport stage parameter (–);
U_c	bedform celerity (LT^{-1})
u	flow velocity (LT^{-1});
$\bar{u}$	depth mean flow velocity (LT^{-1});
u_*	bed–shear velocity (LT^{-1});
z	height above the bottom (L);
α	coefficient (–);
β	bedform coefficient (–);
Δ	$(\varrho_s - \varrho)/\varrho$ = specific density (–);
ε	porosity (–);
θ	Shield's entrainment parameter (–);
$\varkappa$	constant of von Kármán (–);
λ	bedform length (L);
μ	bedform factor (–);
ϱ	fluid density (ML^{-3});
ϱ_s	sediment density (ML^{-3});
τ	bed–shear stress ($ML^{-1}T^{-2}$), and
υ	kinematic viscosity coefficient (L^2T^{-1}).

Index : cr critical value for initiation of motion.

Accent : ′ related to grain roughness; effective, and
″ related to bedform roughness.

Appendix II

Location	$\bar{u}$ (ms^{-1})	h (m)	temp. (°C)	D_{50} (μm)	D_{90} (μm)	H (m)	U_c ($\times 10^{-3} ms^{-1}$)	S_e ($\times 10^{-3} kgm^{-1}s^{-1}$)
Rhine	1,60	10.4	2	3600	14500	1.60	0.166	254
(1)	1.58	9.9	1	3600	14500	1.60	0.131	199
	1.47	8.9	2	3600	14500	1.44	0.057	78
Pannerden	1.70	8.4	10	3800	5000			252
canal	1.76	9.0	10	3800	5000			297
(2)	1.77	9.4	10	3800	5000		no data	339
	1.78	9.5	10	3800	5000		mentioned	368
	1.77	9.1	10	3800	5000			321
	1.68	8.8	10	3800	5000			302
	1.63	8.3	10	3800	5000			249
	1.55	8.0	10	3800	5000			234
Waal	1.65	10.0	9	1050	1750	1.30	0.178	221
(3)	1.57	9.7	9	1050	1750	1.27	0.155	187
	1.50	9.6	10	1050	1750	1.29	0.117	144
	1.47	9.1	10	1050	1750	1.00	0.127	121
	1.41	8.7	11	1050	1750	1.02	0.095	92
	1.34	8.6	11	1050	1750	0.98	0.108	101
Waal	1.20	9.5	9	950	1550	1.16	0.055	61
(4)	1.20	10.0	9	950	1550	1.18	0.074	84
	1.17	9.8	9	950	1550	0.79	0.045	34
	1.13	9.3	10	950	1550	0.95	0.050	45
	1.10	9.0	10	950	1550	0.85	0.046	38
IJssel	0.83	5.3	7	690	1270	0.49	0.072	34
(5)	0.80	5.0	7	690	1270	0.49	0.057	27
	0.82	5.2	7	690	1270	0.57	0.072	39
Hii	0.74	0.59		1440	4000	0.085	1.04	84
(6)	0.93	0.65	no	1440	4000	0.094	1.01	91
	0.80	0.70	data	1440	4000	0.081	1.05	81
	0.81	0.73		1440	4000	0.138	0.70	92
Hii	0.79	0.71		1110	2700	0.250	0.50	119
(7)	0.89	0.85	no	1110	2700	0.224	0.93	194
	0.89	0.88	data	1110	2700	0.174	0.94	156
	0.90	1.03		1110	2700	0.252	1.09	262
Skive Karup	0.6	1.0	10	457	1260	0.09	0.283	24.3
(8)								
Dommel	0.43	0.66	16	406	750	0.050	0.406	9.9
(9)	0.60	0.79	16	370	750	0.042	0.370	16.7
	0.58	0.80	16	476	750	0.045	0.476	12.8
	0.32	0.79	16	452	780	0.030	0.452	4.0
	0.45	0.77	16	506	780	0.027	0.506	5.2
	0.56	0.78	16	433	780	0.024	0.433	9.1
	0.57	0.77	16	374	780	0.037	0.374	11.1
	0.57	0.77	16	407	780	0.042	0.407	11.9
	0.58	0.78	16	406	780	0.037	0.406	14.9
	0.54	0.75	16	445	780	0.038	0.445	9.4

Basic river data used for computations of bed-load transport. For the Hii river, a temperature of 20°C was assumed.

No. 1. *Tidal Computations in Shallow Water*
Dr. J. J. Dronkers† and prof. dr. ir. J. C. Schönfeld
Report on Hydrostatic Leveling across the Westerschelde
Ir. A. Waalewijn, 1959

No. 2. *Computations of the Decca Pattern for the Netherlands Delta Works*
Ir. H. Ph. van der Schaaf† and P. Vetterli, Ing. Dipl. E. T. H., 1960

No. 3. *The Aging of Asphaltic Bitumen*
Ir. A. J. P. van der Burgh, J. P. Bouwman en G. M. A. Steffelaar, 1962

No. 4. *Mud Distribution and Land Reclamation in the Eastern Wadden Shallows*
Dr. L. F. Kamps†, 1962

No. 5. *Modern Construction of Wing-Gates*
Ir. J. C. le Nobel, 1964

No. 6. *A Structure Plan for the Southern IJsselmeerpolders*
Board of the Zuyder Zee Works, 1964

No. 7. *The Use of Explosives for Clearing Ice*
Ir. J. van der Kley, 1965

No. 8. *The Design and Construction of the Van Brienenoord Bridge across the River Nieuwe Maas*
Ir. W. J. van der Eb†, 1968

No. 9. *Electronic Computation of Water Levels in Rivers during High Discharges*
Section River Studies. Directie Bovenrivieren of Rijkswaterstaat, 1969

No. 10. *The Canalization of the Lower Rhine*
Ir. A. C. de Gaay and ir. P. Blokland†, 1970

No. 11. *The Haringvliet Sluices*
Ir. H. A. Ferguson, ir. P. Blokland† and ir. drs. H. Kuiper, 1970

No. 12. *The Application of Piecewise Polunomials to Problems of Curve and Surface Approximation*
Dr. Kurt Kubik, 1971

No. 13. *Systems for Automatic Computation and Plotting of Position Patterns*
Ir. H. Ph. van der Schaaf†, 1972

No. 14. *The Realization and Function of the Northern Basis on the Delta Project*
Deltadienst of Rijkswaterstaat, 1973

No. 15. Fysical-Engineering Model of Reinforced Concrete Frames in Compression
Ir. J. Blaauwendraad, 1973

No. 16. *Navigation Locks for Push Tows*
Ir. C. Kooman, 1973

No. 17. *Pneumatic Barriers to reduce Salt Intrusion through Locks*
Dr. ir. G. Abraham, ir. P. van der Burg en ir. P. de Vos, 1973

No. 18. *Experiences with Mathematical Models used for Water Quality and Water Problems*
Ir. J. Voogt and dr. ir. C. B. Vreugdenhil, 1974

No. 19. *Sand Stabilization and Dune Building*
Dr. M. J. Adriani and dr. J. H. J. Terwindt, 1974

No. 20. *The Road-Picture as a Touchstone for the three dimenbsional Design of Roads*
Ir. J. F. Springer and ir. K. E. Huizinga (also in German), 1975

No. 21. *Push Tows in Canals*
Ir. J. Koster, 1975

No. 22. *Lock Capacity and Traffic Resistance of Locks*
Ir. C. Kooman and P. A. de Bruijn, 1975

No. 23. *Computer Calculations of a Complex Steel Bridge verified by Model Investigations*
Ir. Th. H. Kayser and ir. J. Brinkhorst, 1975

No. 24. *The Kreekrak Locks on the Scheldt-Rhine Connection*
Ir. P. A. Kolkman and ir. J. C. Slagter, 1976

No. 25. *Motorway Tunnels built by the Immersed Tube Method*
Ir. A. Glerum, ir. B. P. Rigter, ir. W. D. Eysink and W. F. Heins, 1976

No. 26. *Salt Distribution in Estuaries*
Rijkswaterstaat, Delft University of Technology, Delft Hydraulics Laboratory, 1976

No. 27. *Asphalt Revetment of Dyke Slopes*
Committee on the Compaction of Asphalt Revetments of Dyke Slopes, 1977

No. 28. *Calculation Methods for Two-dimensional Groundwater Flow*
Dr. ir. P. van der Veer, 1978

No. 29. *Ten Years of Quality Control in Road Construction in the Netherlands*
Ir. C. van de Fliert and ir. H. Schram, 1979

No. 30. *Digital Large Scale Restitution and Map Compilation*
J. G. van der Kraan, H. Rietveld, M. Tienstra and W. J. H. IJzereef, 1980

No. 31. *Policy Analysis for the National Water Management of the Netherlands*
(Netherlands Contributions, related tot the PAWN-study, for the ECE-seminar on Economic Instruments for the Rational Utilization of Water Resources – Veldhoven, Netherlands – 1980)

No. 32. *Changing Estuaries*
Dr. H. L. F. Saeijs, 1982

No. 33. *A Bird's Eye View of the Shipping Traffic on the North Sea*
North Sea directorate, 1982

No. 34. *Contribution to Remote Sensing: Applications of Thermal Infrared*
H. W. Brunsveld van Hulten (ed.), P. Hoogenboom, A. F. J. Jacobs, C. Kraan, G. P. de Loor and L. Wartena, 1984

No. 35. *On the Construction of Computational Methods for Shallow Water Flow Problems*
Dr. ir. G. S. Stelling, 1984

No. 36. *Wrong-way Driving*
Ir. G. A. Brevoord, 1984

No. 37. *The Use of Asphalt in Hydraulic Engineering*
Technical Advisory Committee on Waterdefences, 1985

No. 38. *Recycling of Road Pavement Materials in the Netherlands*
L. C. van Rijn and G. L. Tan, 1985

No. 39. *Groundwater Infiltration with Bored Wells*
National Institute for Water Supply et. al., 1985

No. 40. *Biological Research Ems-Dollard Estuary*
Biological Study of the Ems-Dollard Estuary (BOEDE), 1985

No. 41. *Sutrench-Model*
L. C. van Rijn and G. L. Tan, 1985

No. 42. *Phytoplankton off the Dutch coast*
Dr. R. J. Leewis, 1985

[redacted]

607983 F